DOCTOR OF PHILOSOPHY

Establishing multi-bivalve species Sclerochronology

Reynolds, David John

Award date:
2011

Awarding institution:
Bangor University

ESTABLISHING MULTI-BIVALVE SPECIES SCLEROCHRONOLOGY

BY

David John Reynolds

A thesis presented in partial fulfilment of the requirements of Bangor University for the degree of Doctor of Philosophy

Bangor University
School of Ocean Science
Menai Bridge
June 2011

Acknowledgements

I must acknowledge and give thanks to a host of people and organisations who have provided me not only with financial and technical assistance over the past four years but also much needed direction, reassurance and encouragement, all of which have been critical to me completing this thesis.

Firstly I would like to thank my supervisors Professors James Scourse and Chris Richardson for presenting me with the opportunity to undertake this Ph.D. and for providing much needed and gratefully received supervision, guidance and inspiration throughout this work.

I owe my parents John and Moira Reynolds a great debt for their financial support and eternal encouragement during the entirety of this work; the completion of this PhD would have undoubtedly been in question without them. Similarly I need to thank my girlfriend Sharolyn Parnham for not only her moral support and encouragement, which were much needed along the way, but also for putting up with me particularly during the writing up of this thesis.

Particular thanks must go to my two colleagues and friends Dr Paul Butler and Dr Al Wanamaker who frequently provided much needed advice and critique throughout my PhD (despite working on the "wrong" species). Special thanks must go to Al Wanamaker who, following his departure from Bangor University to Iowa State University, accommodated me in the USA and afforded me the opportunity to use the equipment and facilities within his geochemistry laboratory and this allowed me to generate the stable isotopic data that are presented in Chapter Five.

The Captain and officers of the RV *Prince Madog* are acknowledged and thanked for their part in the collection of shell samples during the 2006 cruise to Western Scotland. Thanks also go to NERC for their financial support (grant No. NFSD/09/01) and to Dr Martin Sayer and the entire NERC Facility for Scientific Diving (NFSD) team for their extensive diving work and collection of various bivalve species in Loch Sunart.

I am grateful to Dr Charlotte Bryant and Dr Pauline Gulliver of the NERC Radiocarbon Facility for their assistance in the applications for radiocarbon support and for undertaking the radiocarbon analysis as well as allowing me to

visit the laboratory to date the shell samples. The NERC are acknowledged and thanked for providing the funds, in two separate applications, for a total of eight ^{14}C determinations (allocation numbers 1419.1009 and 1330.1008). I also thank Dr Jan Heinemeier of the Aarhus Radiocarbon Facility (Denmark) for the analysis of the initial four ^{14}C determinations.

Various museum curators gave me access to their collections of molluscs. Particular thanks go to Professor John Taylor of the Natural History Museum of London, who I would like to thank for accommodating my visit to the molluscan archives, to Dr Ellen Strong of the Smithsonian Institution National Museum of Natural History (Washington) and Sankurie Pye of the Scottish National Museum (Edinburgh) for providing me with details of their shell archives.

I thank Dr Elizabeth Harper, Cambridge University, for undertaking the X-ray diffraction analysis to determine the structural composition of the shells of *Glossus humanus* and *Glycymeris glycymeris*. Professor Ian Hall (Cardiff University) is thanked for enabling me to use his Micromilling system to re-drill samples of shell carbonate for isotopic analysis. Dr Mike Tetley is thanked for running the Glossus humanus data through his habitat suitabilitymodel.

For the generous donation of instrumental data sets I thank Dr Mark Inall (SAMS) for the Tiree Passage Oceanographic series, Dr Ewan Woodley (British Geological Survey) and Dr Neil Loader (Swansea University) for the donation of the Southern Glens dendrochronology series and their assistance in analysing the resulting spatial and temporal climate reconstructions. The British Oceanographic Data Centre (BODC) are acknowledged for providing CTD data from the Tiree Passage region, the Meteorological Office of the United Kingdom for providing historical climate observations and, again, Dr Martin Sayer for providing localised marine environmental datasets.

Furthermore I would like to thank the following organisations for providing the funds needed to complete this work: The EU-funded Millennium project, The Quaternary Research Association for providing funding through the New Research Workers Award and the Radiocarbon Short Course Bursary. NERC supported me as a part-time PDRA during the writing of this thesis.

Summary

This thesis presents statistical and geochemical sclerochronological investigations into three long-lived marine bivalve molluscs, *Arctica islandica*, *Glossus humanus* and *Glycymeris glycymeris,* collected from coastal sites on the west of Scotland. The potential of both *G. humanus* and *G. glycymeris* to become new sclerochronological palaeoenvironmental archives is assessed and the first multi-species master sclerochronology is presented. Cross-matching techniques derived from dendrochronology are used to construct three single species master sclerochronologies, two derived from dead-collected *G. humanus* valves from Salen Bay (Loch Sunart) and the Sound of Mull, and a single absolutely dated sclerochronology from live- and dead-collected *G. glycymeris* collected in the Tiree Passage. Fourteen radiocarbon (^{14}C) determinations were used to validate the cross-matching in each of the chronologies. Significant positive correlations have been identified, using cross-matching techniques, between the *G. humanus* growth increment series (GIS) contained within the Sound of Mull chronology, the GIS of the *G. glycymeris* in the Tiree Passage chronology and the live-collected *A. islandica* enabling the construction of the first absolutely-dated multi-centennial multi-species master sclerochronology. Significant positive correlations have been identified between the *G. glycymeris* and multi-species sclerochronologies and an independent absolutely-dated Scots Pine (*Pinus sylvestris*) dendrochronology from NW Scotland, probably indicating a common response to large scale North Atlantic climatic variability. Spatial field correlation plots and calibration verification models using both shell and tree-ring data show strong association with Gulf Stream/ North Atlantic Current (GS/NAC) sea surface temperatures, northwest European air temperatures and the Atlantic Multi-decadal Oscillation (AMO). These data indicate that the statistical and geochemical analysis of absolutely dated annually resolved chronologies constructed from the long-lived marine bivalve mollusc *G. glycymeris,* in conjunction with *A. islandica* shell- and dendrochronologies constructed in climatically sensitive areas, can facilitate the reconstruction, at high resolution, of past oceanographic and atmospheric variability.

Contents

Chapter 1

Introduction

1.1 Introduction

The Intergovernmental Panel on Climate Change 2007, (IPCC) report states that the generation of detailed high-resolution climatic reconstructions from the hydrosphere, cryosphere and atmosphere are critical for the development of our understanding of the natural amplitude, rate and frequency of past changes within Earth's climatic systems (Pachauri and Reisinger, 2007). The need for such climatic reconstructions stems from the temporal extent of direct climatic observations. These observations are largely constrained to the past *ca.*350 years due to the introduction of meteorological instrumentation. Investigations into past climatic change using these direct quantitative meteorological observations are similarly constrained to the past three centuries. Consequently these data sets act as a record of environmental conditions that are inherently under increasing influence of anthropogenic forcing. In order to examine and understand pre-industrial climatic changes, palaeoclimatologists have developed an array of biological and physical archives that act as naturally occurring qualitative and quantitative recorders of numerous environmental parameters.

A vast array of biological and physical palaeoclimatic archives have been developed that facilitate the investigation of past climatic changes across a broad range of temporal frequency domains from high resolution annually resolved tree-ring chronologies, coral records and ice cores to mid to low frequency (multi-annual to decadal) archives such as sediment cores. These proxy records allow the modern instrumental timeseries to be extended backwards through time over hundreds or even thousands of years. Prior to the

development of molluscan sclerochronological archives, however, investigations into mid-latitude temperate marine environments were largely restricted to sedimentary archives, which can be limited in temporal resolution to mid to low frequency palaeoenvironmental changes. Within this thesis high frequency equates to a period of <3 years, mid frequency 3-35 years and low frequency >35 years.

Although sclerochronology does encompass the examination of skeletal growth within all marine and aquatic organisms, only material regarding molluscan sclerochronology is discussed in this chapter. The following sections attempt to provide the general background of all aspects of molluscan sclerochronology, sclerochronological palaeoenvironmental proxies and the structure to the thesis.

1.2 Sclerochronological archives

Seminal publications during the 1970s and 1980s established the groundwork for the field of sclerochronology, noting that skeletal hard parts of aqueous organisms, particularly molluscs, contained a continuous record of ontogenetic growth (Rosenberg and Runcorn, 1975; Rhoads and Lutz, 1980). Predominantly, past sclerochronological studies have utilized clams as detailed stratigraphies from which biogenic carbonate could be extracted for detailed geochemical analysis (e.g. stable isotope or radiocarbon) (Steuber, 1999; Surge *et al.,* 2003; Schöne *et al.,* 2005; Wanamaker *et al.,* 2011). A number of studies have been published in recent years which examine the ontogenetic growth patterns within populations of bivalves using techniques derived from dendrochronology (Marchitto *et al.,* 2000, Scourse *et al.,* 2006, Butler *et al.,* 2009a). The application of dendrochronological cross-matching (cross-dating) techniques allow the ontogenetic growth patterns derived from long-lived bivalves to form a temporal framework in the form of statistically robust master sclerochronologies. The development of sclerochronologies extending beyond the longevity of a single organism presents an opportunity to investigate high resolution palaeoceanographic conditions beyond the modern instrumental period. Such sclerochronologies have the potential to be utilised within ultra-high-resolution (annual to sub-annual) palaeoclimatic and palaeoceanographic investigations by means of both growth increment analysis and their contained

geochemical proxies (radiocarbon, stable oxygen and carbon isotopes) contained within the shell.

Currently the most important species within the field of sclerochronology is the long-lived marine bivalve mollusc *Arctica islandica* (L.). *Arctica islandica* has been utilised in the construction of all published multi-centennial annually resolved master sclerochronologies (e.g. Witbaard *et al.*, 1997; Scourse *et al.*, 2006; Butler *et al.*, 2009a; Butler *et al.*, submitted; and Wanamaker *et al.*, in prep). It was in 1977 that the use of *A. islandica* as a sclerochronological archive was first voiced - presented to the Annual Meeting of the Geological Society of America, Thompson and Jones, (1977) and later published as Thompson *et al.*, (1980). They argued that *A. islandica* fulfilled four critical biochronicle criteria, which are that (1) growth was synchronous between individuals within given populations; (2) the growth increments were formed with an annual periodicity; (3) the organism is of sufficient longevity to produce timeseries of sufficient length to form statistically robust cross-matches; and (4) the growth increments were continuously formed throughout life. Subsequent publications over the past three decades have gone some way to establishing *A. islandica* as the gold standard of sclerochronological species. *Arctica islandica* reaches a maximum longevity of >500 years (Wanamaker *et al.*, in review), with multiple lines of evidence determining that the periodicity of growth line formation to be annual (Ropes 1988; Weidman *et al.*, 1994; Witbaard *et al.*, 1997) and proven synchrony of growth between individuals within and across populations (Scourse *et al.*, 2006; Butler *et al.*, 2009a). Furthermore recent studies have shown that the annual growth increment widths and geochemistry of the biogenic carbonate within the growth increments of bivalves can be utilised as proxies for sea surface temperature (Strom *et al.*, 2004; Schöne *et al.*, 2004), air temperature (Schöne *et al.*, 2004), productivity dynamics (Witbaard *et al.*, 2003; Wanamaker *et al.*, 2009) and dominant modes of atmospheric (Schöne *et al.*, 2003) and oceanic circulation (Ambrose *et al.*, 2006).

Despite the numerous reasons for concentrating research effort on *A. islandica*, there are reasons why the development of new sclerochronological archives is

deemed advantageous: 1) the distribution of *A. islandica* is patchy through time and space constrained by water depth and sediment type. Therefore, there will be regions of hydrographic and palaeoclimatic interest where there are no known *A. islandica* populations and so without the development of new sclerochronological archives these regions would be void of annually resolved records; 2) it is quite plausible that other bivalve species may be more sensitive palaeoclimatic archives than *A. islandica* and thus provide more accurate reconstructions of palaeoenvironments.

Two bivalve species which could potentially be utilised as sclerochronological archives are the dog cockle (*Glycymeris glycymeris* L.) and the heart cockle (*Glossus humanus* L.). The dog cockle is a common bivalve mollusc which inhabits coarse sand to gravel substrata of European coastal shelf seas to a maximum depth of *ca.* 100m (Hayward and Ryland, 1995). Hitherto Berthou *et al.,* (1986) is the only published study which examines the periodicity of growth line formation within *G. glycymeris* shell valves. By examining the stable isotopic content within the shell matrix in a similar manner to studies conducted on *A. islandica* Witbaard *et al.,* (1994) demonstrated that the growth lines were formed with an annual periodicity. Previous studies have examined the use of *G. glycymeris* shell scars as an archive of fishing trawler disturbance within the Irish Sea (Ramsay *et al.,* 2000, 2001).

Glossus humanus is a large infaunal marine bivalve mollusc that inhabits fine sediments in the European and British coastal shelf seas (Owen 1953; Hayward and Ryland, 1995). *Glossus humanus* shell valves reach a maximum size of *ca.*130mm, which is comparable to *A. islandica* shells from similar hydrographic settings (Owen, 1953). There have been relatively few published articles regarding any aspect of *G. humanus* biology and ecology and, to the author's knowledge, there has been no previous sclerochronological work conducted using their shells. Owen (1953) compared the physiology and morphometrics of *G. humanus* with that of the comparably sized *A. islandica;* as such there is the possibility that the shells of *G. humanus* reach a comparable longevity to that of *A. islandica* on the Hebridean continental shelf.

The geographical range of the modern and historical distributions of both *G. humanus* and *G. glycymeris* are comparable to that of *A. islandica* within the European coastal shelf seas (Nicol, 1951a & b; Dahlgren *et al.,* 2000). These species have complementary preference for specific substrates with *G. glycymeris* inhabiting coarse sands to gravels, *A. islandica* inhabiting fine sand to gravel and *G. humanus* inhabiting soft muds (Hayward and Ryland, 1995). Each species distributions are more extensively discussed within Chapter 6.3. Their complementary distribution provides a basis for the expansion of high resolution palaeoceanographic studies into areas where there are no known modern or historical *A. islandica* populations.

1.3 Molluscan sclerochronologies

There has been a great deal of progress made over the past 15 years in the development of molluscan master sclerochronologies – mean standardised growth index chronologies – constructed from growth increment widths derived from long-lived marine bivalve molluscs. Witbaard *et al.,* (1997) constructed the first centennial *A. islandica* sclerochronology utilising the growth increment widths from live-caught specimens from the northern North Sea. Marchitto *et al.,* (2000) produced the first centennial sclerochronology constructed utilising growth increment from both live- and dead-collected *A. islandica* highlighting the potential for extending sclerochronologies backwards through time beyond the longevity of a single specimen. Witbaard *et al.,* (2003b) found statistically significant correlations between the annually resolved growth increment widths within the multi-centennial *A. islandica* sclerochronology from the North Sea and food availability in the form of zooplankton in the water column. Both the Marchitto *et al.,* (2000) and Witbaard *et al.,* (1997 and 2003b) studies utilised live collected specimens to anchor the sclerochronologies to an absolute date.

Scourse *et al.,* (2006) published the first floating sclerochronology produced from growth increment widths from dead collected *A. islandica* from the North Sea. Floating sclerochronologies – chronologies that have no absolute temporal anchor in the form of a cross-match to a specimen with a known date of death – provide a window into the past, but are less "useful" than an absolutely dated sclerochronology. An absolutely dated sclerochronology, which has been

anchored by cross-matching between fossil and a modern specimen with a known year of death, can be compared to instrumental data allowing for direct comparisons to be made between the growth increment and target environmental data. A floating sclerochronology, however, such as the one constructed by Scourse *et al.,* (2006), has no contemporaneous data to be compared with and, as such, palaeoclimatic reconstructions are limited to geochemical proxies that may also come with caveats which may reduce precision.

Although the studies of Marchitto *et al.,* (2000), Witbaard *et al.,* (1997 & 2003b) and Scourse *et al.,* (2006) all present sclerochronologies that may be perceived to represent relatively short timescales, they present significant grounding and proof of concept that has subsequently allowed the construction of much longer sclerochronologies, such as the 489 year Irish Sea sclerochronology (Butler *et al.,* 2009a) and the 1357 year Icelandic sclerochronology (Butler *et al.,* submitted; Wanamaker *et al.,* in review.).

Hitherto only a single paper has been published regarding the use of a multi-species sclerochronology. Witbaard *et al.,*. (2006) examined the growth increment widths within *A. islandica* and two other relatively short-lived marine bivalve molluscs, *Mya truncata* and *Chamelea striatula*, from the northern North Sea. Significant correlations were identified between the growth patterns across the three species but no attempt was made to construct a single master multi-species sclerochronology. This paper does, however, indicate that it may be possible to utilise a spectrum of bivalve species to construct a single absolutely-dated master multi-species sclerochronology.

Other studies have alluded to common growth signals being identified between the growth of species across taxa. Black (2009) examined growth increment series within the yelloweye rockfish (*Sebastes ruberrimus*), splitnose rockfish (*Sebastes diploproa*) and the Pacific geoduck (*Panopea abrupta*). Significant commonality was identified within chronologies (decadal in length) constructed from the sites within the region of the study area. Furthermore the principal components reflect dendrochronologies constructed in western North America.

Helama *et al.*, (2007 & 2010) also found significant coherence between growth increment series within dendrochronologies and sclerochronologies constructed from specimens of *A. islandica* and the Scots pine. Years with "particularly low winter and high summer North Atlantic Oscillation indices" showed increased synchronisation between the dendrochronologies and the sclerochronologies (Helama *et al.*, 2007). These studies demonstrate the sensitivity of a broad array of annually resolved marine and terrestrial palaeoenvironmental archives to climatic variability. Further development of these principles may allow for the reconstruction of large scale climatic indices.

1.4 Sclerochronological proxies

Sclerochronologies act as powerful temporal frameworks that facilitate the detailed investigation of ultra high resolution palaeoenvironmental conditions by means of geochemical or growth increment proxies. It has been shown that by means of geochemical analysis or statistical analysis of growth increment widths it is possible to reconstruct parameters such as air temperature (Schöne *et al.*, 2004), seawater temperature (Strom *et al.*, 2004), productivity dynamics (Witbaard *et al.*, 2003b; Wanamaker *et al.*, 2009), and dominant modes of atmospheric (Schöne *et al.*, 2003) and oceanic circulation (Ambrose *et al.*, 2006). The underlying principle behind both geochemical and growth increment proxies is the Uniformitarianism Principle, which implies that the relationships between proxies and the target parameters are the same at present as they have been in the past, thus conforming to the Uniformitarian Principal pioneered by James Hutton (Fritts, 1976). Significant relationships identified between a proxy and a target environmental parameter over the instrumental period, are assumed to be significant for the entirety of the record, thus allowing for the accurate reconstruction of the target parameter. The following two sub-sections detail the key hypotheses and methods within both increment width and geochemical proxies (1.4.1 and 1.4.2 respectively)

1.4.1 Increment width reconstructions

The application of the increment width chronology directly as a climatic proxy is a widely used technique within dendrochronology. Within sclerochronology, however, the construction of climatic reconstructions based solely on the growth

increment widths has hitherto not been fully utilised. Statistical techniques such as linear regression analysis and data scaling (Esper *et al.*, 2005) can be used to directly calibrate proxy series to instrumental target series over the instrumental period. Standard methods of calibration and verification of increment width series to target environmental parameters have been commonly used within the dendrochronological community over the past three decades to provide a robust test of the proxy calibration (Fritts, 1976; Cook and Kariukstis, 1990; Visser *et al.*, 2010). The calibration verification process works by separating two halves of the target environmental timeseries; one half is applied to the calibration with the proxy record and the second half is set aside for independent verification of the calibration. Detailed methods of the calibration verification techniques as well as the methods for the statistical assessment of the precision and skill of the climatic reconstruction are given in Chapters 3.7 and 3.8.

1.4.2 Geochemical reconstruction

Geochemical proxies form the foundation of the majority of published sclerochronological palaeoenvironmental reconstructions (e.g. Schöne *et al.*, 2004 & 2005; Wanamaker *et al.*, 2008 & 2011), utilising stable carbon and oxygen isotopes ($\delta^{13}C$ and $\delta^{18}O$ respectively) as well as the radioactive carbon isotope (^{14}C). The bias within the published peer reviewed literature towards geochemical proxies over growth increment width proxies is largely due to the established theories dictating the uptake of stable isotopes within the marine environment and the uptake of this material into the calcium carbonate shell matrix, whilst the connection between inter-annual growth and environmental parameters, such as sea water temperature, is yet to be established. The following sub-sections detail the key theories and hypotheses associated with the use of carbon and oxygen isotopes in sclerochronology.

There are several advantages of utilising geochemical proxies for palaeoenvironmental reconstructions over using increment width proxies. The principal advantage of geochemical proxies is that they are largely independent of any ontogenetic trends (carbon may be an exception; see section 1.4.2.2). As a result geochemical proxies are able to replicate climatic signals across all

temporal frequency domains, something that currently impedes growth increment series due to the detrending process. Furthermore, the temporal resolution of growth increment reconstructions is constrained by the periodicity over which the increments are formed; geochemical proxies, however, are constrained by the mass and hence volume of material required for the desired analysis, and the width of the growth increments from which the material originates. Generally this allows for sub-annual resolution analysis of carbon and oxygen stable isotopes, whilst typically allowing for precise multi-annual resolution radiocarbon sampling. The single disadvantage of the use of geochemical analysis is cost.

1.4.2.1 Stable oxygen isotopes ($\delta^{18}O$)

Analysis of the ratio of stable oxygen isotope (16:18, denoted as $\delta^{18}O$) concentrations within biogenic carbonates has been widely used within sclerochronology as a natural recorder of ambient seawater temperatures (Schöne *et al.*, 2004 & 2005; Wanamaker *et al.*, 2008 & 2011). The mechanisms of $\delta^{18}O$ fractionation are well established within the marine environment and can be driven by seasonality in temperature, evaporation and salinity (through the influx of fresh water). It is also well established that the biogenic aragonite shell matrix of bivalve shells incorporate oxygen in equilibrium or at constant offset from equilibrium with the ambient sea water (Urey, 1947). As a result measureable fluctuations within the $\delta^{18}O$ of the ambient sea water caused by temperature can be reconstructed by the measurement of the $\delta^{18}O$ composition of the aragonite shell matrix. Palaeothermometry equations have developed over the past thirty years which, when taking into account the effects of salinity, allow for the direct conversion of $\delta^{18}O_{aragonite}$ into absolute ambient seawater temperatures (Grossman and Ku, 1986; Dettman *et al.*, 1999).

1.4.2.2 Stable carbon isotopes ($\delta^{13}C$)

Measurements of $\delta^{13}C$ can be determined either as a "by product" of ^{14}C dating (Butler *et al.*, 2009b), or by standard mass spectrometry as a ratio of carbon 12:13 denoted as $\delta^{13}C$ (Cage and Austin, 2010). Examination of the long-term variability within the $\delta^{13}C$ record in the marine environment shows relative

stability during the pre-industrial era going back to the last millennium (Cage and Austin, 2010). Since the industrial revolution, however, the trend within marine $\delta^{13}C$ records from the Irish Sea and Scottish sea lochs shows a distinctive shift towards depleted $\delta^{13}C$ values (Butler *et al.*, 2009b; Cage and Austin, 2010). These trends have been attributed to the ^{13}C Suess effect. The Suess effect is the relative depletion in ^{13}C relative to ^{12}C due to the increased burning of fossil fuels (which contain higher concentrations of ^{12}C) (Suess, 1953). Hitherto the archives of both pre- and post-industrial $\delta^{13}C$ within the waters of NW Britain have been conducted at low resolution (>10 years), (Butler *et al.*, 2009b; Cage and Austin, 2010). There is scope therefore to produce an annually resolved record of $\delta^{13}C$ within Scottish waters using micro-sampling and stable isotope techniques from absolutely dated shell material.

1.4.2.3 AMS radiocarbon dating

Accelerator mass spectrometer (AMS) radiocarbon (^{14}C) dating has become an integral part of many scientific disciplines allowing for the relatively accurate (± *ca.*100 years, 2σ error) dating of historical and fossil material. Calibration of marine derived ^{14}C determinations are complicated due to reservoir effects. Modern ^{14}C, which is generated within the upper atmosphere, is relatively homogenous in concentrations within the atmosphere. The modelled marine radiocarbon calibration curve compensates for the global offset of the marine system due to the time taken for the atmospheric ^{14}C to enter the marine system (Hughen *et al.*,2004; Einer *et al.*, 2009). Regional offsets (ΔR) are present within the ^{14}C age of the oceans due to differences in the rate of transportation of carbon from the atmosphere to the oceans. These rates are driven by cryospheric, hydrographic and oceanographic conditions, so that the relative ^{14}C age of water can differ significantly across geographical areas. Radiocarbon determinations derived from absolutely dated material facilitate the accurate calculation of such regional offsets allowing for precise calibration of ^{14}C data with unknown temporal origins.

Bivalve molluscs have been shown to incorporate ^{14}C in equilibrium with the ambient sea water in which they live and as such can be used to accurately determine ΔR through time. Although ΔR could prove problematic in other areas

of marine research, when the ^{14}C determinations are sourced from an absolutely dated material they can be used as an archive of the source of oceanic waters. Wanamaker *et al.*, (in review.) used ^{14}C determinations from a 1357 year absolutely dated sclerochronology to reconstruct the temporal variations in ΔR on the North Icelandic shelf. The long-term instabilities that Wanamaker *et al.*, (in review.) found can be attributed to changes in the water masses as they cross the North Icelandic shelf from relatively older Arctic waters to relatively younger North Atlantic waters.

1.5 Project rationale

The rationale behind the research presented within this thesis is aimed at further increasing the scope of sclerochronology by broadening the spectrum of environments which can be investigated using molluscan archives. The distribution of *A. islandica*, which is currently the most widely used molluscan sclerochronological archive, is patchy through time and space, and is constrained by water depth and sediment type. Consequently there are large areas of coastal shelf seas in which there are no *A. islandica* present, either as dead or living populations. Developing other long-lived molluscs into palaeoenvironmental archives would allow for these areas to be investigated and further increase the number of habitats and environments which can be investigated, incorporating areas of particular hydrographic and oceanographic interest where there are no living or fossil populations of *A. islandica.*

1.6 Project objectives

This project has the following primary objectives:

I. Construction of sclerochronologies from the three long-lived species, *Arctica islandica, Glycymeris glycymeris* and *Glossus humanus.*

II. Construction of the first multi-centennial multi-species sclerochronology.

III. Comparison of high resolution molluscan archives with other available archives of Holocene environments (dendrochronological and sedimentary records).

Where appropriate, further investigation of the growth increment series and geochemical data was undertaken to assess key hypotheses (e.g. periodicity of growth line formation) and the potential use of these data in palaeoenvironmental reconstructions.

1.7 Thesis structure

Chapter 1: introduction

Chapter 2: Practical Materials and Methods

This Chapter describes the methods used during the various practical aspects of the research contained within this thesis and it covers a) the study area and sample collection, b) the sectioning strategies adopted, c) the construction of the digital photo-mosaics of the shell sections, d) how the records of the growth increment series are constructed, e) the determination of the calcium carbonate crystalline form within *G. humanus* and *G. glycymeris* shells and f) the sampling approach used to radiocarbon date shells and obtain samples for stable isotopic analysis. Details are given of oceanographic and meteorological observations that have been examined within this thesis.

Chapter 3: Statistical Methods

This Chapter details the statistical methods used for the analysis and interrogation of the growth increment records; this involves high-pass detrending for cross-matching to allow each increment to be absolutely positioned in time, as well as the detrending process for chronology construction. Methods for chronology "quality assurance" are also outlined. All three species examined were treated identically unless otherwise stated.

Chapter 4: Biological and chronological results

This Chapter describes the raw biological data collected during the completion of this study. Where possible the published distribution maps have been up-dated using collection data from various sources. The growth rates of

specimens are compared with recorded morphological traits such as shell length. Inter- and intra-species cross-matching results are also described.

Chapter 5: Geochemistry results

This Chapter details the geochemical results including the AMS ^{14}C determinations, and examination of the stable oxygen and carbon concentrations derived from *G. humanus* and *G. glycymeris* shell valves. The crystalline form of the calcium carbonate within the shells of *G. humanus* and *G. glycymeris*, determined by X-ray diffraction is described. The results of every sample analysed are presented within Appendix A-GC.

Chapter 6: Discussion: Biology and Chronology

This Chapter draws on, and reviews, data from Chapters 4 and 5, and discussing the differences and similarities between the constructed master chronologies. The first annually-resolved multi-species sclerochronology is presented and the results discussed. Each of the sclerochronologies are compared to a dendrochronology constructed from tree ring series within the Southern Glens of Scotland.

Chapter 7: Discussion: Palaeoenvironmental Reconstructions From Growth Increment Series

This Chapter discusses the temporal and spatial correlations between the master *G. glycymeris* chronology and the multi-species chronologies and compares these chronologies with localised and gridded oceanographic and meteorological instrumental datasets.

Chapter 8: Discussion: Geochemistry

The radiocarbon determinations used to verify independently the nature of the cross-matching, presented in Chapter 4, are used to determine the localised offset from the global marine reservoir (ΔR). These values are compared to previously published values calculated for Scottish coastal waters. Analysis of stable isotopic concentrations, presented in Chapter 4, are analysed and compared with other geochemical archives from Scotland and the Irish Sea.

Chapter 9: Conclusion

This chapter concludes the results and discussions encompassing the biology, geochemistry, chronological analysis and palaeoenvironmental reconstructions. It also sets out some ideas and recommendations for possible future work.

Chapter 2

Materials and Methods

2.1 Introduction

This chapter describes the methods used during the various practical aspects of the research contained within this thesis and it covers a) the study area and sample collection, b) the sectioning strategies adopted, c) the construction of the digital photo-mosaics of the shell sections, d) how the records of the growth increment series are constructed, e) the determination of the calcium carbonate crystalline form of the *Glossus humanus* and *Glycymeris glycymeris* shells and f) the sampling approach used to radiocarbon date some selected shells and obtain samples for stable isotopic analysis and seawater temperature reconstruction. Finally, details are given of the oceanographic and meteorological data that have been used in this thesis. Details of the statistical methods used in the cross-matching and chronology construction, as well as information regarding the oceanographic and meteorological instrumental time series analysed are given in chapter 3.

2.2 Study area

This study was conducted on the shells of three bivalve molluscs, the heart cockle *Glossus humanus*, the dog cockle *Glycymeris glycymeris* and the ocean quahog *Arctica islandica,* which were live- and dead-collected from sites within Loch Sunart and the surrounding environments on the west coast of Scotland. This area is of key oceanographic significance due to its location on the eastern limits of the North Atlantic Current (NAC) (Figure 2 – 1). The coastal waters within the Tiree Passage and the Sound of Mull are largely comprised of two main components, the Scottish Coastal Current (SCC) and the North Atlantic Slope Current (NASC), a branch of the NAC. These currents bring hydrographically distinct water masses onto the Hebridean Shelf through the

Tiree Passage and the Sound of Mull and into Loch Sunart. The NASC brings relatively warmer and more saline (*ca.*35.5 PSU, Prcatical Salinity Units) waters from the central North Atlantic whilst the SCC brings colder less saline waters (ca. 1% dilution due to riverine input throughout the Irish Sea and Clyde Sea (Inall *et al.*, 2009).

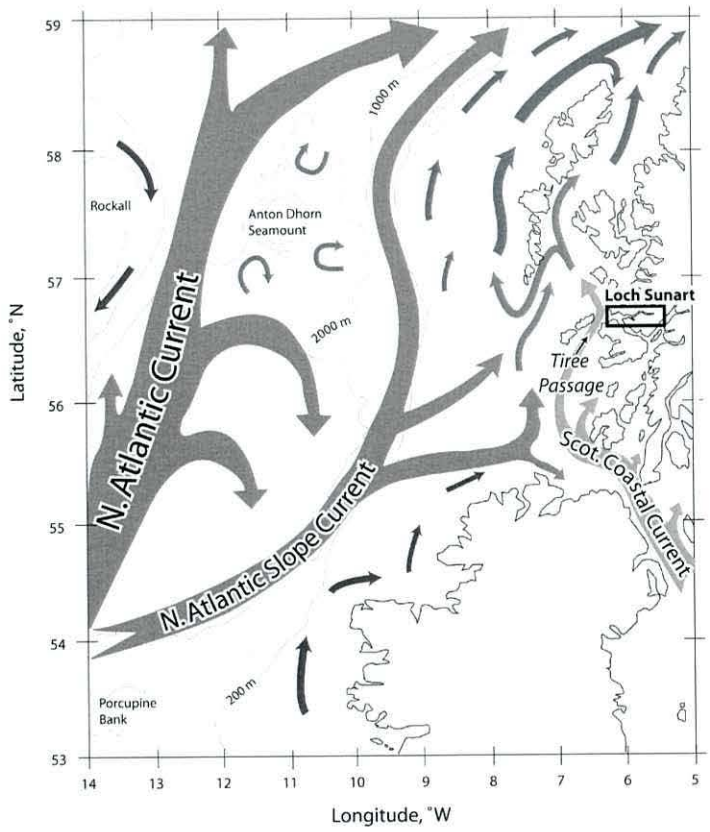

Figure 2 - 1: Map highlighting ocean and shelf sea currents along the west of Scotland, UK. The location of Loch Sunart and the Tiree Passage are also indicated (Figure 1, Cage and Austin, 2010).

Loch Sunart is a large sea loch ~33km in length with a mean width of ca.1.5km situated at the northern end of the Sound of Mull (Figure 2 – 2) (Gillibrand *et al.*, 2005). Loch Sunart is sub-divided into three main basins by two sills, situated *ca.*7km and *ca.*21km from the mouth of the loch, which are 33m and 8m below mean sea level (Gillibrand *et al.*, 2005). The outermost sill has a negligible impact on the through-flow of coastal waters into or out of the loch (Cage and Austin, 2010). Tidal forcings within the loch are semidiurnal with the tidal ranges varying between 1m and 4m during neap and spring tides respectively. The geology and topography of the Loch Sunart 299km^2 catchment area facilitate a

relatively rapid transfer of precipitation into the surface waters of the loch, of which ~50% is discharged into the upper-most basin (Cage and Austin, 2010).

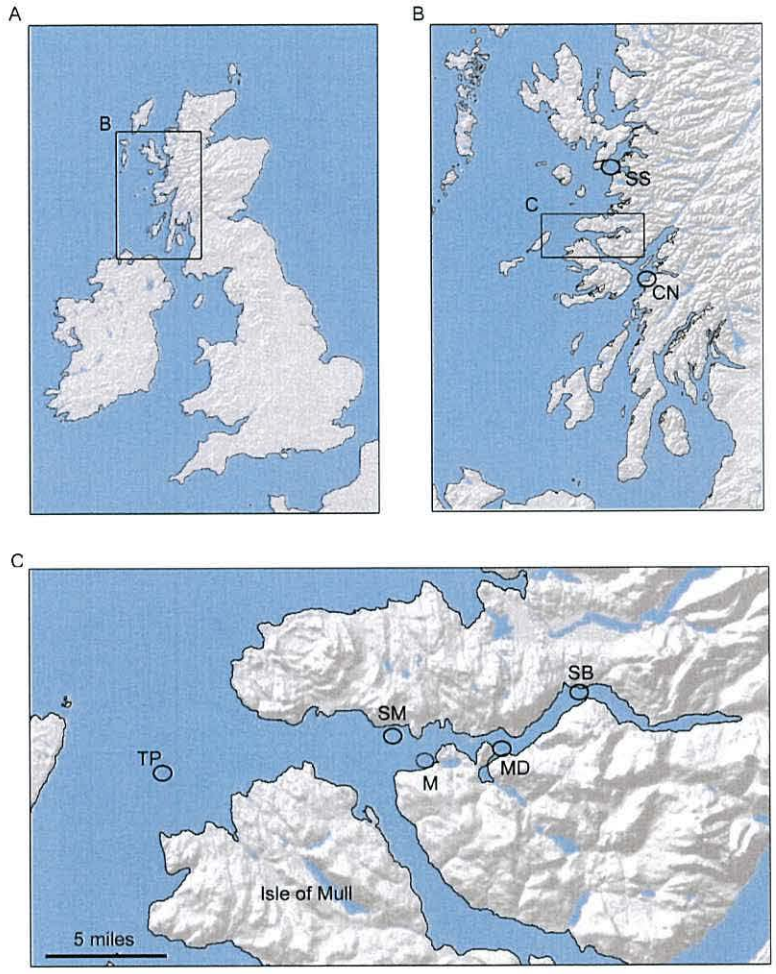

Figure 2 - 2: A) General locality where the shells were collected in this study. B) Location where live Glossus humanus shells were collected from the Sound of Sleat (SS) and Camas Naithas (CN). C: The sites within Loch Sunart/ Sound of Mull which yielded specimens of Arctica islandica and Glossus humanus (SM = Sound of Mull, MD = the Marion Dufresne collections and SB = Salen Bay) and Glycymeris glycymeris from the Tiree Passage (TP). Despite dredging efforts no samples were collected from Mourvern (M).

2.2.1 Site selection and sample collection

The shells in this study were predominantly collected from within Loch Sunart and the surrounding coastal shelf seas of north west Scotland, UK (Figure 2 – 2). Fossil *G. humanus* shell material was also examined which had been collected from sites in the Irish Sea and North Sea as well as from archived collections housed in the Natural History Museum (London) and the National Museum of Scotland (Edinburgh).

The sites where the shells were collected were initially selected on the basis of the suitability of the habitat to yield numbers of the three different species of long-lived bivalves as well as the interesting hydrographic setting where the shells were living. These bivalves were then used to produce robust sclerochronologies that could be compared with environmental data recorded by an oceanographic mooring recording environmental data in the Tiree Passage, and to compare these data with hindcast models produced from sedimentary data cored within Loch Sunart, (Figure 2 – 2 for locations also see Cage and Austin, (2010). The various bivalve species were collected from five sites (see Table 2 – 1). These sites covered a range of environments from a high energy "open water" setting in the Tiree Passage and the Sound of Mull to three sheltered sites within the main basin of Loch Sunart (see figure 2 – 2 for locations).

			Numbers of *A. islandica* (*Ai*), *G. humanus* (*Gh*) and *G. glycymeris* (*Gg*) specimens collected		
Station	**Latitude**	**Longitude**	**Live**	**Dead, single valves**	**Dead, paired valves**
SB	56°42.00 N	5°45.50 W	2 *Ai*	3 *Ai*, 20 *Gh*	1 *Ai*
SM	56°40.50 N	6°0.25 W	-	1 *Ai*, 19 *Gh*	3 *Gh*
M	56°39.35 N	5°58.00 W	-	-	-
TP	56°37.75 N	6°24.00 W	4 *Gg*	133 *Gg*	3 *Gg*
MD	56°40.00 N	5°52.00 W	-	59 *Ai*, 28 *Gh*	2 *Ai*, 1 *Gh*
Totals			2 Ai, 4 *Gg*	63 *Ai*, 67 *Gh*, 133 *Gg*	3 *Ai*, 4 *Gh*, 3 *Gg*

Table 2 - 1: Summary of the numbers of live-collected and fossil shell valves of various species of bivalves collected during a research cruise conducted in 2006 aboard the RV Prince Madog II in the Tiree passage and Loch Sunart. SB = Salen Bay, SM = Sound of Mull, M = Mourvern, TP = Tiree Passage, MD = Marion Dufresne sampling site (Cage and Austin, 2010).

Shells used in this study were predominantly collected using a 1m mechanical bespoke dredge (Figure 2 – 3) deployed from the RV *Prince Madog II* during a research cruise to the West of Scotland in 2006. Numbers of fossil *A. islandica*, *G. glycymeris* and *G. humanus* were collected (Table 2 – 1). However, a lack of live-collected shell material required further collections. To this end an application was made to the NERC Facility for Scientific Diving (NFSD) to employ divers to search for and collect live bivalves. However the water depths

at the original sites (given in Table 2 – 1) precluded the use of divers for sampling, so the sites were moved slightly inshore of the original sample locations to shallower depths so that divers could search safely for living animals (Table 2 - 2). Also to minimize the effect of depth related growth trends sampling was undertaken using a depth transect.

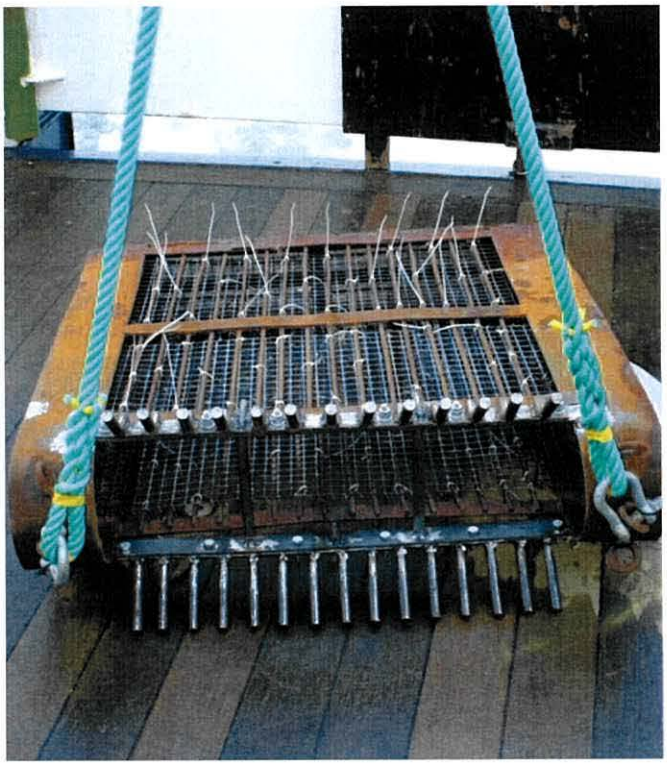

Figure 2 - 3: A bespoke mechanical dredge was used to collect a majority of the samples during the RV Prince Madog II cruise in 2006.

Site	Latitude	Longitude
Sun01	56º 41.712 N	5º 46.115 W
Sun02	56º 40.703 N	5º 59.657 W
Sun03	56º 39.919 N	5º 52.066 W
Sun04	56º 41.042 N	5º 40.501 W

Table 2 – 2: Latitude and longitude co-ordinates of the four sites sampled by the NFSD team within the main basin of Loch Sunart (Sun01 to 04).

The shell length (anterior-posterior axis), shell height (umbo-rim axis), maximum shell height, shell width (Figure 2 – 4) and wet body mass together with the

shell condition i.e. the preservation of the periostracum, the ligament preservation, shell margin damage, and condition of the inner shell surface nacre were recorded. Although not an absolute measure of shell age or the year of death, the shell biometrics and shell condition can be used as a rough estimate of the longevity of each bivalve species (see Butler, 2009). Using these data it was possible to distinguish between those shells that were of likely antiquity from those that had recently died, thus increasing the likelihood of potential cross-matches between live-collected and dead-collected shells.

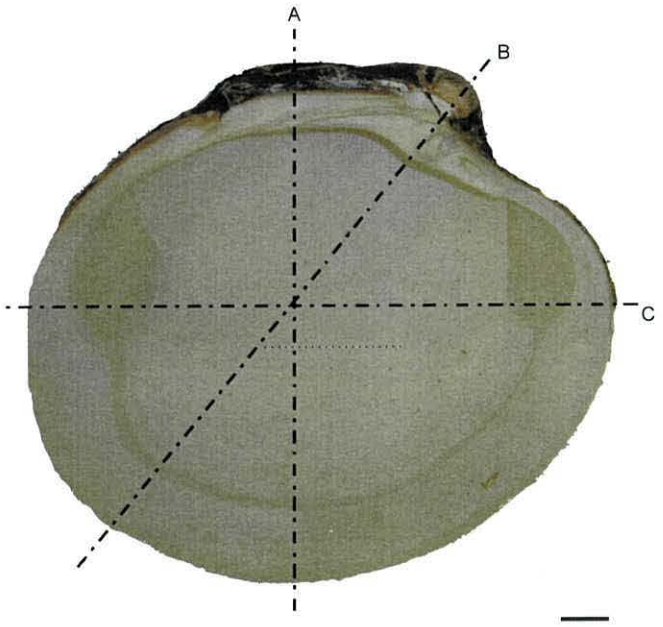

Figure 2 – 4: Diagram to illustrate the axes of measurement for A) shell height, B) maximum shell height and C) shell length of an Arctica islandica shell valve. Scale bar ~1cm.

2.3 Sectioning Strategy

Adopting the correct sectioning strategy was critical for ensuring that the internal growth series could be viewed in their entirety. The methods used for sectioning *G. glycymeris* and *A. islandica* shell valves were adapted from those used previously (see section 2.3.1), (Ramsay *et al.*, 2000 and Scourse *et al.*, 2006 respectively). In the case of *G. humanus* with its complex turbinate nature of growth at the umbone it was not possible to use the same sectioning strategy as that used on *A. islandica* and *G. glycymeris*. A line of section directly through the umbo to the shell margin in *G. humanus* would have resulted in the loss of the oldest growth increments and incorrect assessment of the longevity of the

individual (see Figure 2 – 5 illustrating the difference in shape of the umbone between the two species). An initial sequential sectioning strategy was employed to investigate how the direction of the growth lines would change as the line of section progressed through the central cardinal tooth of one *G. humanus* shell valve (see section 2.3.2).

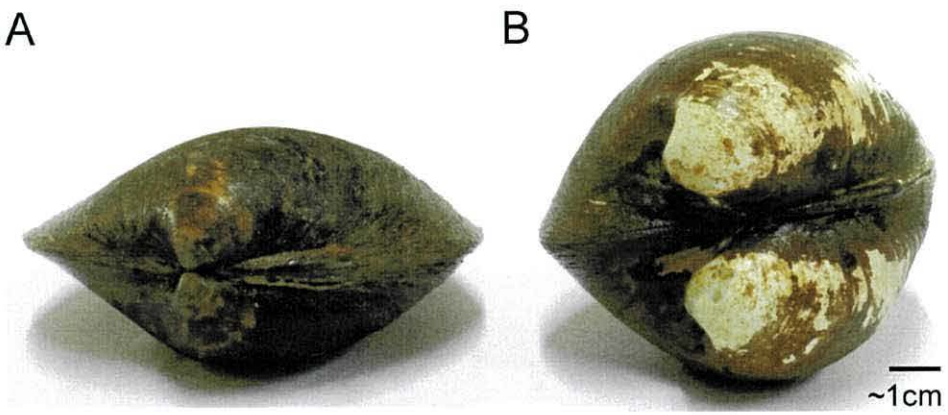

Figure 2 – 5: Photographs comparing the umbiones of A) Arctica islandica and B) Glossus humanus to illustrate the turbinate nature of the umbone of Glossus humanus which precludes the standard sectioning strategy.

2.3.1 *Arctica islandica* and *Glycymeris glycymeris* sectioning

A 1cm – 2cm shell section was cut from the umbone to the shell margin (Figure 2 - 6A) from the left shell valves of *A. islandica* and *G. glycymeris*, using a rotary grinding saw with a diamond edged blade. These shell slices were then embedded in MetPrep Kleer-set epoxy resin (Figure 2 - 6B). The embedded blocks were sectioned a second time along the axis of maximum growth from the umbone to the shell margin but fractionally offset from the apex of the cardinal tooth.

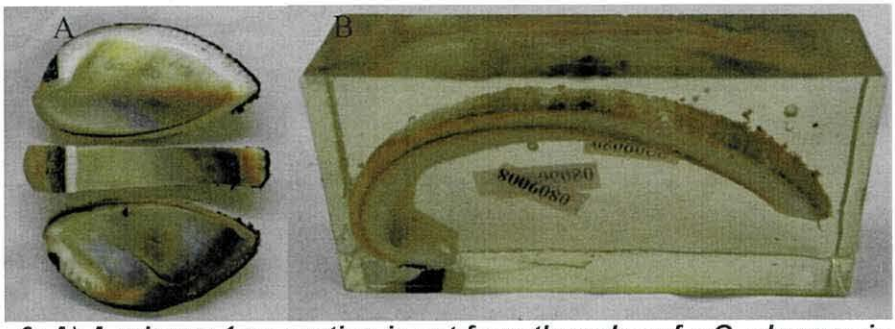

Figure 2 – 6: A) A primary 1cm section is cut from the valve of a G. glycymeris along the axis of maximum growth and B) The 1cm section is then embedded in epoxy resin prior to further sectioning.

The shell section containing the apex of the cardinal tooth was then ground using grit paper of grades from 120 through to 4000 lubricated with water so that the apex of the cardinal tooth was exposed and ground smooth. The ground surface was then polished, using 0.3µm diamond solution on two grades of magnetic felt polishing pad on an auto-rotating polishing table until a glass-like polished shell surface was achieved. The shell surfaces were etched using 0.1M HCl for 2mins. by immersing the resin block containing the shell section. Acetate peel replicas were then prepared of the dry, polished and etched shell section (see section 2 – 4).

2.3.2 Sequential sectioning of *Glossus humanus*

Sequential sectioning through the umbone region of one *G. humanus* valve (gh0005), (Figure 2 – 7), was undertaken to investigate the direction of shell deposition through the cardinal teeth in the umbone to assess the optimal position for sectioning and measuring the growth increment record. The left valve of *G. humanus* was initially sectioned perpendicular to the axis of maximum growth, separating the ventral margin from the umbone region. The umbone region was then embedded in epoxy resin using methods described in section 2.4.1.

The first section (Figure 7C line D) of the embedded umbone region was cut perpendicular to the side of the anterior and central cardinal tooth. The cut surface was then ground smooth and polished using methods described in section 2.4.1 and an acetate peel replica of the polished and etched tooth was

constructed prepared (see section 2.4). A further five sections were then ground at different positions through the central cardinal tooth and for each section acetate peel replicas were constructed for comparison.

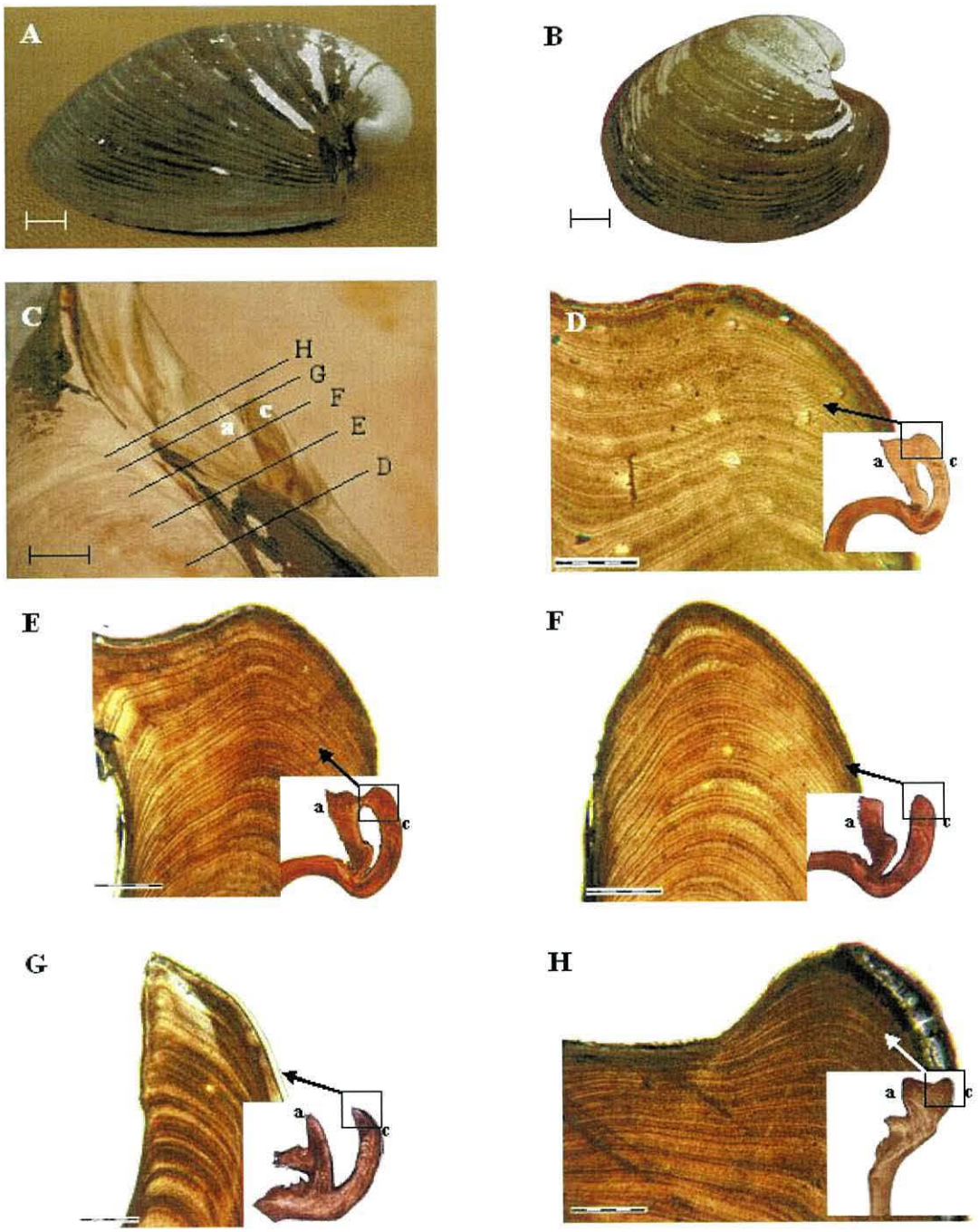

Figure 2 - 7; Appearance of A) the side view to highlight the complex curvature around the umbonal region (U) and B) the complete right valve of Glossus humanus; scale bars = 1cm. C) the hinge area of G. humanus to show the direction of the five sections (D-H) taken through the anterior (a) and the central (c) cardinal teeth, used to investigate the optimum positions for the sections that appear in figures D – H. The photomicrographs D – H, demonstrate the appearance of the section through the hinge (insets) and the growth lines in a selected cardinal tooth (arrow). D & E) the anterior and the central cardinal teeth are connected and the growth lines are indistinct, F & G) the cardinal and central teeth are separate allowing a clear image of the growth lines in the cardinal tooth and (H) both teeth have coalesced and the growth lines are unclear. Scale bars are 500µm.

2.4 Shell etching and acetate peel replicas

Arctica islandica and *G. glycymeris* polished shell sections were etched using routine methods (e. g. Butler *et al.*, 2009a & 2009b). The polished shell section was immersed in 0.1M hydrochloric acid (HCl) for 120 seconds, and then rinsed with distilled water to halt the etching process. Hitherto no studies have examined the internal growth lines in *G. humanus* shell valves, therefore the methods that had been used on *G. glycymeris* and *A. islandica* were assessed as potential techniques. Examination of the acetate peel replicas revealed that the shell section was over etched using a time of 120 seconds, but a slightly quicker etching period of 90 seconds gave optimal appearance to the growth lines. Once air dried the etched shell surface was covered with ethyl acetate and a piece of acetate sheet (35µm thick) was delicately positioned onto the etched surface ensuring no air bubbles were trapped beneath the acetate sheet. The peels were left to dry in a fume hood for about one hour. Once dry the acetate sheets were peeled from the blocks and placed on a labelled microscope slide ready for photographing.

2.5 Digital photo-micrographs and digital photo-mosaics

The acetate peel replicas were digitally photographed using a digital camera mounted on a transmited light microscope under x2.5 to x20 magnification. The imaging system used was initially AnalySIS (version 3.2) coupled with a SIS three megapixel CCD camera mounted to a Leica light transmitting microscope; this was later upgraded to a U-Eye three megapixel CCD camera mounted on a Meiji microscope coupled to the image capture and analysis software Omnimet (version 9,0 rev. 4). Both systems allowed for the complete manual adjustment of both microscope and camera settings to maximize optical quality. The aperture of the light source was set at the maximum allowable to maximise the depth of field in each of the photographs, with a shutter speed of *ca.*200ms. The colour balance of the camera was modified to enhance contrast to optimise the visibility of the growth lines.

The size of the shell sections and their acetate peel replicas prevented a single digital photomicrograph being taken to visualize the entire growth record at high magnification. It was therefore necessary to construct photomosaics –

montages of multiple digital photomicrographs – to allow the full growth record to be captured at high resolution. Initially the mosaics were constructed by manually aligning the individual photomicrographs using Adobe Photoshop (version 7). However, subsequent software updates (Photoshop CS4 and the Omnimet system) enabled the automation of this process.

2.6 Construction of growth increment series

The incremental growth series in the hinge of all three species were digitally recorded using image analysis software AnalySIS V3.2 and subsequently using Omnimet (version 9,0 rev. 4). The growth increments were measured in the shell hinge as opposed to the main portion of the shell through to the ventral margin as the umbone required far fewer photomicrographs to capture the entire growth record and thus processing time was reduced. The growth series were recorded along the axis of maximum growth (Figure 2 – 8).

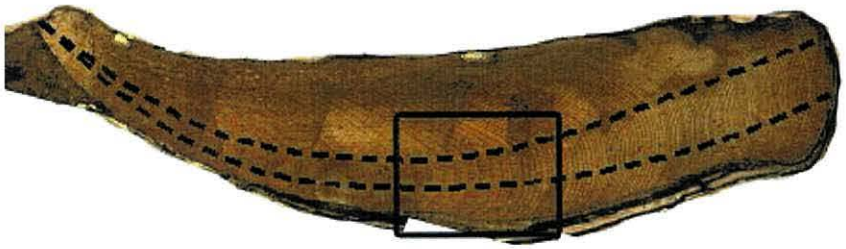

Figure 2 – 8: Photomosaic of an acetate peel replica from the polished and etched section of an embedded Glycymeris glycymeris hinge. The two dashed lines highlight the axes of maximum growth, the desired axis along which the increment widths were measured. The solid black box highlights the area of the acetate peel replica shown in Figure 2 - 9.

The incremental growth series were measured three times in the hinge sections of all species (Figure 2 – 9). The mean of these three growth series was calculated to reduce human observational error associated with slight differences in the line of measurement along the hinge section. The mean growth increment series were then exported as a two column text file, with the corresponding calendar years (arbitrary years if a growth series was from a fossil shell). These files were then imported into SHELLCORR for cross-matching (see chapter 3.2).

Figure 2 – 9: A section of a digital photo-mosaic (position indicated by the black box in figure 2 –8). Three series of growth measurements have been taken from this image, (blue, red and green lines). These series were then used to compile an average growth series for the specimen and it is this average growth series which was used in the SHELLCORR analyses. Scale bar = 200um.

2.7 AMS Radiocarbon sampling

Accelerator mass spectrometer (AMS) radiocarbon (^{14}C) dating is a powerful tool both in constraining and constructing chronologies. Radiocarbon dating allows independent determinations of the age of a shell by determining the relative abundance of ^{14}C within the calcium carbonate. These determinations can range in accuracy from a few years during the post-nuclear bomb testing period (post 1950) to 200 years for the pre-bomb testing period (pre 1950), depending upon the shape of the marine radiocarbon curve (2σ error level).

Calcium carbonate samples (30mg) were taken from strategic positions in the *G. humanus* and the *G. glycymeris* increment chronologies (Table 2 – 3) in order to provide an independent validation of the increment cross-matches between shells (see chapter 3) as well as providing evidence regarding the hypothesis that the growth lines in *G. humanus* and *G. glycymeris* are formed annually.

Species	Shell ID#	No. of Samples Taken	Position of sample taken	Rationale
G. humanus	0003	1	Ventral margin	Constrain the chronology
G. humanus	0013	2	Hinge and ventral margin	Constrain the chronology and test of annual banding hypothesis
G. humanus	0015	1	Hinge	Constrain the chronology
G. humanus	0024	1	Ventral Margin	Constrain the chronology
G. humanus	0046	2	Hinge and ventral margin	Constrain the chronology and test of annual banding hypothesis
G. humanus	0051	2	Hinge and ventral margin	Constrain the chronology and test ofannual banding hypothesis
G. humanus	0054	1	Ventral Margin	Constrain the chronology
G. glycymeris	0020	2	Hinge and ventral margin	Constrain the chronology and test of annual banding hypothesis
G. glycymeris	06004	2	Hinge and ventral margin	Constrain the chronology and test of annual banding hypothesis

Table 2 - 3: Summary of the sampling position and rationale for taking each shell sample for AMS ^{14}C dating.

A total of fourteen radiocarbon determinations were undertaken, four at the AMS dating facility at the Aarhus Radiocarbon Facility, Denmark, and a further ten determinations using the AMS at the NERC Environmental Radiocarbon Facility in East Kilbride, UK, (allocation numbers 1419.1009 and 1330.1008).
The shell samples were either drilled from the cleaned external shell surface, using a dental drill bit or pieces of shell (chips) were broken from the shell valves. The calcium carbonate chips and powder were placed into plastic vials and submitted to the relevant radiocarbon laboratory. The samples were prepared using the standard procedures for calcium carbonates. Samples were weighed and the calcium carbonate powder reacted with orthophosphoric acid to release carbon dioxide (CO_2) and this was then converted to graphite via a zinc/ iron (Zn/ Fe) reduction which was condensed into a pellet ready for loading into the AMS.

2.8 Determining the aragonitic nature of the shell of *Glossus humanus* and *Glycymeris glycymeris*

In order for the oxygen isotopic composition of shell derived calcium carbonate to be used in a palaeotemperature reconstruction, it was first necessary to

establish the form in which the calcium carbonate was present within the shell of both species, *i.e.* one of the two forms of calcium carbonate, aragonite or calcite. These two forms differ in the fractionation/composition of their oxygen isotopes and thus it is necessary to know the composition of the shell in order to correctly convert from $\delta^{18}O$ values into sea water temperature using the correct palaeotemperature equation.

Previous studies have shown that the shell structure of *A. islandica* is 100% aragonite so it was unnecessary to reassess the composition of this species. The crystalline structure of *G. humanus* and *G. glycymeris,* however, have never been examined and thus, prior to these species being used as an archive of palaeotemperature by means of isotopic ratios it was necessary to identify which form of calcium carbonate was present within the shell valves of both these species.

About $20mm^2$ sections of shell material were cut from the ventral margins of individual *G. humanus* and *G. glycymeris*. These shell pieces included portions of both inner and outer shell material and were subject to X-ray diffraction analysis (XRDA) by Dr E. Harper at Cambridge University, UK. Prior to analysis the shell portions were ground into a powder. The XRD determines the crystalline form of calcium carbonate – or any crystalline substance – by producing an x-ray diffraction pattern for the substance. These patterns act as finger prints as each crystal form has a distinct x-ray diffraction pattern. Thus analysis of the XRD plots for the shell samples against known aragonite or calcite XRD plots will identify the crystalline form of the structure.

2.9 Stable isotope sampling

The stable isotopic composition of calcium carbonate shell material is a valuable archive of the environmental conditions (seawater temperature) at the time of shell precipitation. This fact allows the isotopic composition of the shell material to be used as an archive of the environmental conditions throughout the life span of an individual and is largely independent of the growth of the animal, although ontogenetic trends have been found in the $^{12}C:^{13}C$ ratios during the earliest periods of shell growth within *A. islandica (*Butler *et al.,*

2011). The isotopic composition of the calcium carbonate incremental record in the shell valves of *G. humanus* and *G. glycymeris* were examined at ultra high sub-incremental resolution in order to test the hypothesis that the growth lines are formed annually. Additionally a series of shell samples were drilled, one from each increment, from a 28 year growth series in the shell valve of a "long-lived" live collected *G. glycymeris* for comparison with environmental seawater temperatures.

Calcium carbonate samples were drilled using the Merchantek Micromill system at the Iowa State University Department for Geology and Atmospheric Studies Isotope facility, USA. The polished shell resin blocks were mounted onto the stage of a dissecting microscope using thermoplastic glue (figure 2 – 9). The surface of the shell was then photographed and three dimensionally mapped to allow for exact drilling precision. The drilling paths were then mapped onto the shell (see figure 2 – 10).

Figure 2 - 9: An embedded sectioned shell mounted on the stage of the Merchantek micromill ready for drilling.

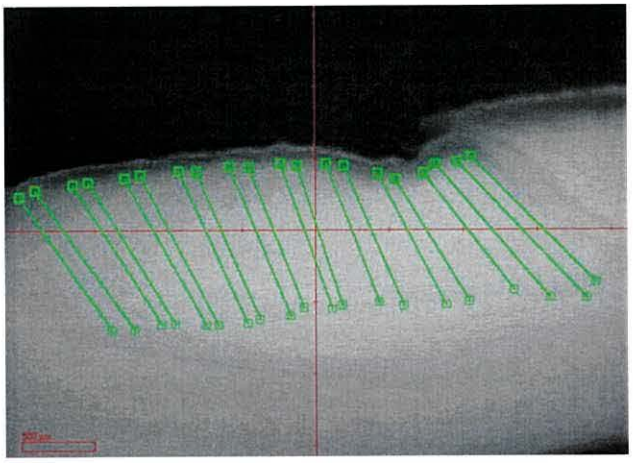

Figure 2 - 10: Reflected light image of the polished embedded G. glycymeris shell surface. The green lines indicate the mapped path along which individual growth increments were micromilled.

Each of the proposed mapped paths could be programmed and individually drilled by altering the drilling speed and drill depth. The increments were drilled to a depth of no more than 1mm and the drilled shell samples were collected using a scalpel blade and a fine brush and placed into small vials. The samples were placed overnight in an oven at 35°C to remove volatiles. The isotopic composition of the samples was determined using a ThermoFinnigan Delta Plus XL mass spectrometer.

2.10 Sources of instrumental data

Meteorological and oceanographic timeseries were obtained for various locations from published sources (Figure 2 – 11 and Table 2 – 4 respectively) together with indices of large scale climatic oscillations (Table 2 – 5). These data were compared with the mean standardized growth series and stable isotopic determinations. The following subsections (2.10.1 and 2.10.2) provide details of each of the meteorological and oceanographic observations and climatic indices respectively.

2.10.1 Oceanographic and meteorological timeseries

Numerous sources of oceanographic and meteorological timeseries were obtained covering a wide geographical area across Western Scotland and the Irish Sea, (Figure 2 – 11). Table 2 – 4 summarises the key information regarding each of these datasets. The oceanographic mooring in the Tiree

Passage is situated in close proximity to both the site within the Tiree Passage from where the *G. glycymeris* were collected, but also the mouth of Loch Sunart and as such may provide representative data for this area. However significant periods of missing data may constrain the use of this data set for providing detailed SSTs and for developing a robust calibration tool for the sclerochronologies. As a result these data were used to assess the reliability of utilising other marine environmental timeseries which cover a larger time period. These analyses are described in Chapter 7.2.

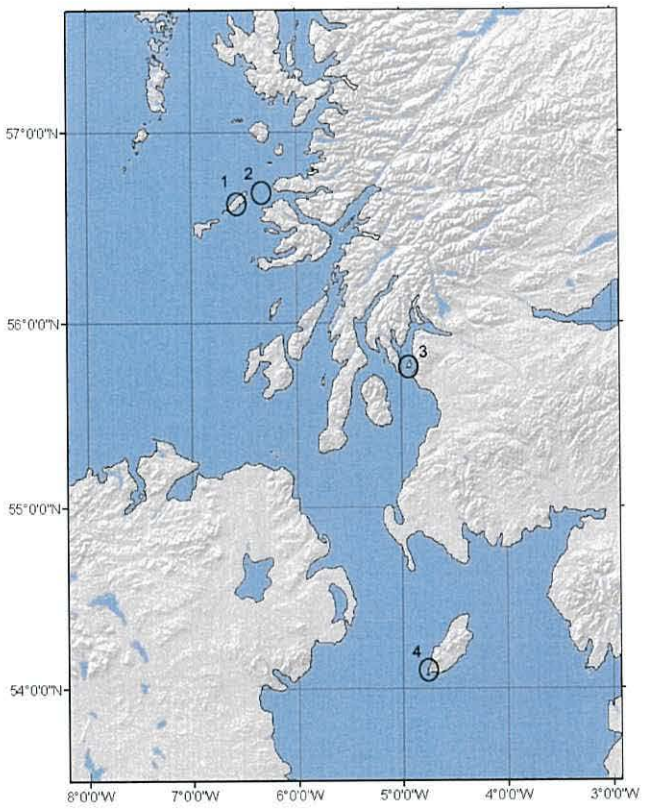

Figure 2 - 11: Location of the instrumental series used in the study. 1) Tiree Airport Meteorological Office Station; 2) Tiree Passage oceanographic mooring; 3) Keppel Pier sea surface temperature series; 4) Isle of Man Cypris and Port Erin Breakwater sea surface temperature timeseries.

Name of Series	Lat. (N)	Long. (W)	Parameter recorded	Temporal resolution	Period	Source
Tiree Airport Met.	56°29	06°52	Air temp. Precipitation	Monthly	1930 - present	UK Met Office
Tiree Passage	56° 37	06° 23	SST	Daily	1975 – 2006*	Inall *et al.*. 2009 / SAMS
Keppel Pier	55°45	04°55	SST	Monthly	1952 – 2006	NFSD/ SAMS
Cypris	54° 05	04° 50	SST, Salinity.	Monthly	1954 – 1992	IOM Gov
Port Erin Breakwater	54° 05	04° 46	SST	Daily	1904 – 2006	IOM Gov.

Table 2 - 4: Details of the meteorological time series examined within this thesis. The positions refer to the map in Figure 2-10. *The Tiree Passage timeseries contains periods of missing data.

2.10.2 Large scale climatic indices

Given the potential climatic sensitivity of the Tiree Passage and Loch Sunart to large scale climatic variability due to their proximity to the eastern fringes of the North Atlantic Current (NAC), timeseries were obtained through the Koninkjk Nederlands Metereologisck Instertuut (KNMI) climate explorer facility. Table 2 – 5 summarises each of the climatic timeseries that were examined either by means of spatial correlation analysis (see Chapter 7.3) or standard dendrochronological data scaling and linear regression methods (Esper *et al.*, 2005).

Series name	Environmental parameter	Spatial resolution	Temporal resolution	Period	Source
CET	Air temperature	NA	Daily/ monthly	1659 - present	Parker *et al.*, 1992/ Met office
HadISST1	SST	1°	Monthly	1870 – present	Rayner *et al.*, 2003 / UK Met office
HadISST2	SST	5°	Monthly	1850 – present	Rayner *et al.*, 2006/ UK Met office
NAO	Atmospheric pressure index	NA	Monthly	1821 – present	Jones *et al.*, 1997/ CRU
AMO	SST index	NA	Monthly	1850 - present	NOAA derived from HadISST2

Table 2 - 5: Details of the gridded time series and climate indices used for comparison with the sclerochronologies. CET = Central England Temperature series, NAO = North Atlantic oscillation and AMO = Atlantic multi-decadal oscillation.

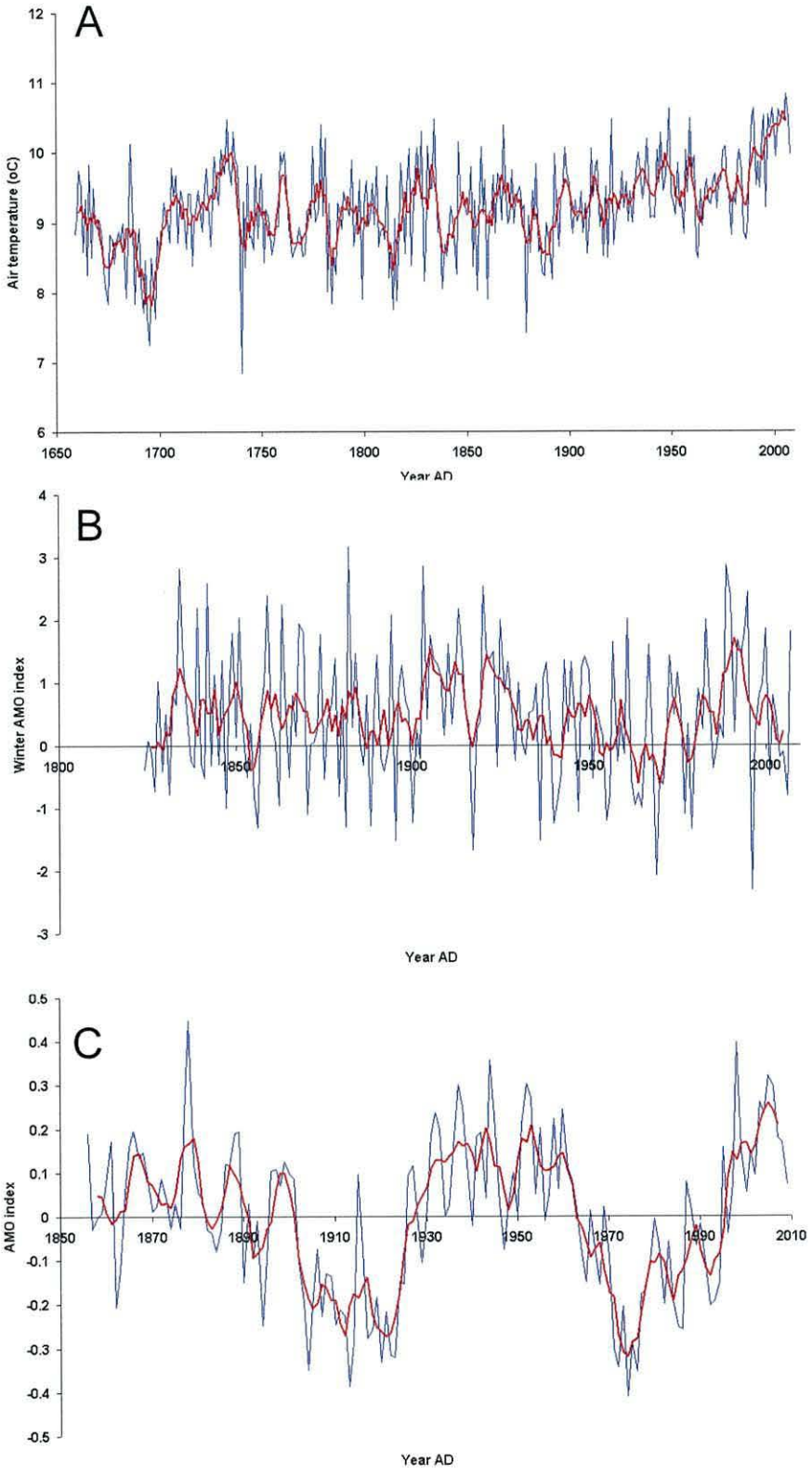

Figure 2 – 12: A) Central England temperature series (CET); B) Winter North Atlantic Oscillation index (NAO); and C) Atlantic multi-decadal oscillation (AMO). Blue lines denote annual or seasonal (winter NAO) data whilst the red lines display the 5 year running mean.

Figure 2 – 12 displays the high resolution (blue lines) and low pass filtered (5 year running mean), (red lines) North Atlantic Oscillation (NAO) index, Atlantic Multi-decadal Oscillation (AMO) index and Central England Temperature series (CET). The following paragraphs briefly describe each of the climate indices as well as the HadISST1. HadISST2 and CRU TS3 series. The North Atlantic Oscillation (NAO) index, first defined by Walter and Bliss, (1932), is generally recorded as a sea level pressure gradient between Iceland and the Azores (Cullen *et al.*, 2001). Hurrel (1995 and references therein) identified the NAO as one of the dominant modes of climate variability within the Northern Hemisphere accounting for 32% of variability within winter temperatures and ca.30% SLP (Sea Level Pressure) variability during the second half of the twentieth century.

The Atlantic Multi-decadal Oscillation (AMO) is an index of mid to low frequency variability within the Atlantic system linked with SSTs (Tourre *et al.*, 2010) and the thermohaline circulation (Zhang, 2007). It has been shown that the AMO can account for variability within hemispheric and global weather systems (Zhang and Delworth, 2006). The Central England Temperature series (CET) was originally presented as a mean monthly timeseries from AD1659 (Manley, 1974) and was later updated to mean daily from AD 1772 (Parker, 1992). This data set represents the longest continual series of direct climate observations in existence. The area represented within the CET is a triangular region covering middle England broadly from London in the East, Bristol in the West and Manchester in the north west. The HadISST1 and HadISST2 are global gridded SST timeseries at 0.5^{o} and 1^{o} from AD1871 and 1850 to present day respectively (Rayner *et al.*, 2003, 2006). These data were obtained through the KNMI Climate Explorer online utility for spatial analysis or were downloaded to construct climate indices for inclusion in temporal correlation analyses.

Chapter 3

Statistical Methods

3.1 Introduction

This chapter details the statistical methods used for the analysis and interrogation of the growth increment records constructed in Chapter two. This involves high-pass detrending for cross-matching to allow each increment to be absolutely positioned in time, as well as the detrending process for chronology construction. Methods for chronology "quality assurance" are also outlined. All three species examined were treated identically unless otherwise stated.

3.2 Raw Growth Series Analysis

Similarl to dendrochronological archives, sclerochronological archives such as *A. islandica* exhibit strong ontogenetic growth trends such as that shown in Figure 3 - 1A. The average rate of shell growth during the juvenile life phase is significantly greater than that during the mature and senile life phases, as is the inter-annual variability in growth (Figure 3 - 1B) which is calculated by first differencing the raw increment widths using the following equation:

Equ. 3.1 $$\delta W = W_Y - W_{Y-1}$$

where W_y and W_{y-1} are increment widths in successive years

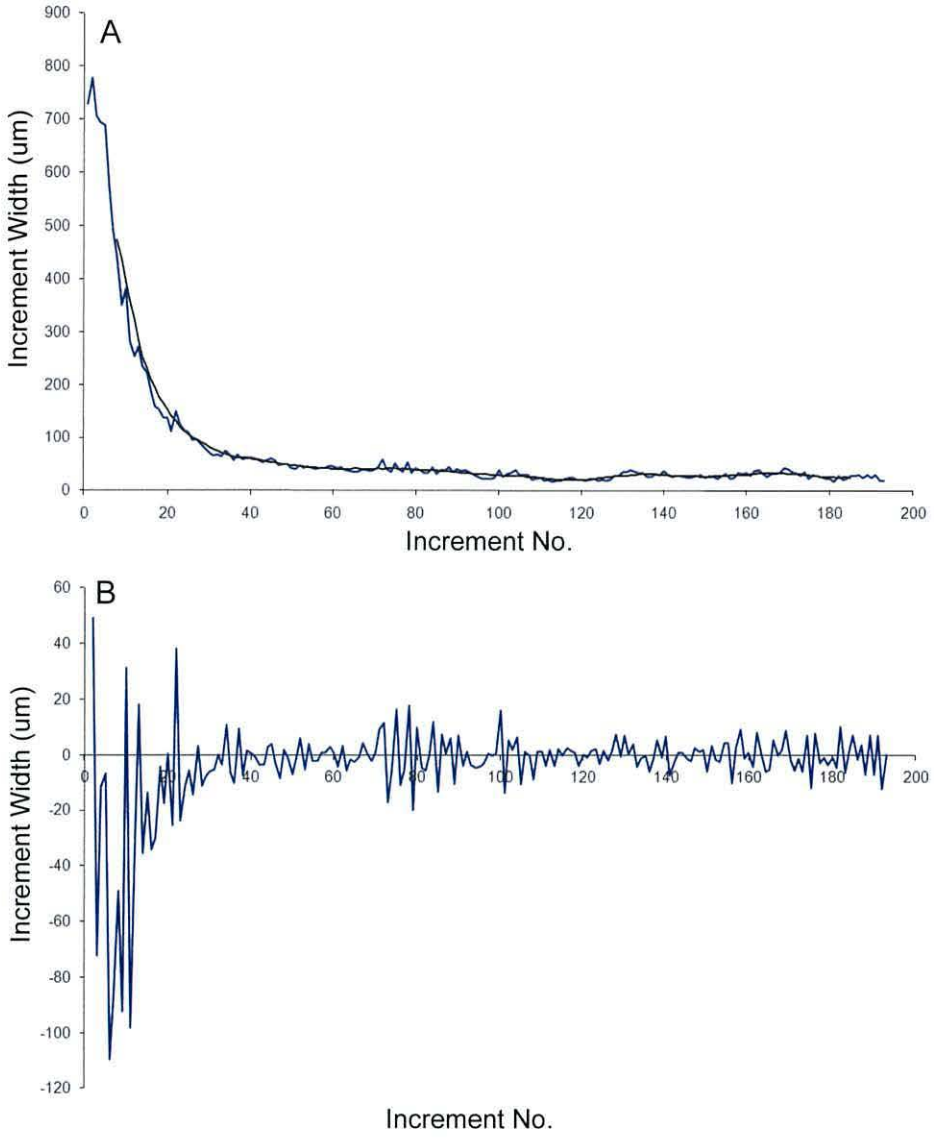

Figure 3 - 1: A) Generalised representation of average raw growth increment widths (blue line) for a long-lived, large, sub-tidal marine bivalve mollusc fitted with a 15year moving average (black line) and B) the corresponding inter-annual variability calculated by first differencing the raw growth series. Data derived from the mean growth increments of twenty G. glycymeris, G. humanus and A. islandica.

Such ontogenetic growth traits hinder the identification of any growth variability that may be of an external environmental nature. In order to construct robust sclerochronologies, statistical methods have to be employed to remove these ontogenetic effects. Recent sclerochronological studies have demonstrated that methods derived from dendrochronology can successfully facilitate the removal of such ontogenetic trends and allow the construction of statistically robust sclerochronologies. The following sections (3.3 and 3.4) provide a detailed

outline of the methods used within this thesis for cross-matching (cross-dating) incremental growth series and constructing master sclerochronologies.

.

3.3 Cross-matching

Growth increment series were cross-matched using SHELLCORR, a macro program run within Matlab v13. SHELLCORR is a development of the dendrochronological application COFECHA (Scourse *et al.*, 2006) which allows for the cross comparison of multiple individual growth series generating graphical outputs facilitating the detailed investigation of the growth increment series (Scourse *et al.*, 2006; Butler *et al.*, 2009a)

The growth increment series for individual shells were archived as two column text delimited files (.txt), - year with corresponding increment width. The last complete growth increment was assumed to represent the last complete year of growth. For live collected shells, this meant that the outermost growth increment could be assigned the absolute calendar year corresponding to the year preceding the date of collection and earlier growth increments could then be dated in relation to it. Dead collected specimens were initially dated in the same way, with the last complete increment being assigned the year preceding the collection year.

Flexible splines (smoothing spline, see Cook and Peters 1981) and log transformations were used to allow the comparison of the growth increment series at ultra high to moderate frequencies (Figure 3 – 2), (Scourse *et al.*, 2006). The more flexible splines calculated from a moving average over a smaller window (7-15 years) allowed for the removal of the low, mid and some of the higher frequency growth trends; the resulting residuals highlight the inter-annual fluctuations in growth which may result from changing external environmental conditions. More rigid splines (generally calculated over a 45 year window) were used to examine correlations between growth increment series over broader temporal frequencies, incorporating both mid and high frequency growth trends (Figures 3 – 3 and 3 – 4).

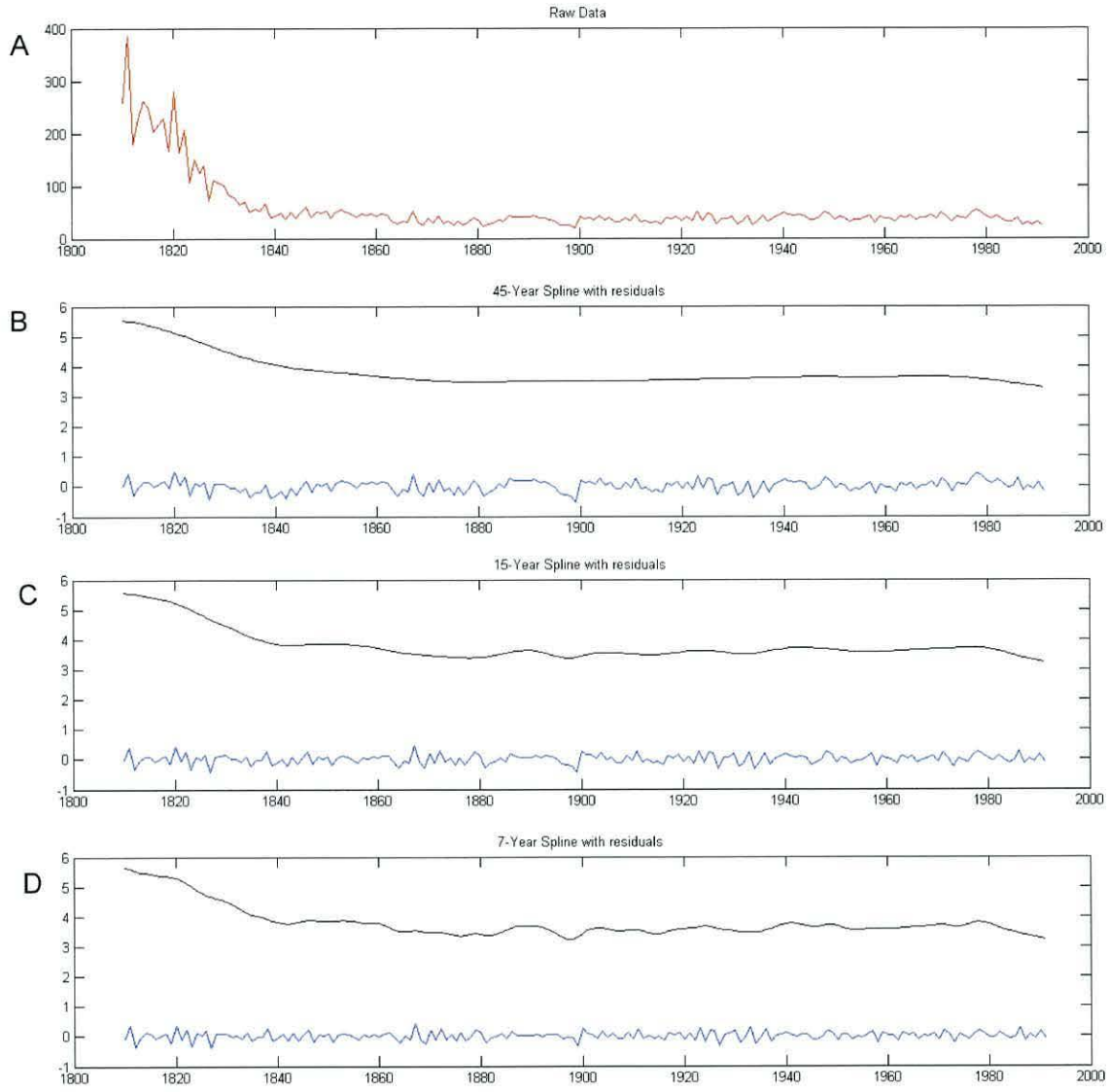

Figure 3 – 2: Diagrams showing the effect of using different length splines (splines shown as black lines) in detrending a a raw increment growth series. A) The raw growth increment series derived from G. glycymeris 00020; B – D) the raw growth increment series detrended with a 45, 15 and 7 year spline respectively (blue lines).

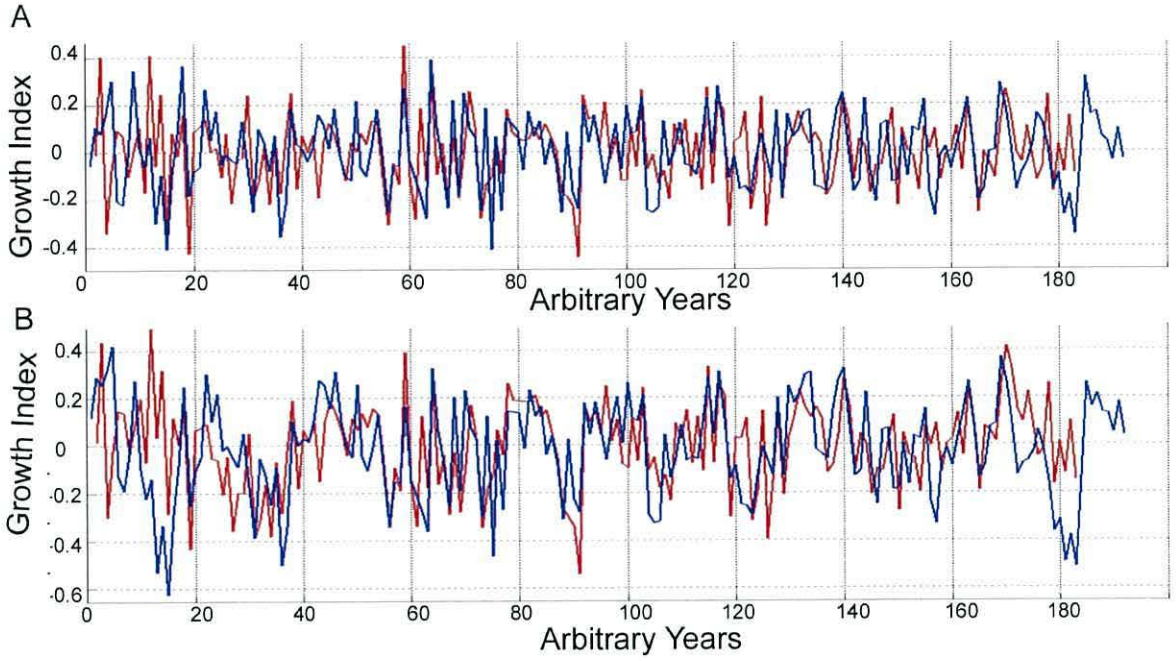

Figure 3 – 3: A) Matlab SHELLCORR outputs showing the detrended growth increment series of two cross-matched shells using a log function and A) a 15 year spline to remove the mid and low frequency trends and B) a 45 year spline to preserve the mid frequency trends.

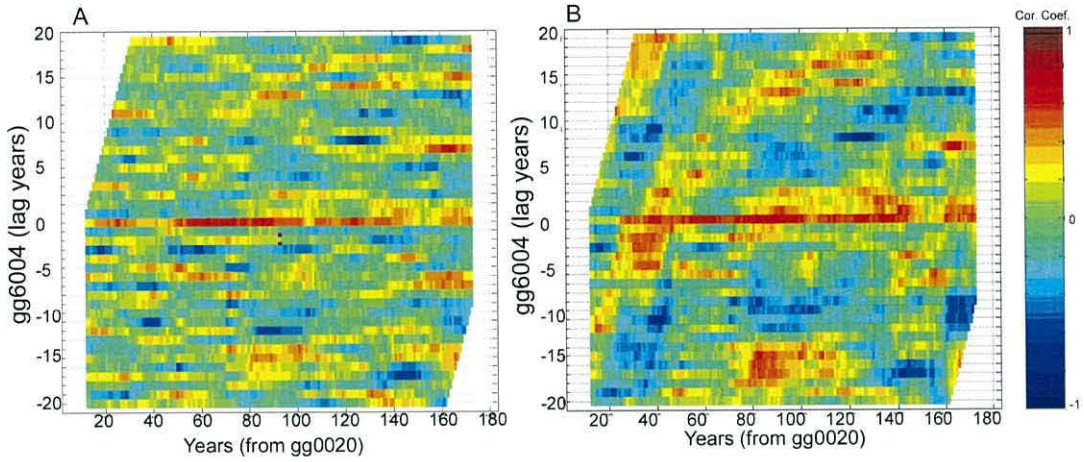

Figure 3 - 4: Matlab SHELLCORR outputs showing 21-year running correlations between the growth increment series of shells gg0020 and gg06004, at yearly lag offsets from +20 to -20 years, which have been detrended using A) a 15 year spline and B) a 45 year spline.

The graphical SHELLCORR outputs (Figure 3 - 5) were interrogated to correct any shifts/jumps in temporal lags between the growth increment series caused by the incorporation of spurious non-annual lines or the exclusion of faint or missing annual lines (*cf.* Scourse *et al.*, 2006). Comparison of the SHELLCORR

outputs generated from the growth increment series of multiple shells (>3) allowed the identification of error; a series with an error will always contain a jump in the temporal lag when compared with multiple growth series not containing any errors. The SHELLCORR outputs of the correlations between two shells which have been correctly aged and aligned will show no jumps or offset in temporal lag, thus comparison of three or more shells allows for the shell with the error to be identified. Once the position of the spurious or missing increment had been identified, the digital photomosaics of all the shells could be re-examined to determine the most appropriate re-interpretation.

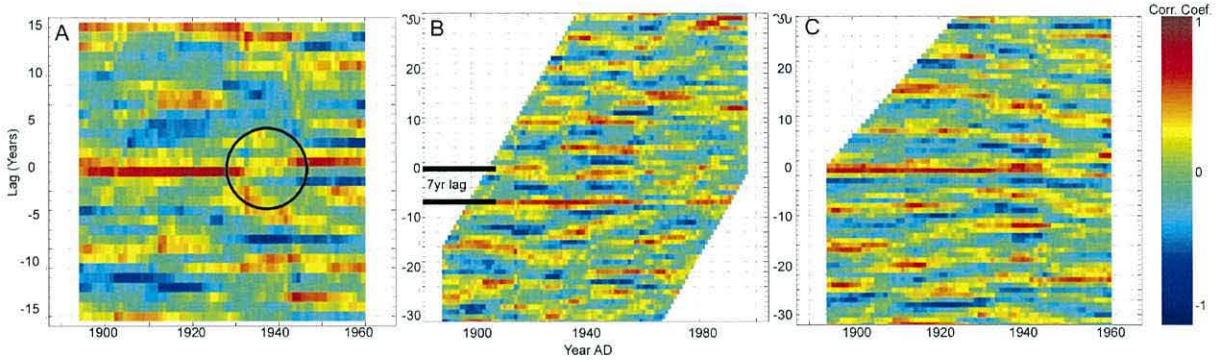

Figure 3 – 5: Matlab SHELLCORR outputs of the 21-year running correlation coefficients between two shell series illustrating A) a shift in positive correlations (highlighted within the black circle) caused by a mis-match in the identification of growth lines; B) the use of the correlation plots to identify temporal lags between individual series allowing for the shells to be aligned and C) correctly aligned growth increment series.

3.4 – Construction of master sclerochronologies using ARSTAN

The master sclerochronologies – mean standardized growth indices (MSGI) – were constructed using the dendrochronological application ARSTAN for Windows (Cook and Krusic, 2007). ARSTAN enables a variety of dendrochronological transformations (such as adaptive power transformation) and detrending methods (linear, negative exponential) to be applied to the growth increment series before the MSGI is produced.

All the correctly dated (by cross-matching) raw growth increment series, stored as two column text delimited (.txt) files, were composited into a single compact (.CMP) formatted file using the FMT executable – supplied through the

dendrochronological program library (www.ltrr.arizona.edu). The CMP formatted file retains the raw increment growth series with corresponding years. Using ARSTAN, an adaptive power transformation was initially applied to all the raw increment series to compensate for the ontogenetic trend in variance (Cook and Peters, 1997) and a negative exponential function was used to remove the trend in the mean. Negative exponential detrending was selected as it is commonly used in the construction of sclerochronologies and dendrochronologies (e.g. Scourse *et al.*, 2006, Butler *et al.*, 2009a). Regional curve standardisation (RCS), a detrending curve generated from the mean ontogenetic growth of a single species (Briffa *et al.*, 1992), was not deemed suitable as it requires large sample sizes over a wide temporal range, the number of suitable *G. humanus and G. glycymeris* collected therefore precludes the use of RCS detrending. The growth increment series were then exported from Arstan both as MSGIs and individual detrended growth increment series (Cook and Krusic, 2007).

3.5 Chronology quality assurance

Assessing the statistical significance of any chronology is a critical step if the chronology is to be used as part of any palaeoenvironmental study. Identifying and understanding any caveats which are associated with the master chronology is critical in developing the chronology as a palaeoenvironmental archive. The method predominantly used within dendrochronology is the expressed population signal, (EPS) which can be calculated using equation 3.2 (Wigley *et al.*, 1984).

Equ. 3.2

$$EPS = \frac{n.\bar{r}}{n.\bar{r} + (1 - \bar{r})}$$

where $\bar{r}$ signifies the mean correlation between the series over the period of interest and n is the sample depth over the same period. The EPS can be referred to as the expressed common signal to noise ratio, and represents the degree to which the sample of shells in the chronology is expressing the common signal of the whole population. Wigley *et al.*, (1984) set the widely

used guideline that a chronology with an EPS of ≥0.85 would suggest that the shells indicated within the chronology represent the wider population.

The rearranged EPS equation (Equ. 3.3, Wilson & Elling, 2004), was used to estimate the sample depth required to achieve the recommended EPS, given the mean correlation between growth increment series.

Equ. 3.3

$$N = \frac{(\bar{r}\text{-}1)\ EPS}{\bar{r}\ (EPS - 1)}$$

where $\bar{r}$ is the mean Pearson correlation coefficient of the shells included within the chronology and *EPS* represents the target EPS level.

3.6 Climate reconstruction

Both the spatial extent and temporal stability of correlations between the master sclerochronologies and environmental parameters were analysed. The spatial analysis utility within the Koninkjk Nederlands Metereologisck Instituut (KNMI) Climate Explorer facility (http://climexp.knmi.nl/) was used to assess the spatial extent of the correlations between the mean standardised chronologies and the gridded spatial environmental parameter timeseries including the HadISST1 sea surface temperature series (SST) and the CRU TS3 air temperature and precipitation record. The KNMI spatial analysis utility is a graphical statistical tool which identifies geographical areas of statistical significance (e.g. Figure 3 – 6). The spatial resolution of these outputs is defined by the spatial resolution of the input environmental dataset. As the utility is purely a graphical qualitative tool for the identification of correlations, further temporal analysis and calibration of the proxy to the target parameter are required.

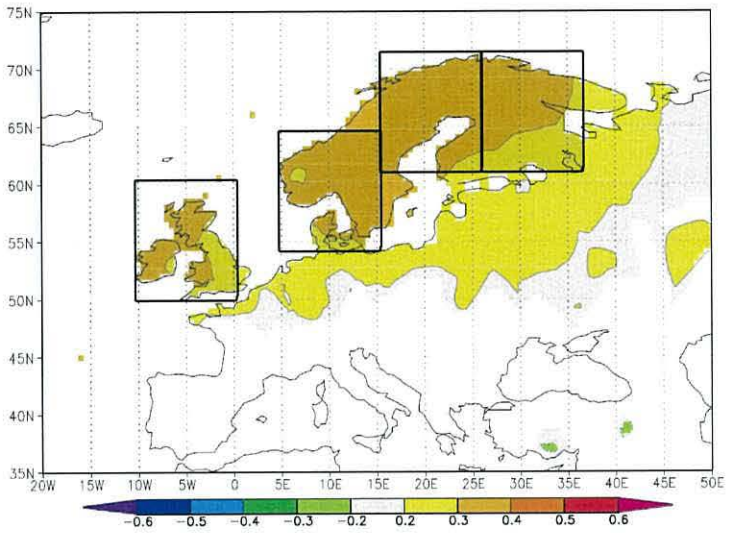

Figure 3 – 6: an example of a spatial correlation plot between a mean standardised chronology and mean land air temperatures. The black boxes represent the defined areas for which timeseries of environmental parameters were acquired through the KNMI climate explorer facility. White regions contain correlations of ca. zero.

Composite environmental parameter series were constructed from the monthly resolved target environmental parameters through the KNMI facility. The KNMI facility allows the acquisition of environmental timeseries over customisable geographical areas. Multiple larger sub-grid boxes were used to define complex areas to allow for the data from the widest area to be downloaded and incorporated. The resolution of these sub grid boxes was constrained by the complexity of the area, but generally they were $10^{\circ}x10^{\circ}$ in resolution. The resulting timeseries for each of the sub-grid boxes was then combined by averaging each of the mean monthly timeseries individually to retain the monthly temporal resolution. The resulting composite time series could then be examined using standard temporal dendrochronological statistics.

3.7 Proxy calibration

The master sclerochronologies were calibrated to the target environmental parameters using the widely used calibration verification methods (Fritts, 1976). The calibration-verification approach splits the target environmental series into two independent time series. One half is used to calibrate the proxy whilst the second half, which is independent of the calibration process, is used to verify that the calibration is statistically robust.

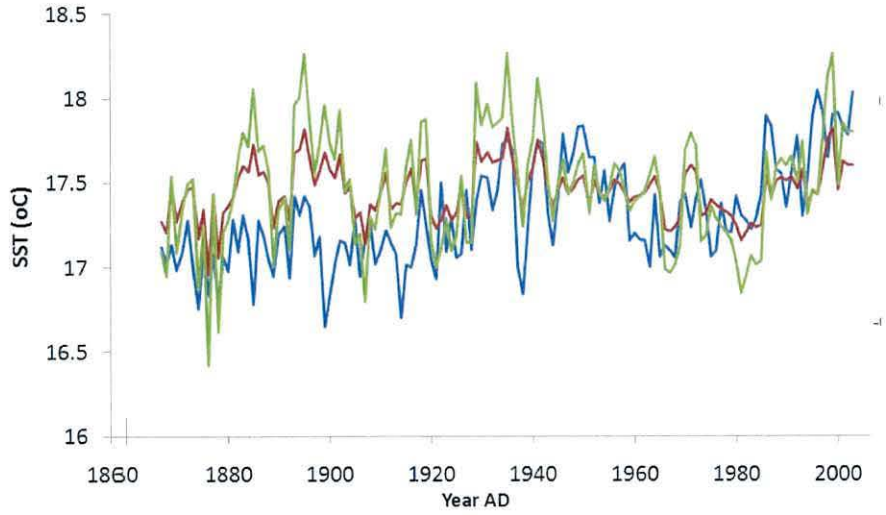

Figure 3 – 7: Comparison of two SST reconstructions from the same proxy using (green line) data scaling and (red line) linear regression methods. The blue line shows the target instrumental data.

Reconstructions can be implemented using two primary methods which can usefully be compared – data scaling and linear regression. Figure 3 – 7 illustrates two reconstructions that have been constructed from a single proxy using both the linear regression and the data scaling methods of proxy calibration. It is apparent that the variability within the linear regression reconstruction (red line) is significantly reduced by comparison to the data scaled reconstruction (green line). This inherent difference results from the way that the two methods incorporate error. Data scaling involves the homogeneous distribution of the variability – the proxy standard deviation equals that of the target – throughout the proxy reconstruction and this results in periods of over inflated variability within the reconstruction (Esper *et al.*, 2005). The linear regression approach attempts to generate the best fit between the proxy and the target parameter throughout the calibration period. The generation and application of the linear regression model however (Figure 3 – 8) results in the reduction of amplitude of variability caused by multiple growth increments being formed at the same temperature, denoted by the grey circles in Figure 3 – 9. These points will generate an over and under estimate of temperature respectively causing a reduction in the overall amplitude of variability.

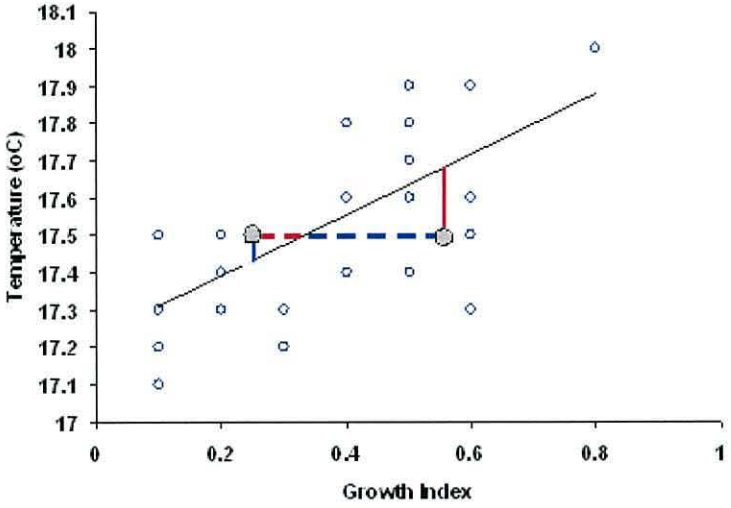

Figure 3 – 8: Linear regression analysis of a hypothetical growth index chronology against a hypothetical temperature timeseries. The black line denotes a statistically significant regression line (r^2 ca. 0.4). The grey circles represent two independent growth increments formed during relatively cooler and warmer years respectively (indicated by solid blue and red lines respectively). The red and blue dashed lines indicate the likely reconstructed values from the linear regression equation.

Data scaling techniques transform the standard deviation and average of the proxy archive to equal that of the target instrumental series using the equation:

Equ. 3.4 $$T(^{o}C) = (g-G)^{*}(\sigma_t/\sigma_p)+I$$

where g represents increment widths of a single year, G represents mean increment widths over the calibration period; σ_t represents the standard deviation of the target parameter over the calibration period, σ_p represents the standard deviation of the growth increment widths over the calibration period and I represents the mean value of the target parameter over the calibration period. The data scaling approach, while accurately representing the mean and standard deviation, tends to be less precise overall.

3.8 Assessment of reconstruction error

Various methods have been utilised within the published dendrochronological and sclerochronological communities to quantify the degree of error within palaeotemperature reconstructions derived from increment width chronologies,

including general statistical approaches such as mean squared error (MSE, Equ. 3.5):

Equ. 3.5 $$MSE(\check{Y}) = \frac{1}{n}\Sigma(Y_t - \check{Y}_t)^2$$

where Y_t represents the target parameter and $\check{Y}_t$ denotes the proxy values respectively at year t; n corresponds to the number of years being analysed. This approach was used rather than percentage error (Schöne *et al.*, 2005), as the percentage error approach can cause a biased result. Such a bias would be generated within reconstructions with mean values close to zero; for example a 0.25°C error on a value of 3°C (8.3% error) is significantly larger than the same 0.25°C error on a value of 25°C (1%).

3.9 Reconstruction precision

Standard dendrochronological methods were used to assess the precision and skill of each proxy reconstruction over the respective calibration and verification periods. Three statistical approaches were applied, reduction of error statistics (RE, Equ. 3.6) coefficient of efficiency (CE, Equ. 3.7) and correlation coefficients (r and r^2, Equ. 3.8) (Fritts, 1976):

Equ. 3.6 $$RE = 1 - \frac{MSE(\check{Y})}{MSE(Y_c)}$$

where $MSE(\overline{Y}_c)$ denotes an "unreal" estimate error based on a linear reconstruction derived from the target mean calculated over the calibration period.

Equ. 3.7 $$CE = 1 - \frac{MSE(\check{Y})}{MSE(Y_i)}$$

where $MSE(\overline{Y}_i)$ denotes an "unreal" estimate error based on a linear reconstruction derived from the target mean calculated over the period of interest/verification period.

Equ. 3.8

$$r^2 = \frac{[\Sigma (Y_t - \overline{Y_i})(\check{y} - \overline{\check{y}})]^2}{\Sigma (Y_t - \overline{Y_i})^2 (\check{y} - \overline{\check{y}})^2}$$

where Y_t represents the target parameter and $\check{y}_t$ denotes the proxy values respectively at year t.

Reduction of error and coefficient of efficiency statistics compare the mean squared error (MSE) of the proxy reconstruction to the MSE of a fictional linear reconstruction based on the mean target parameter value over the calibration and verification periods respectively. As the RE and CE statistics are based on reconstructions of separate linear mean reconstructions, they essentially test the predictive skill of the proxy reconstruction to detect a shift in the mean value of the target parameter between the calibration and the verification period. Reduction of error and coefficient of efficiency values can range from negative infinity to one, with significant values being greater than zero.

A multi-statistical approach is necessary because the RE and CE statistics are more sensitive to mid and low frequency fluctuations within the data sets whilst the correlation coefficients are more senitive to high frequency changes within each dataset. As such it is possible for a proxy timeseries to have insignificant RE and CE statistics despite having an r value of one (red line in Figure 3 – 9). Similarly it is possible for a proxy timeseries to have statistically significant RE and CE statistics yet not reflect the highest frequency fluctuations within the target series (Black line in Figure 3 – 9).

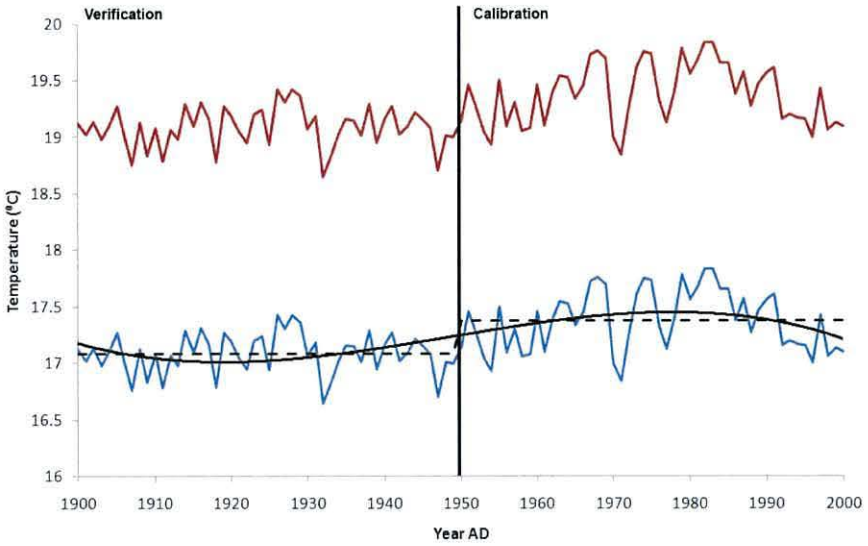

Figure 3 – 9: Blue line) Hypotheticval temperature timeseries over the period AD 1900-2000. Red and black lines) Fictional proxy timeseries. Dashed black line) mean value of fictional temperature data over the calibration and verification periods. (Figure adapted from NRC, 2006).

Chapter 4

Biological and Chronological Results

4.1 Introduction

This chapter provides the results of 1) the sampling efforts by means of diving and mechanical dredge; 2) the biometrics of the samples collected with analysis of the growth increments of each of the three species; 3) growth and longevity within each of the species; and 4) cross-matching within each of the species and the construction of the master sclerochronologies.

4.2 Collection data

Table 4 – 1 details the number of shells obtained using the mechanical dredge during the 2006 *Prince Madog* cruise to Loch Sunart and surrounding environment. In total four of the five sites sampled yielded shell material. *Glycymeris glycymeris* were collected in large numbers from the Tiree Passage (TP) but were absent at all of the other sites sampled. The site within Salen Bay yielded the only live *A. islandica*, in addition to three dead specimens. Six live clams were collected in total, four *G. glycymeris* from the Tiree Passage and two *A. islandica*, which could potentially be used to provide an absolutely dated anchor for a master sclerochronology. Of the three sites where both *A. islandica* and *G. humanus* were obtained, (SB, SM and MD) each site showed a bias towards one of the species, with SM and SB yielding greater numbers of *G. humanus* whilst MD yielded a greater proportion of *A. islandica*. None of the three target species were obtained from the Mourvern site (M).

Due to the deficiency of live-collected shell material further collections were undertaken utilising the NERC Facility for Scientific Diving (NFSD allocation number NFSD/09/01). Depth constraints due to diving protocols required minor

modification of the sampling positions to areas adjacent to the dredging locations within the divers' depth range. Moderate numbers of *A. islandica* were obtained from four of the sites sampled by the NFSD team (Table 4 – 2). Only one live *G. humanus* was found by the divers, but additional specimens, obtained as bycatch in the Sound of Sleat by a local *Nephrops* trawler, were donated to this study (station SS).

Station	Latitude			Longitude			Numbers of Shells collected		
							Live	Dead, single valves	Dead, paired
SB	56°	42.00	N	5°	45.50	W	2 Ai	3 Ai, 20 Gh	1 Ai
SM	56°	40.50	N	6°	0.25	W	-	1 Ai, 19 Gh	3 Gh
M	56°	39.35	N	5°	58.00	W	-	-	-
TP	56°	37.75	N	6°	24.00	W	4 Gg	133 Gg	3 Gg
MD	56°	40.00	N	5°	52.00	W	-	59 Ai, 28 Gh	2 Ai, 1 Gh
					Totals		**2 Ai, 4 Gg**	**63 Ai, 67 Gh, 133 Gg**	**3 Ai, 4 Gh, 3 Gg**

Table 4 – 1: Details of the number of shells collected from each of the sites dredged during the 2006 Prince Madog cruise to Loch Sunart. A. islandica (Ai), G. humanus (Gh) and G. glycymeris (Gg) specimens collected.

Station	Latitude			Longitude			Number of live shells collected	
							Arctica islandica	*Glossus humanus*
SUN01	56°	41.712	N	5°	46.115	W	16	0
SUN02	56°	40.703	N	6°	59.657	W	3	1
SUN03	56°	39.919	N	5°	52.066	W	5	0
SUN04	56°	41.042	N	6°	40.501	W	15	0
SS*	57°	7.011'	N	5°	46.012'	W	0	13
					Totals		**39**	**14**

Table 4 – 2: Details of shells collected live by the NERC Factility for Scientific Diving (SUN01 – SUN 04) and as bycatch from a Nephrops trawler within the Sound of Sleat (SS). *Exact co-ordinates within the Sound of Sleat are unknown.

4.3 Biometrics

Biometrics of all the shells used in this thesis were digitally measured and recorded (±0.1mm and ±0.01g precision). Table 4 – 3 summarises of the mean shell length, height, maximum height and shell mass, (see Figure 2 – 4 in Chapter 2.2) for each species.

Species	Length (mm)	Height (mm)	Max Height (mm)	Width (mm)	Mass (g)
A. islandica	59.7 *(18.4)*	51.3 *(15.7)*	55.7 *(17.9)*	18.0 *(5.7)*	20.0 *(20.2)*
G. humanus	68.2 *(10.8)*	73.8 *(9.9)*	73.4 *(12.7)*	29.6 *(5.9)*	26.7 *(12.5)*
G. glycymeris	57.6 *(7.7)*	57.0 *(8.2)*	57.7 *(8.7)*	18.6 *(5.1)*	26.4 *(8.1)*

Table 4 - 3; Average shell length, height, maximum height, width and mass (with standard deviations) of the A. islandica, G. humanus and G. glycymeris examined.

The percentage size class distribution for each of the three species (Figure 4 – 2) indicates key differences within the size class distribution (shell length and maximum height) of the dead- and live-collected shell valves. The *G. humanus* size class distributions, for both shell length and shell height, are normally distributed. The *G. glycymeris* appears to be positively skewed towards the larger size classes, this is likely due to a selection bias within the sampling. The *A. islandica* size class distribution (Figure 4 – 2C) shows a bimodal distribution with peaks in maximum shell height and length (45-50mm and 75-80mm).

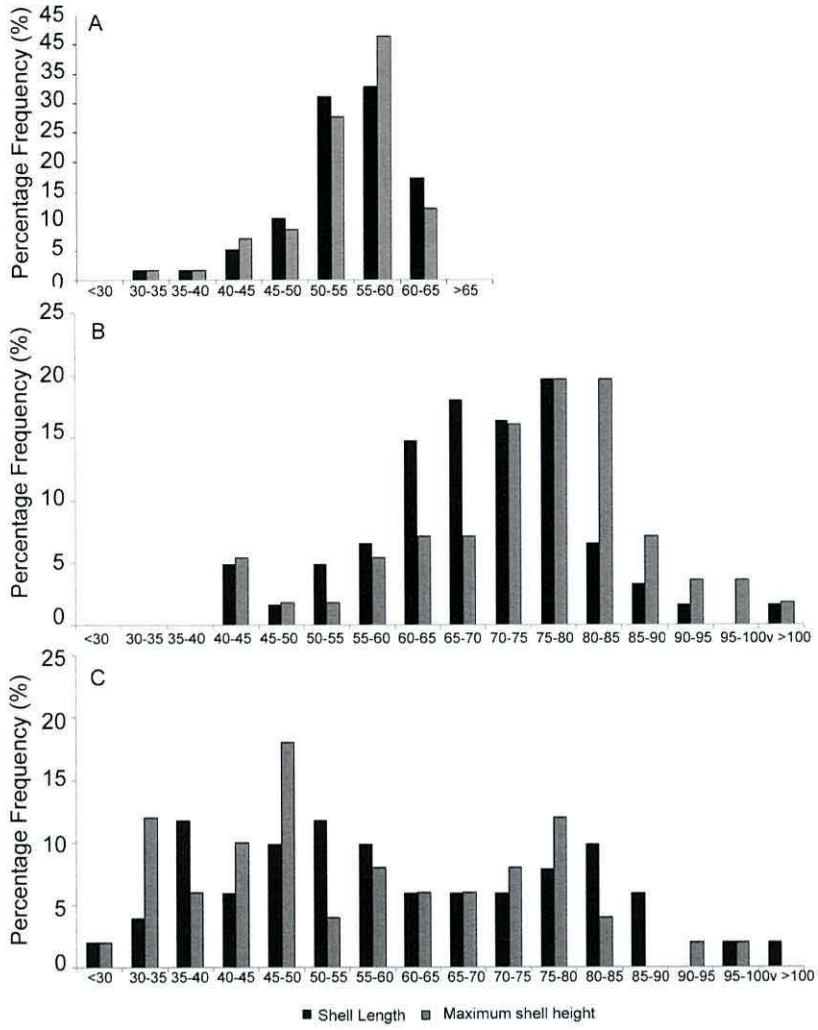

Figure 4 – 2; Percentage size frequency distributions of the shell length (dark grey) and maximum shell height (light grey) of A) G. glycymeris, B) G. humanus and C) A. islandica collected by the mechanical dredge in 2006 from the four principle sites examined in this thesis.

Linear regression analysis of the natural log of the shell length versus the natural log of shell height (Figure 4 – 3) identifies significant linear trends for all three species.

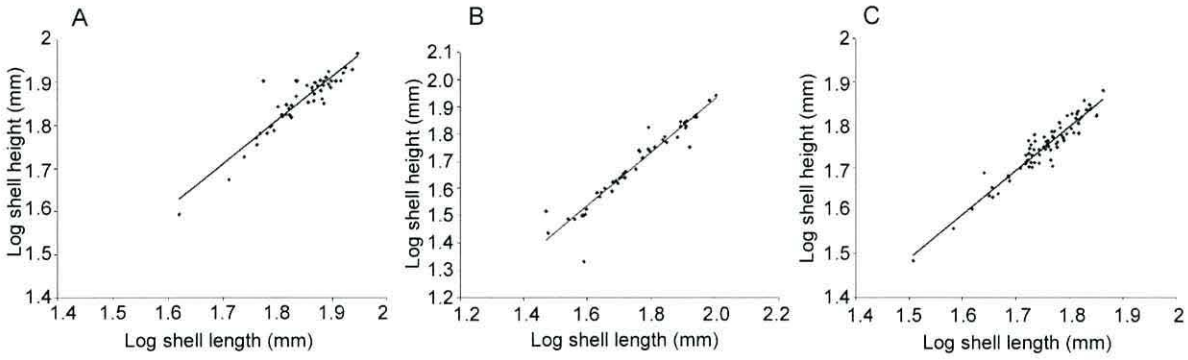

Figure 4 – 3; Linear regression analysis between the natural log of shell length and natural log of shell height for A) G. humanus (H= 1.014L-0.131, n= 49, r=0.913 and P<0.0001), B) A. islandica (H= 0.9746L-0.0225, n= 49, r=0.956 and P<0.0001) and C) G. glycymeris (H= 1.0209L-0.0421, n= 79, r=0.952 and P<0.0001), where H represents the log of shell height and L the log of shell length.

4.4 Growth increment analysis

Acetate peels of etched polished shell sections of all three species yielded reproductions of the internal growth lines suitable for the digital measurement of the growth increment widths. Figure 4 – 4 demonstrates that although growth increments were visible and could be measured in all three species the clarity varied significantly across the species. Figure 4 – 4 shows typical examples of the clarity for all three species with *G. glycymeris* providing the clearest records and *G. humanus* providing significantly poorer records than both *A. islandica* and *G. glycymeris*. The degree of clarity ultimately has an impact on the accuracy of the measurements as well as the speed at which the measurements can be taken.

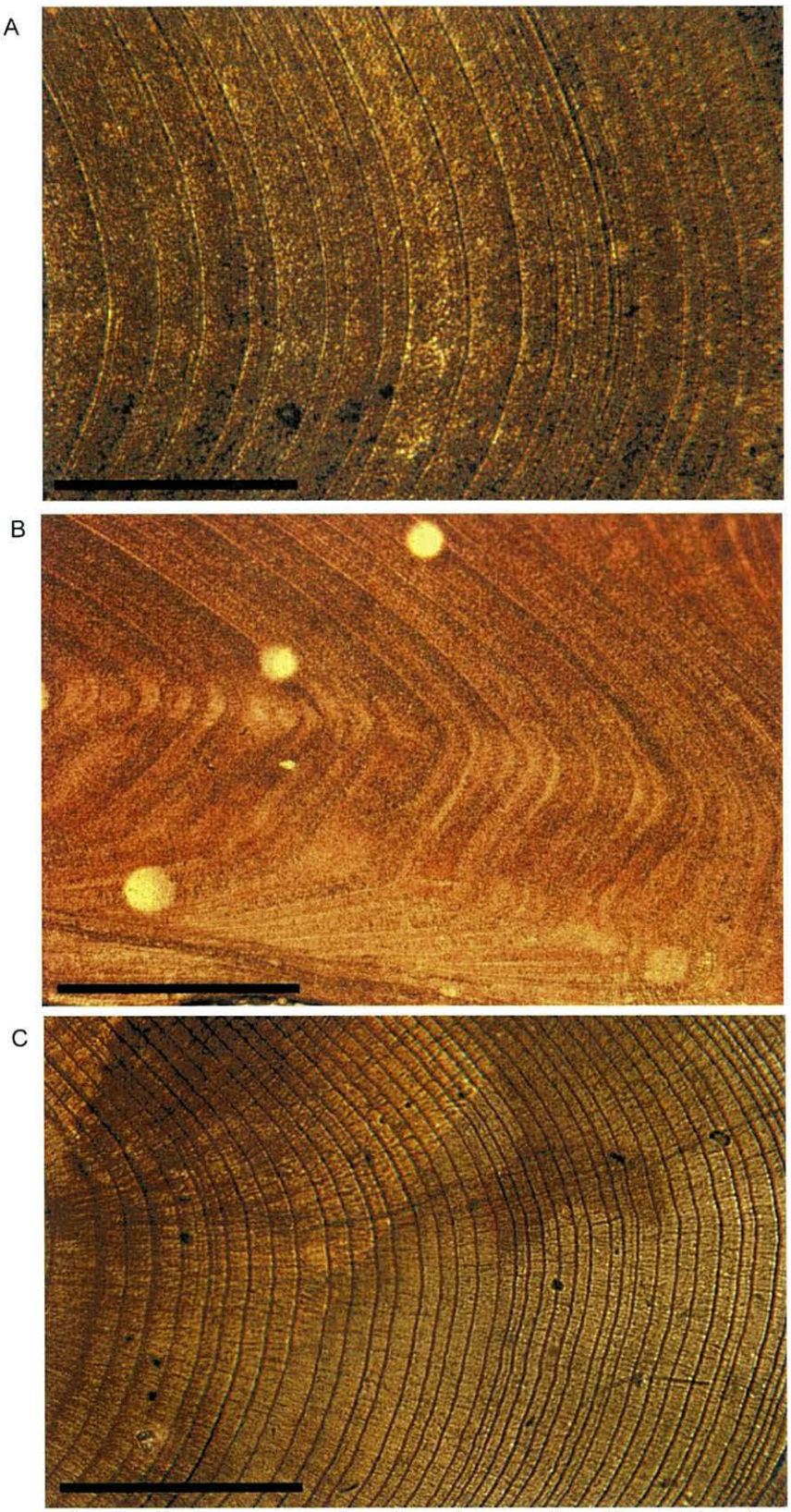

Figure 4 – 4; Photomicrographs of acetate peel replicas taken from the umbone of A) Arctica islandica B) Glossus humanus and C) Glycymeris glycymeris shell valves. Direction of growth in all pictures is from left to right. Scale bars ca.300µm.

4.5 Growth and longevity

The growth increment measurements recorded from the internal growth lines in *G. humanus*, *G. glycymeris* and *A. islandica* shell valves show strong ontogenetic trends in mean, standard deviation and inter-annual variability (Figure 4 – 5).

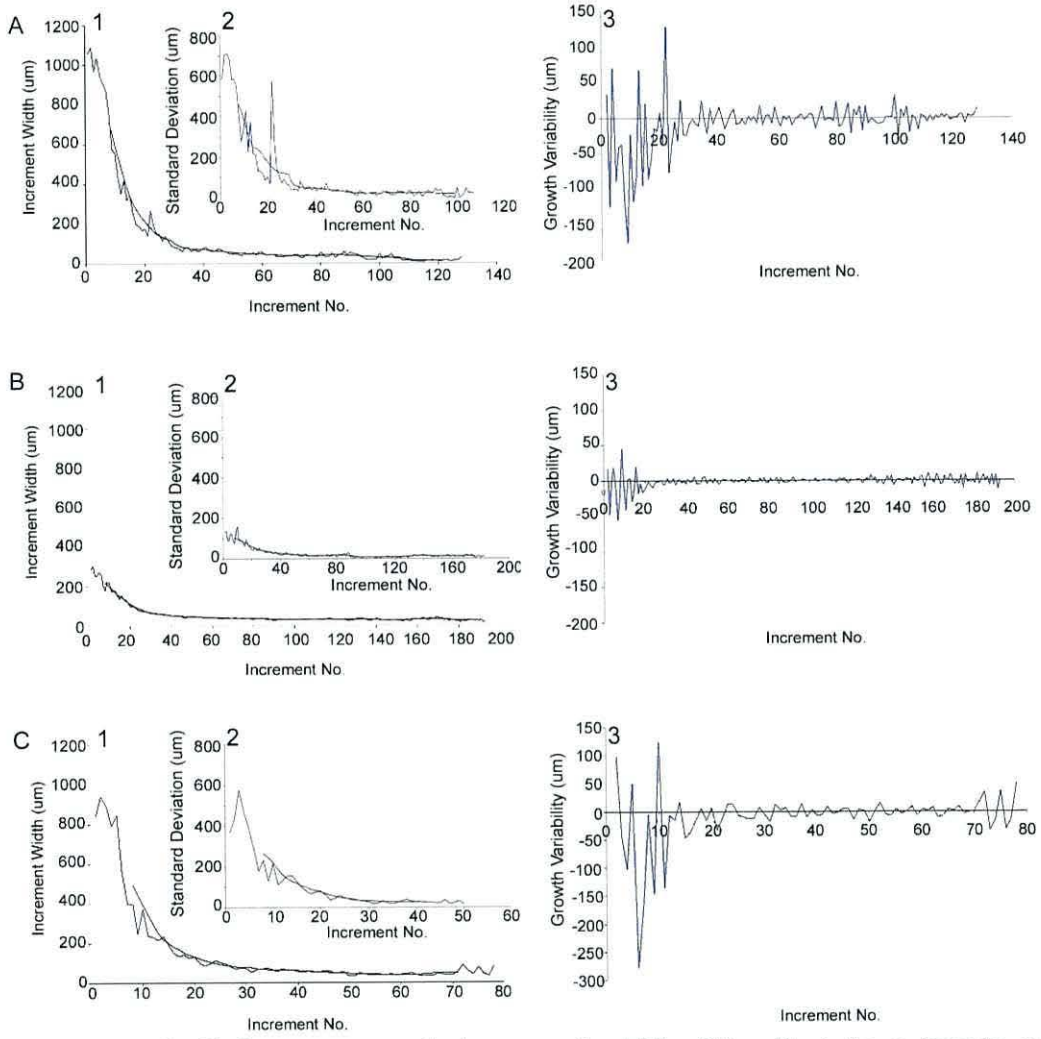

Figure 4 – 5: 1) Average growth increment widths (blue line) from twenty randomly selected specimens for each of the three species A) Arctica islandica B) Glycymeris glycymeris and C) Glossus humanus, fitted with a 15-year moving average (black line). 2) Standard deviation of increment widths across the twenty measured shells (blue line) fitted with 15-year moving average (black line). 3) Average inter-annual variability calculated by means of first differencing.

The ontogenetic trend in the growth increment series resembled that of a negative exponential curve. A rapid decline in the average growth from year to

year over the first 40 growth increments is apparent in all the individuals examined. The magnitude of the slope in the *G. glycymeris* growth curve (Figure 4 – 5.C1) is significantly reduced in comparison with those of *A. islandica* and *G. humanus. Glycymeris glycymeris* also exhibits a reduced amplitude in variance between individuals measured over the first four growth increments in comparison with *A. islandica* and *G. humanus.* The maximum standard deviation between individuals for *G. glycymeris* being <200µm compared to *ca.*600 and 800µm for *G. humanus* and *A. islandica* respectively.

The degree of inter-annual variability within the growth increment series is significant because of its importance for cross-matching. Complacent records – a growth series with little or no inter-annual variability – significantly constrain or prohibit cross-matching which relies on high frequency inter-annual fluctuations in growth. The *G. glycymeris* record shows significantly muted inter-annual variability in comparison with those of *A. islandica* and *G. humanus*.

4.6 Cross-matching

The primary objective of cross-matching was to produce absolutely-dated series from live- and dead-collected shell valves. The initial focus was to produce independent cross-matched series for each of the three species (*G. humanus*, *G. glycymeris* and *A. islandica*). Shells sectioned were selected on the basis of shell size and condition. The largest shells (shell length) with the least degradation of the ventral margin, most intact periostracum and ligament preservation were selected as these shells were likely to yield the greatest longevities. The shell condition criteria increased the likelihood of the shells being contemporary. These criteria were used for the selection of all the dead collected shells examined. The following three subsections (4.5.1 – 4.5.3) detail the results from the cross-matching of each of the three species.

4.6.1 *Glossus humanus*

Of the 43 shells selected for sectioning based on their biometrics and shell condition, 30 contained >40 growth increments, which, for the purposes of cross-matching, was deemed sufficient to produce statistically significant periods of overlap for robust cross-matches. Of these shells only seven growth

series cross-matched with statistically significant Pearson correlation coefficients (Figure 4 – 6). Of these seven shells three originated from the Sound of Mull site and four from Salen Bay. These shells were incorporated into a single master chronology, pending ^{14}C validation, despite the shells being collected at separate sites, due to the relative close proximity of the sites and the apparent statistically significant cross-matches between the respective shell series.

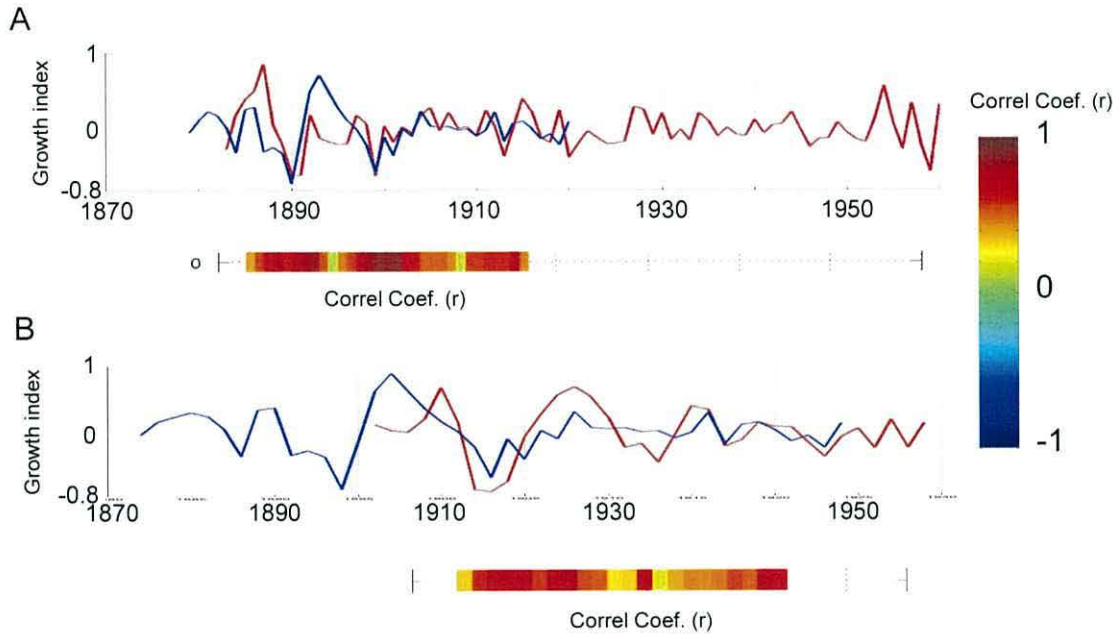

Figure 4 – 6: Matlab SHELLCORR outputs showing the detrended growth series for G. humanus A) 00013 and 00051 and B) 00051 and 00024, which have been cross-matched with corresponding Pearson correlation coefficients shown in a moving window of 15 years.

4.6.2 *Glycymeris glycymeris*

Of the 137 dead collected *G. glycymeris* valves, 75 were severely bored and were therefore considered unlikely to yield usable growth records. The growth increment series of ten out of the 50 dead-collected shells sectioned and aged cross-matched with a statistically robust period of overlap and statistically significant correlation coefficient (Figure 4 – 7). Similarly the growth increment series of the two "long-lived" live-collected *G. glycymeris* significantly cross-matched. While the Pearson correlation coefficients between the dead and the "long-lived" live-collected shells were statistically significant, the length of the overlap period was not sufficient (sufficient length determined using standard

correlation statistics) to allow the cross-match between the live and the dead shells to be reliable without independent validation by means of AMS radiocarbon dating (^{14}C).

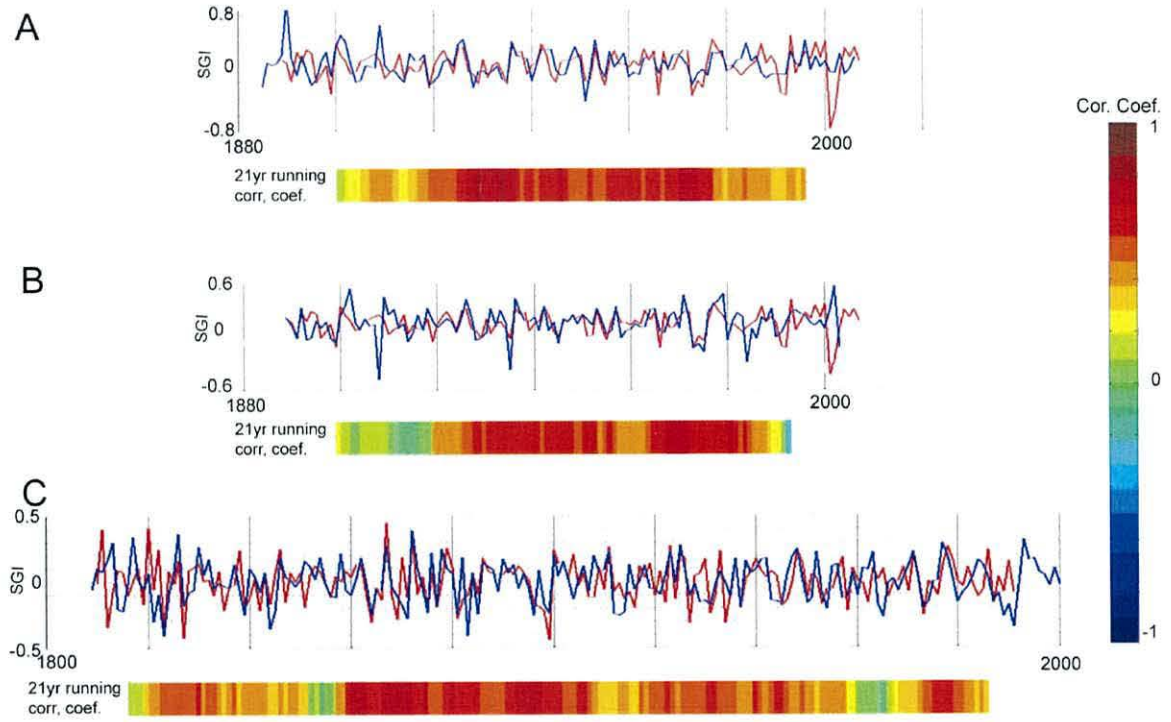

Figure 4 – 7: Matlab SHELLCORR outputs showing the detrended growth series for Glycymeris glycymeris A) 0001 and 0050, B) 0001 and 00008, C) 0020 and 06004, which have been cross-matched, with corresponding Pearson correlation coefficients shown in a moving window of 15 years.

4.6.3 *Arctica islandica*

It was not possible to fully examine all of the *A. islandica* within the scope of this thesis due to time constraints. Therefore in order to provide absolutely dated specimens to compare with the Sound of Mull *G. humanus* sclerochronology and the Tiree Passage *G. glycymeris* sclerochronology, priority was given to cross-matching the *A. islandica* that had been collected from the sites near the mouth of Loch Sunart (See Table 2 – 3 in Chapter 2.2). The growth increment series from the largest live-collected (>60mm shell length) shells were examined using the cross-matching techniques detailed in Chapter 3.3. In total six, of the live-collected *A. islandica were* successfully cross-matched, providing absolutely dated material with which to compare the *G. humanus* and *G.*

glycymeris sclerochronologies constructed from the Sound of Mull and the Tiree Passage respectively.

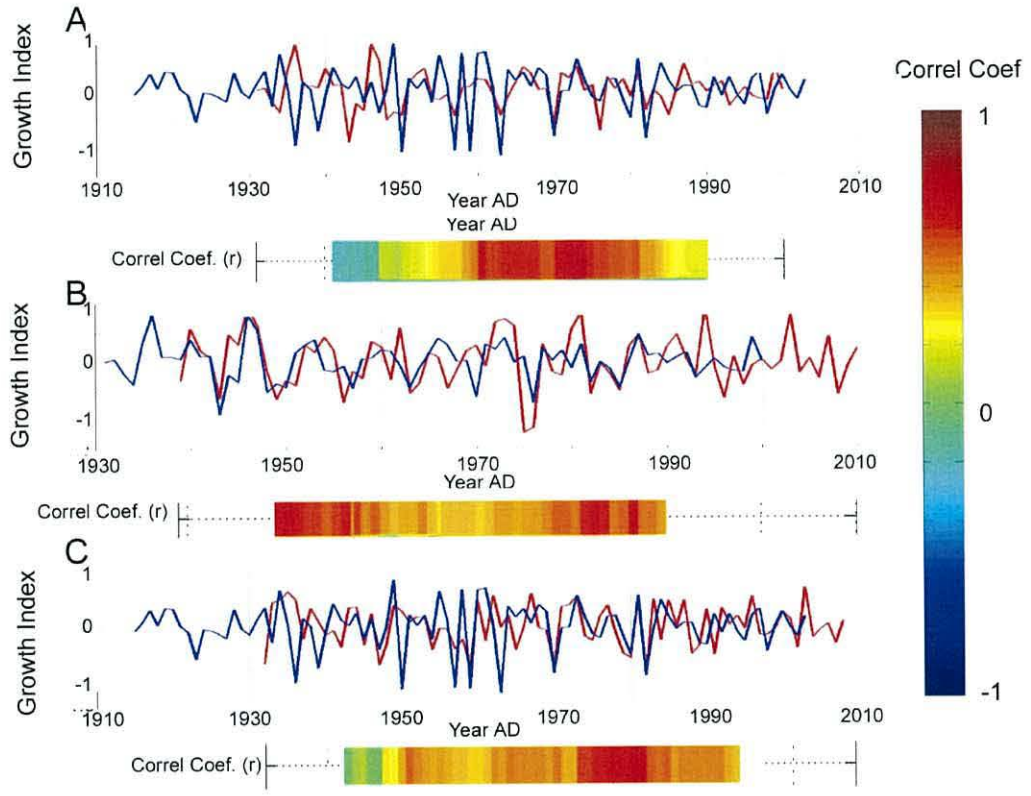

Figure 4 – 8: Matlab SHELLCORR outputs of A. islandica standardised growth indexes highlighting three statistically significant cross-matches between A) Ai108002 and Ai108024; B) Ai108010 and Ai108002: and C) Ai108024 and Ai108025, with the associated 21-year running correlation coefficients.

4.7 Master sclerochronologies

Following the independent validation of the cross-matching by means of radiocarbon dating (see chapter 5) master sclerochronologies were constructed using methods as described in chapter 3. A total of three chronologies are produced from ARSTAN, (Standardised, Residual and Arstan). These chronologies differ in the degree of autoregressive modelling which is re-incorporated into the master growth series. The standardized chronology incorporates no autoregressive modelling. The residual chronology is comprised of the average residuals from the autoregressive modelling. The autoregession which is common or synchronous amongst the growth series and which is likely due to climatological forcing, is reincorporated to the residual chronology to form the Arstan chronology. For more details regarding the construction of the chronologies see the ARSTAN guide by Cook and Holmes, (1986). The

following sub-sections present the *G. humanus* and *G. glycymeris* master sclerochronologies constructed from ARSTAN and details the general chronology statistics as well as assessments of robustness (EPS) for each of the chronologies constructed.

4.7.1 *Glossus humanus* chronologies

Initially seven dead-collected shells were used to construct the first floating sclerochronology derived from *G. humanus* growth lines. Verification of the cross-dating by means of ^{14}C radiocarbon dating (for methods see Chapter 2.7 and results see Chapter 5.2), indicated that the shell specimens from the two sites should not be used to construct a single sclerochronology. The shells from Salen Bay significantly pre-dated those from the Sound of Mull. The ^{14}C determinations confirm the dating of all except one of the shells from each of the respective sites.

In accordance with the ^{14}C results, two separate floating chronologies were constructed using the methods described in Chapter 3.4 (Figure 4 – 9). The single live-collected *G. humanus,* (from SUN02), was of insufficient longevity to be cross-matched with the floating sclerochronologies and could not be used as an anchor to absolutely date the series.

The EPS statistics (see chapter 3.5) for each of the floating chronologies fell below the recommended value of 0.85 and are thus deemed not representative of the common population signal. The average EPS of the Sound of Mull and Salen Bay chronologies are 0.75 and 0.52 respectively. As both chronologies were statistically non-robust, principally due to the relatively low sample depth, - sample depth is defined as the numberof shells in the chronology for a given period - efforts were made to calculate a prediction of the required sample depth for any given year to produce a statistically robust *G. humanus* sclerochronology. Using the Wilson and Elling, (2004) equation (see Chapter 3.5 Equ. 3.3), given the mean correlations of each of the *G. humanus* chronologies, each chronology would need to contain twelve or more series to produce a coherent common signal with a significant EPS.

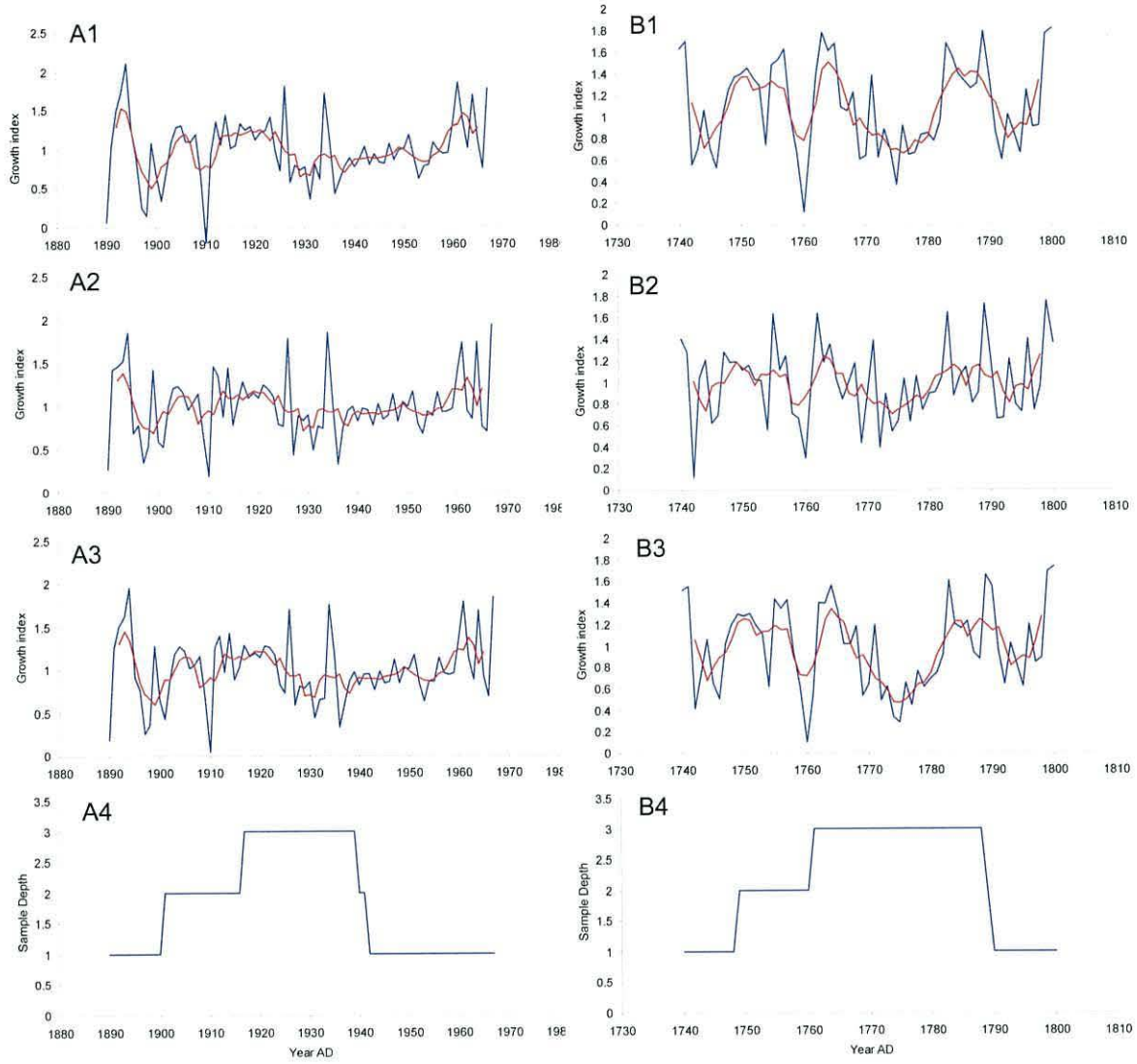

Figure 4 – 9: 1) Standardised 2) Residual and 3) Arstan chronology outputs produced from ARSTAN for A) the Sound of Mull and B) the Salen Bay Glossus humanus floating sclerochronologies, with 4) the corresponding sample depth. Blue lines represent annually resolved data and the red lines display the five year running means. Dates have been determined by means of calibrated ^{14}C dating (see Chapter 5.2).

4.7.2 *Glycymeris glycymeris* chronology

In total ten dead and the two long-lived live-collected shells were used to construct the first absolutely dated sclerochronology derived from internal *G. glycymeris* growth increment widths (Figure 4 – 10). However, the period of overlap between the live and the dead-collected specimens was of insufficient length (<25 years) to be statistically robust. The ^{14}C determinations which were dated to being post-bomb pulse allowed greater precision in calibration (See

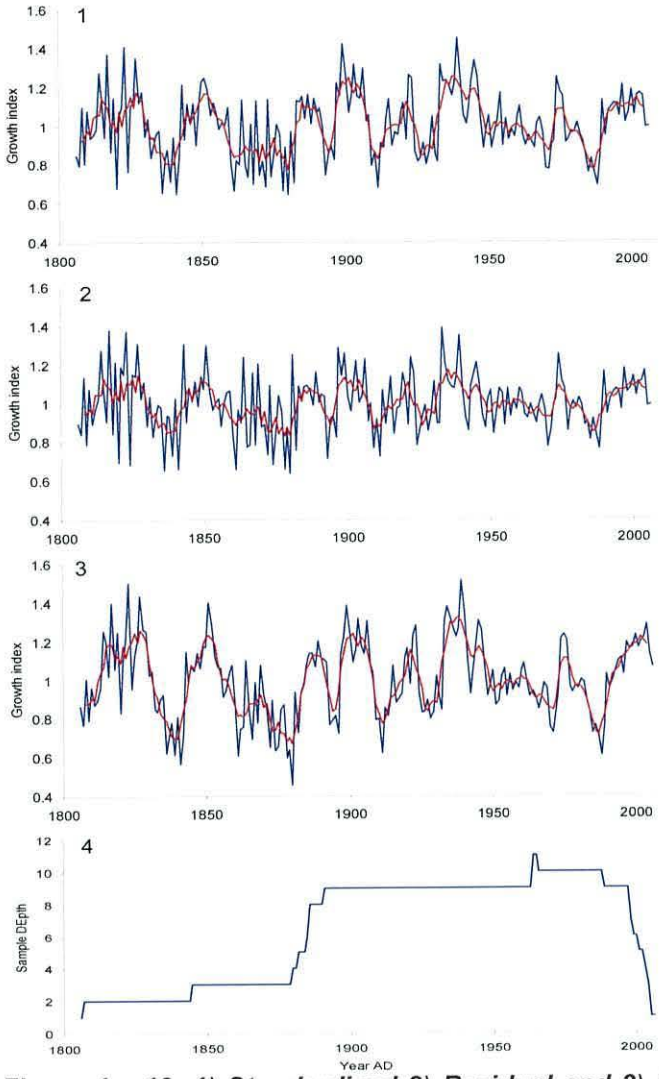

Figure 4 – 10; 1) Standardised 2) Residual and 3) Arstan chronology outputs produced from ARSTAN for the absolutely dated master Glycymeris glycymeris sclerochronologies, with 4) the corresponding sample depth. Blue lines represent annually resolved data and the red lines display the five year running means.

Chapter 5. 2) and therefore greater confidence in the accuracy of the cross-dating over the period.

A running EPS calculated over a fifty year window indicates that the chronology is statistically robust over the period AD 1880-2000 (EPS=0.853). During the periods prior to AD1880 there is a significant reduction in the sample depth which, despite the statistically significant Pearson correlation coefficients between the shells over this period, reduces the EPS below the guide value of 0.85.

Chapter 5

Geochemistry Results

5.1 Introduction

This chapter details the geochemistry results including the AMS ^{14}C determinations, and examines the stable oxygen and carbon concentrations derived from *G. humanus* and *G. glycymeris* shell valves. The crystalline form of the calcium carbonate within the shells of *G. humanus* and *G. glycymeris*, determined by x-ray diffraction determination is described. The results of every sample analysed are presented within appendix A-GC.

5.2 AMS radiocarbon determinations

In total 14 AMS ^{14}C determinations were undertaken, four at the Aarhus radiocarbon Dating Centre (Denmark) using *G. humanus* shell material, and a further ten at the NERC radiocarbon laboratory using both *G. humanus* and *G. glycymeris* shell material. The following subsections describe the raw ^{14}C determinations (5.2.1) and the calibration of the post-bomb (modern, post 1950) determinations (section 5.2.2) and the pre-bomb derived ^{14}C determinations (section 5.2.3).

5.2.1 Raw ^{14}C determinations

Table 5 – 1 summarises the results of the primary ^{14}C determinations obtained from the Aarhus AMS Radiocarbon Dating Centre, Denmark. The uncalibrated determinations indicate that one sample (AAR11601), taken from the ventral margin of the longest-lived *G. humanus* (00013), incorporated shell material which was formed from carbonate precipitated in the modern, post-bomb, era. The modern ^{14}C age precludes the use of the conventional ^{14}C calibration curve, instead requiring a regional bomb-pulse calibration curve (see section 5.2.2). The remaining three samples run by the Aarhus laboratory were all

returned with conventional ^{14}C ages and were calibrated using the conventional ^{14}C Marine09 calibration curve (see section 5.2.3).

The ^{14}C determinations derived from the ventral margin and the umbone of *G. humanus* 00046, collected from Salen Bay, (AAR11603 and AAR11604 respectively) were returned with "inverted" ^{14}C results. As this is biologically impossible, it is concluded that the inversion is likely due to misidentification/mislabelling of the samples at some stage in the process.

Lab ID #	Shell ID #	Sample position	Site	C14 age (years BP ± 1σ)
AAR11602	00015	Umbone	Sound of Mull	389 ± 33
AAR11601	00013	Ventral Margin	Sound of Mull	Modern
AAR11603	00046	Ventral Margin	Salen Bay	657 ± 42
AAR11604	00046	Umbone	Salen Bay	555 ± 31

Table 5 - 1; Raw ^{14}C determinations analysed at the Aarhus Radiocarbon Dating Centre, Denmark. Samples were derived from three G. humanus valves within the chronology.

The calibration of the primary ^{14}C determinations identified the Salen Bay *G. humanus* (00046) as being significantly older than the Sound of Mull shells (see section 5.2.3). The growth series from these shells had been cross-matched into a master chronology, so a second radiocarbon submission was undertaken to verify the cross-matching (see chapter 4.5) and to decide whether the shells from both sites (Salen Bay and Sound of Mull) should be combined into a single Loch Sunart sclerochronology or whether they should be used to construct two independent sclerochronologies for each site.

Lab ID #	Shell ID #	Sample position	Site	C14 age (years BP ± 1σ)
SUERC-23419	00013	Umbone	Sound of Mull	411±35
SUERC-23420	00003	Ventral Margin	Sound of Mull	494±37
SUERC-23424	00054	Ventral Margin	Salen Bay	555±37
SUERC-23421	00051	Umbone	Salen Bay	627±35
SUERC-23422	00051	Ventral Margin	Salen Bay	562±37
SUERC-23423	00024	Ventral Margin	Salen Bay	1203±37

Table 5 - 2; Raw ^{14}C determinations analysed at the NERC Radiocarbon Laboratory, Scotland. Samples were derived from G. humanus valves from both the Salen Bay and the Sound of Mull the chronologies.

Table 5 – 2 shows that all of the secondary *G. humanus* samples that were analysed by the NERC Environment Radiocarbon Laboratory, Scotland, were returned with conventional ^{14}C determinations and were calibrated using the conventional ^{14}C Marine09 calibration curve.

The two *G. glycymeris* samples which were derived from $CaCO_3$ drilled from the umbones of the two longest-lived *G. glycymeris* were returned with conventional ^{14}C determinations (Table 5 – 3). The conventional *G. glycymeris* ^{14}C determinations were calibrated using the conventional Marine09 calibration curve (see section 5.2.3) The corresponding ventral margin samples from the same two shells, however were returned with modern, post-bomb, ^{14}C determinations and were calibrated using the regional bomb-pulse curves (see section 5.2.2).

Publication Code	Sample Identifier	Sample Position	Site	C14 age (years BP ± 1σ)
SUERC-28452	06004u	Umbone	Tiree Passage	471 ± 37
SUERC-28453	06004v	V. margin	Tiree Passage	Modern
SUERC-28454	0020u	Umbone	Tiree Passage	455 ± 35
SUERC-28455	0020v	V. margin	Tiree Passage	Modern

Table 5 - 3; Raw uncalibrated ^{14}C determinations from two fossil G. glycymeris valves collected from the Tiree Passage. Samples analysed at the NERC Radiocarbon Laboratory, Scotland.

5.2.2 Post-bomb ^{14}C calibration

The doubling in the concentration of atmospheric ^{14}C caused by atmospheric nuclear bomb testing is reflected within the marine system. Elevated ^{14}C concentrations are incorporated into all organisms living during or following the nuclear bomb testing (post AD1950). These peaks in ^{14}C concentration therefore facilitate far greater precision in ^{14}C dating assuming that a relevant regional calibration curve is available. Samples which contain these elevated ^{14}C concentrations are termed "modern" i.e. post AD1950 and are calibrated using bomb pulse calibration curves (see Figure 5 – 1).

Three samples were determined to have a modern ^{14}C age, sample numbers AAR11601, SUERC-28453 and SUERC-28455, (see table 5 – 1 and table 5 –

3), These determinations were calibrated using regional post-bomb marine radiocarbon calibration curves (Figure 5 – 1, Scourse *et al.*, in prep).

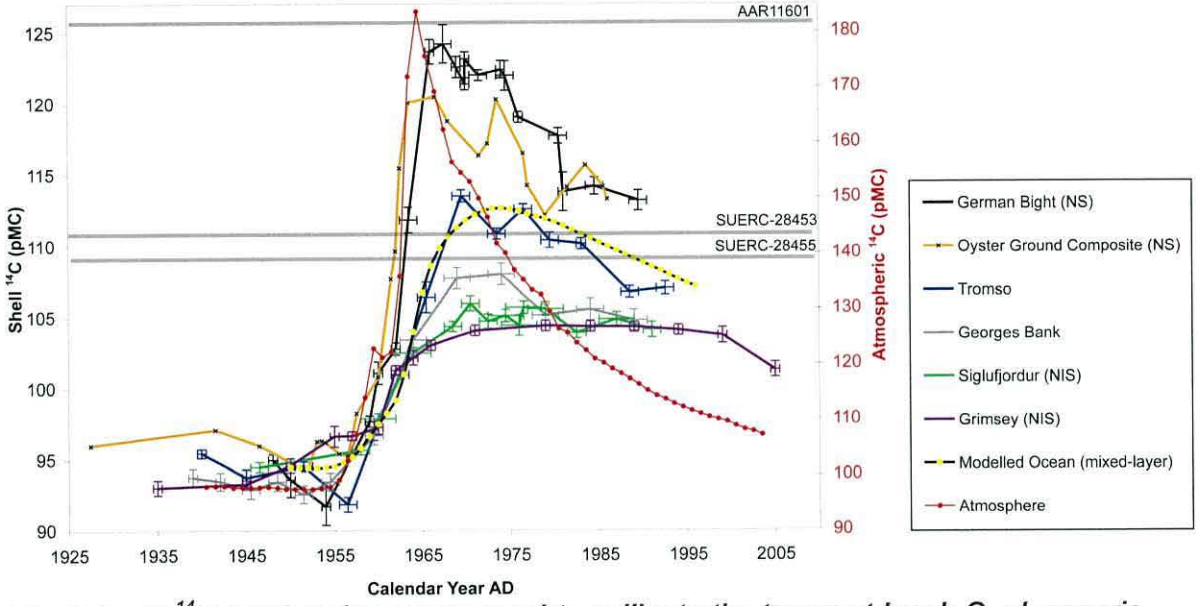

Figure 5 - 1: ^{14}C bomb pulse curves used to calibrate the two post-bomb G. glycymeris ^{14}C determinations (Scourse et al., in prep). NS= North Sea, NIS = North Icelandic Shelf.

Sample AAR11601, derived from the ventral margin of the longest-lived dead-collected *G. humanus* valve (00013), contained the highest ^{14}C concentration of the three modern determinations, (126.12 ±0.47pMC).This likely dates the sample to the peak in the calibration bomb pulse curves at AD1967 ±10yrs. As the concentration places the sample at the peak of the calibration curve the error bars are principally determined by the degree of sclerochronological error, i.e. the number of growth lines deposited within the piece of drilled shell sample.

The two modern ^{14}C determinations (SUERC-28453 and SUEERC-28455), derived from the ventral margins of the two longest–lived dead-collected *G. glycymeris* valves, were not as enriched in ^{14}C as those of the *G. humanus* modern sample (AAR11601). As a result the calibration of these ^{14}C determinations were not as precise, as they could have two possible solutions on the calibration curves, on the incline and decline respectively. Both modern *G. glycymeris* samples were calibrated using the modelled ocean mixed layer ^{14}C marine bomb pulse calibration curve (Figure 5 – 1). The resulting calibrated ^{14}C dates range from AD1965 – AD1994 and AD1968 – AD 1984 ±10years.

5.2.3 Pre-bomb ^{14}C calibration

Calibration of all the conventional ^{14}C determinations (pre AD1950) was undertaken using the online ^{14}C calibration software OxCal version 4.1 (http://c14.arch.ox.ac.uk/) (Bronk Ramsay, 1994 & 2001). Oxcal V4.1 facilitates the calibration of both marine and terrestrial ^{14}C determinations using a range of ^{14}C calibration curves. The Marine09 calibration curve (Reimer *et al.*, 2009) was utilised to calibrate all of the conventional ^{14}C determinations derived from both *G. humanus* and *G. glycymeris* shell valves.

All except one shell (sample id no. SUERC-23423, calibration code R_date GH24M) of the conventional ^{14}C determinations were dated to the later half of the last millennium (Figure 5 – 2). The ^{14}C determination SUERC-23423 that originated from *G. humanus* shell (00024), whose shell growth series had been cross-matched with the Salen Bay *G. humanus* chronology, had a radiocarbon date compatible with being alive during the 11th or 12th Century AD. By contrast the other shells that were cross-matched into the Salen Bay *G. humanus* sclerochronology originated during the 15th to 17th centuries AD respectively. Thus on the basis of the ^{14}C date of *G. humanus* (00024), this shell was not included in the Salen Bay chronology and it was concluded that the initial cross-match was spurious.

The calibrated ^{14}C determinations derived from the shell material drilled from the shells incorporated within the *G. humanus* Sound of Mull sclerochronology suggests that all three shells lived during the 17th century AD at the earliest. The two conventional ^{14}C determinations derived from the umbones of the two long-lived *G. glycymeris* shells incorporated within the Tiree Passage sclerochronology were calibrated to the 18th century AD. Both the two *G. glycymeris* ^{14}C determinations and the ^{14}C determinations derived from the Sound of Mull *G. humanus* lack precise ^{14}C calibrations as there is a plateau in this part of the Marine09 calibration curve during this period is relatively flat extending the probability range, (Figure 5 – 3).

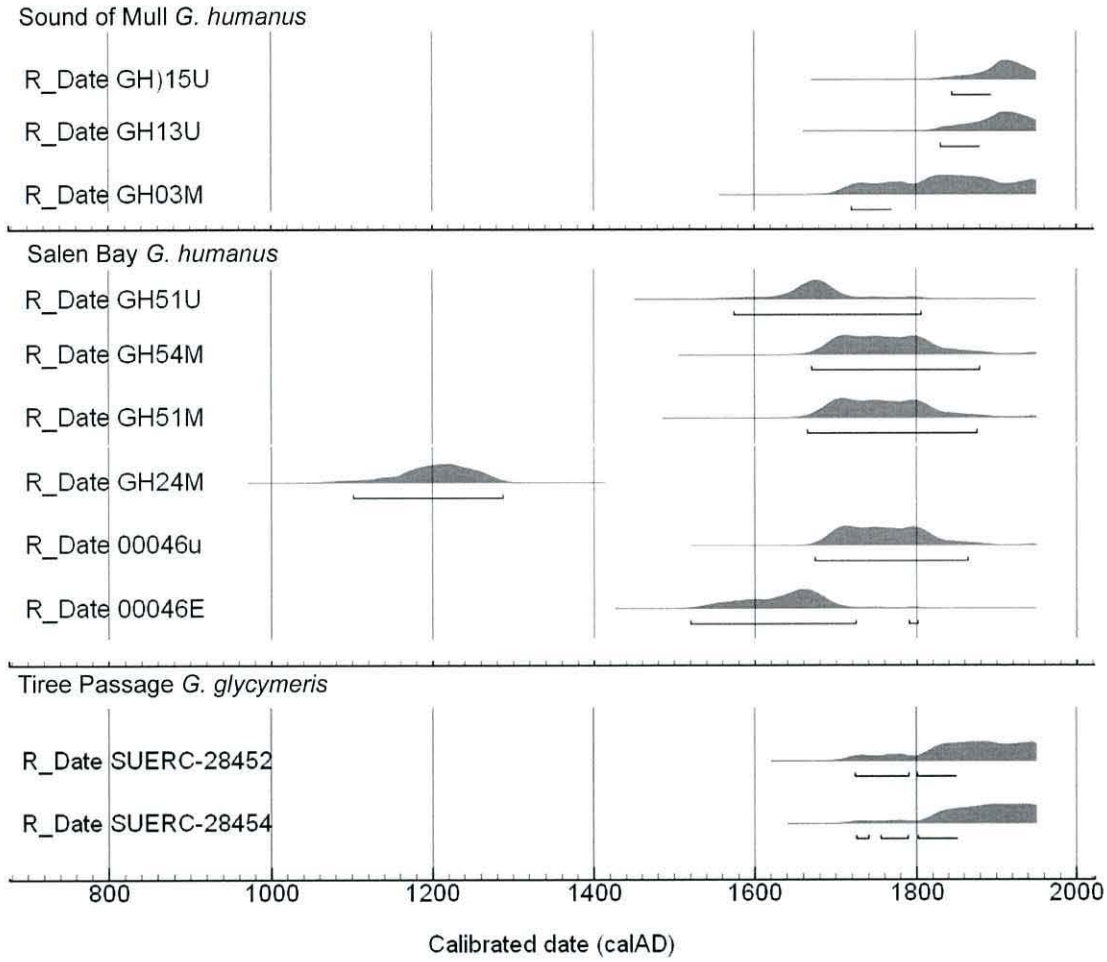

Figure 5 – 2: OxCal ^{14}C probability distributions of calibrations of nine Glossus humanus and two Glycymeris glycymeris conventional ^{14}C determinations calibrated using the Marine09 radiocarbon calibration curve.

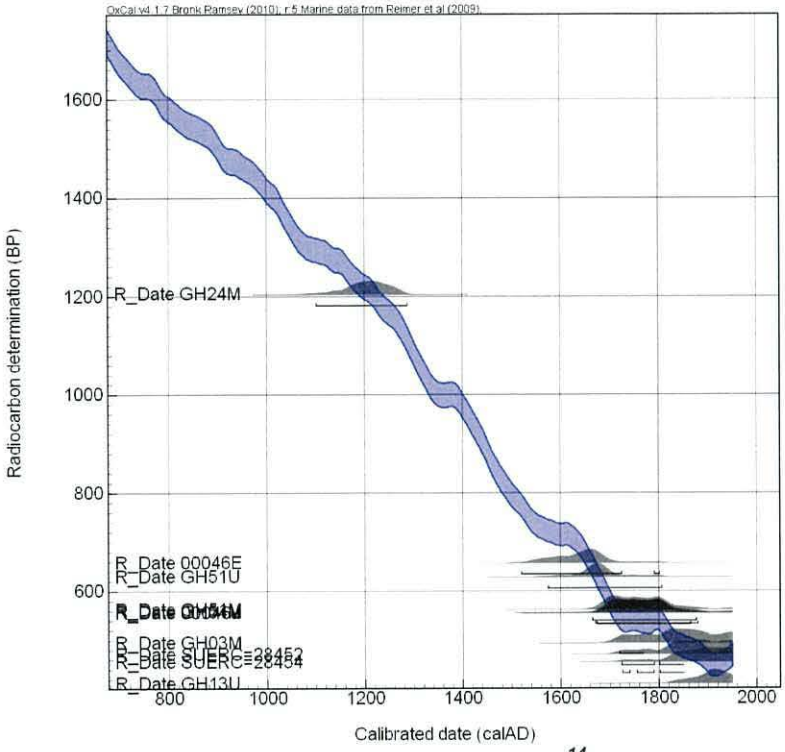

Figure 5 – 3: Oxcal plot of the Marine09 ^{14}C calibration curve with the probability distribution plots of each of the conventional ^{14}C determinations derived from the G. humanus and G. glycymeris shell valves.

5.3 X-Ray diffraction

Pieces (~10mm^2) of shell were cut using a carborundum cutting wheel attached to a hand-held dremel saw from the ventral margins of a dead-collected *G. humanus* and a dead collected *G. glycymeris* shell. These shell pieces were ground to a fine powder and small pellets of this material were analysed using X-ray diffraction (XRD) at Cambridge University (courtesy of Dr E. Harper) to determine the form of the calcium carbonate crystals of the shell, either aragonite, calcite, or a combination of both. These data are needed so that the correct palaeotemperature equation applicable to calcite or aragonite can be applied in the reconstruction of seawater temperature. Figures 5 – 4 and 5 – 5 show the XRD spectral outputs for the *G. glycymeris* and *G. humanus* samples respectively. Both the XRD outputs indicate that the calcium carbonate crystalline structures of both *G. humanus* and *G. glycymeris* are 100% aragonite (pers. comm. Dr E. Harper). In subsequent analyses the stable oxygen isotope composition of the shell was transformed to palaeotemperatures using the aragonite palaeotemperature equation (see Chapter 8.4).

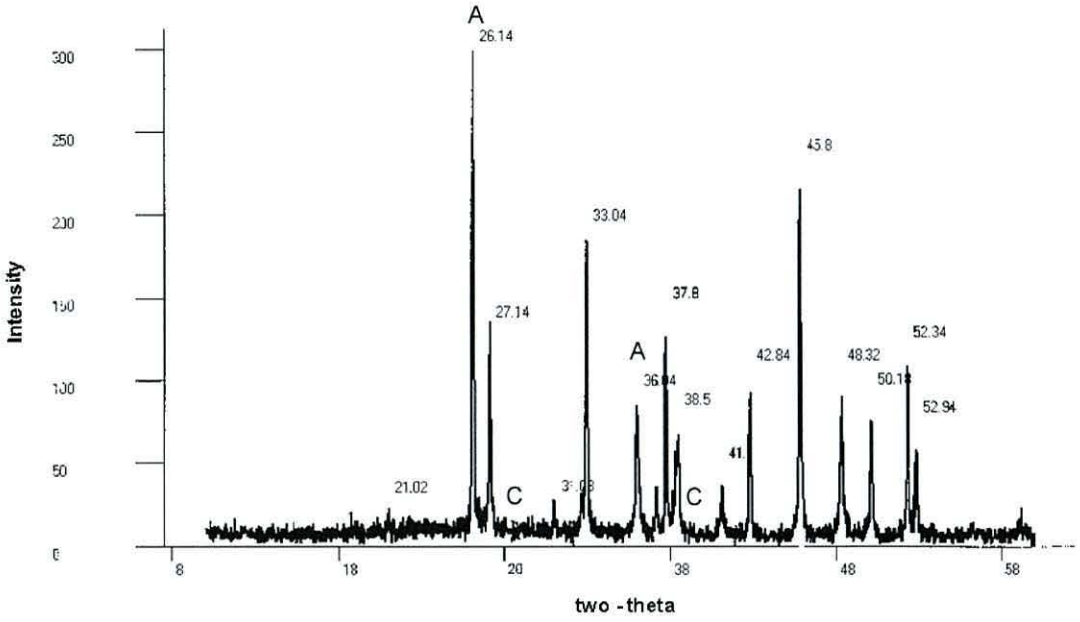

Figure 5 – 4: An X-Ray Diffraction (XRD) plot for calcium carbonate derived from a Glycymeris glycymeris shell (00015), (courtesy of Dr E. Harper). Aragonite and calcite peaks are denoted by A and C respectively (Stepkowsa et al., 2003)

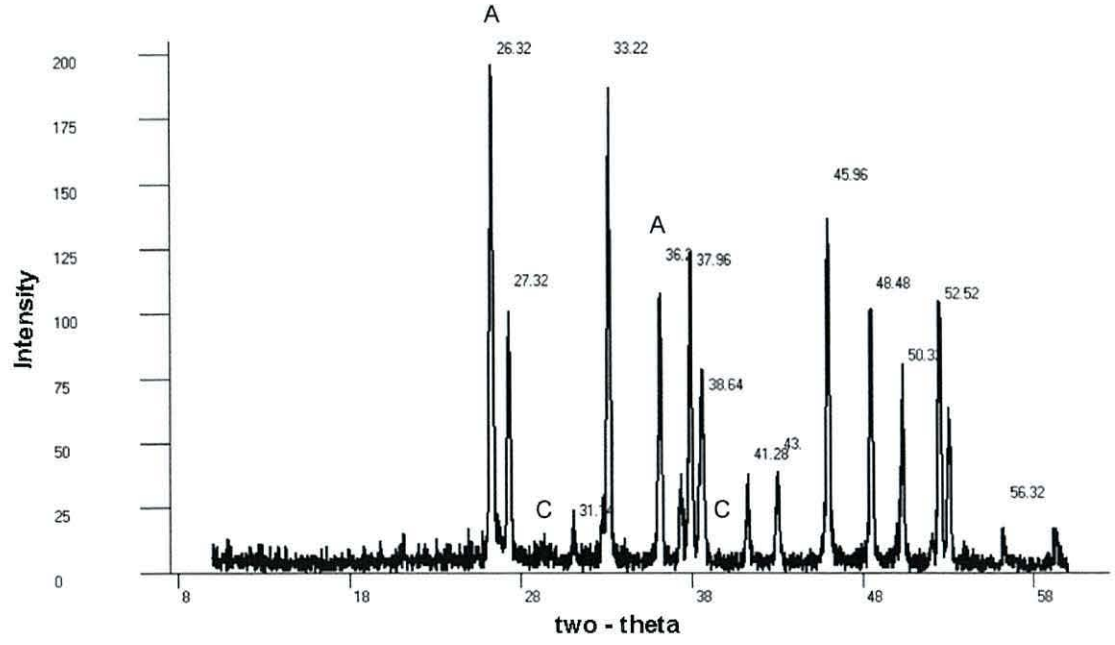

Figure 5 – 5: : An X-Ray Diffraction (XRD) plot for calcium carbonate derived from a Glossus humanus shell (00020), (courtesy of Dr E. Harper) . Aragonite and calcite peaks are denoted by A and C respectively (Stepkowsa et al., 2003).

5.4 Stable isotopic analysis of *Glossus humanus* and *Glycymeris glycymeris*

The data presented in sections 5.4.1 and 5.4.2 (below) were corrected by comparison with laboratory standards, which were analysed simultaneously to the calcium carbonate samples, the laboratory standards had been compared with international standards that had been run through the same machine at an earlier date. Full details of individual samples are given in Appendix A - GC. These data were analysed at Iowa State University (USA) stable isotope facility courtesy of Dr Alan Wanamaker Jr.

5.4.1 Sub incremental isotope analysis

To investigate the timing and annual periodicity of growth line deposition in *G. humanus* and *G. glycymeris*, calcium carbonate shell samples were drilled at high resolution (sub-incrementally/intra-annually) from within selected growth increments from a single dead-collected *G. humanus* and a live-collected *G. glycymeris* shell valve and their stable oxygen and carbon isotopic composition determined. Should the growth increments be formed annually the isotopic content, which reflects the water temperature, should return a seasonal cycle. It has not been possible to complete this investigation because of technical difficulties resulting in the loss of the samples during the analysis process. Those samples that have been analysed can be found in Appendix A-GC.

5.4.2 Incremental isotopic analysis

Further to the ultra high resolution sub incremental samples, single calcium carbonate samples were drilled from each growth increment spanning AD1976 – 2004 from one live-collected *G. glycymeris* valve (gg00024). Although the specimen was collected live in 2006, the narrow width of the growth increments in 2005 and 2006 prevented annually resolved samples being collected. The next two sub-sections detail the results for the carbon and oxygen stable isotopes respectively.

5.4.2.1 Stable carbon isotopes

$\delta^{13}C$ in the calcium carbonate samples (Figure 5 – 6) shows a statistically significant linear decline (r^2=0.886 p<.0001 n=28) from *ca.*2.7‰ to *ca.*1.5‰ over

the 28-year period from 1976 to 2004. Superimposed upon the linear decline in $\delta^{13}C$ is an apparent multi-annual (6-8 years) oscillation, which exhibits four repeated cycles over the 28 year period

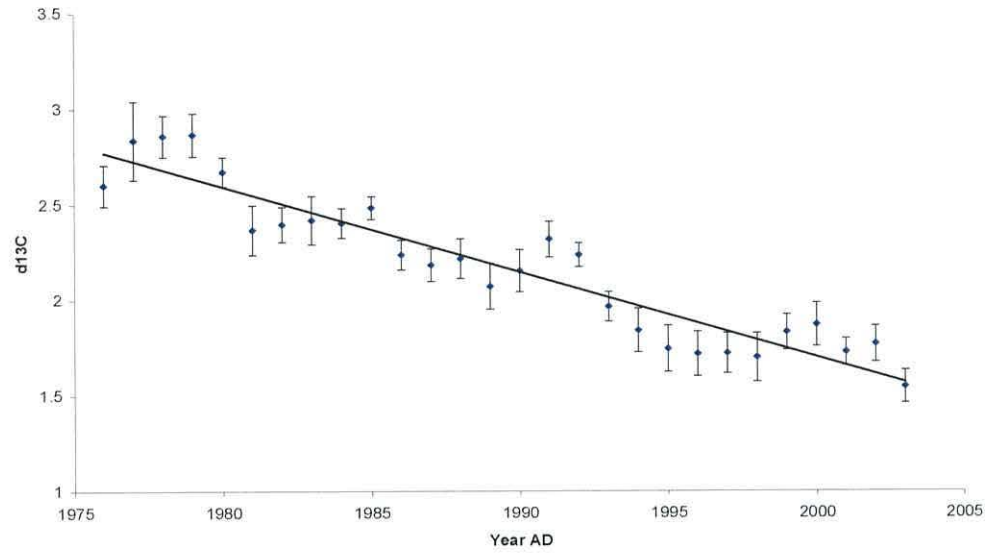

Figure 5 – 6: Raw $\delta^{13}C$ values (‰) of calcium carbonate samples micro-milled from single growth increments, showing a linear decline of 0.0445‰ per year (r^2=0.886 p<.0001) during the period of AD1976 to AD2003. Values derived from G. glycymeris 00024.

5.4.2.2 Stable oxygen isotopes

Figure 5 – 7 displays the $\delta^{18}O$ values derived from the calcium carbonate samples micromilled from 28 annually resolved growth increments in *G. glycymeris* shell no. 00024. The $\delta^{18}O$ values show a small but non-significant trend of 0.325‰ over the 28 year period. The $\delta^{18}O$ values and the mean annual seawater temperatures, taken from records collected at Keppel Pier, in the Firth of Clyde, the nearest station to the locations of the *G. glycymeris* shell indicates a significant positive Pearson correlation (r= 0.52 n= 28 P<0.005) (Figure 5 – 8). Discussion of these results are given in Chapter 7.4.

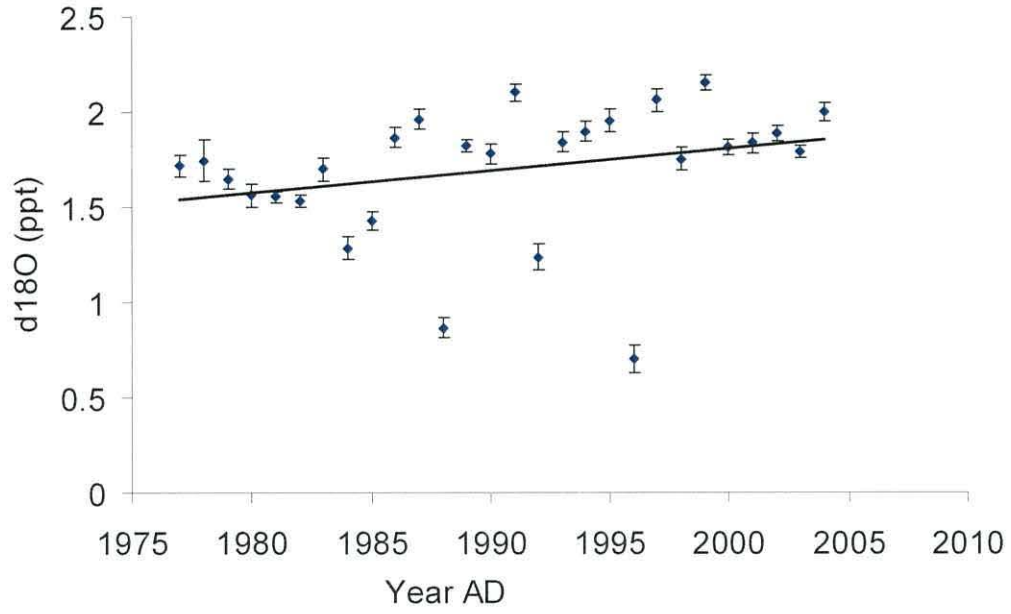

Figure 5 – 7: Raw $\delta^{18}O$ values (‰) derived from 28 calcium carbonate samples micromilled at annual resolution from one G. glycymeris (gg00024). Error bars are determined by the standard deviation of the ten analyses which comprise each isotopic determination. The black line represents the statistically non-significant linear regression is described by the equation y = 0.0116x - 21.381 (r^2= 0.0784 p=0.0753 n=28)

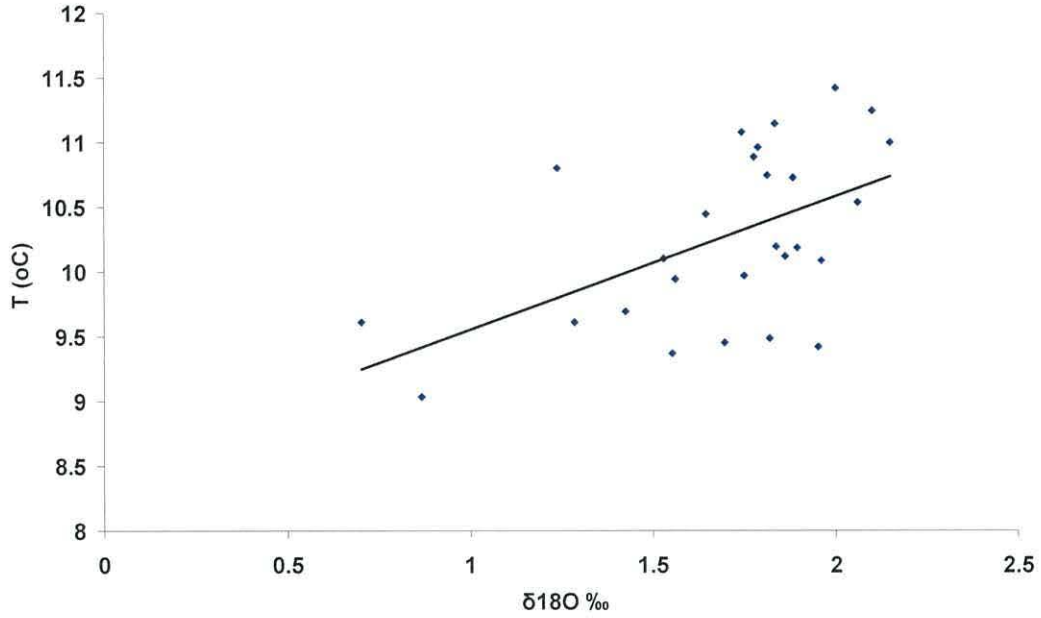

Figure 5 – 8: Linear regression analysis between raw $\delta^{18}O$ values (‰) and mean annual sea surface temperatures from Keppel Pier over the period AD1976 to AD2004. The black line is described by the equation y = 1.0269x + 8.5256 (n = 28 r^2=0.281 P<0.005).

Chapter 6

Discussion: Biology and Chronology

6.1 Introduction

This chapter draws on and reviews data from chapters four and five discussing the innate differences and similarities between the constructed master chronologies. The first annually resolved multi-species sclerochronology is constructed and the results discussed. Each of the sclerochronologies are compared to a dendrochronology constructed from a tree ring series from the Southern Glens of Scotland.

6.2 Sample collection and suitability

The sampling methods (mechanical dredge and diver collection) used to obtain the different bivalve species were not designed to provide a quantitative population sample of each of the three species studied. However they collected sufficient shells for chronology construction from each location. The mechanical dredge was towed a total of 15 times, covering a total distance of 8,848m, across five sites within Loch Sunart and the Sound of Mull. Table 6 – 1 details the number of tows of the mechanical dredge completed at each of the sites and the corresponding dredging efficiency (number of specimens collected.metre^{-1} dredged). Table 6 – 2 gives the details of the diver collected specimens and the related efficiency of sample collection using this method.

Site	No. of Tows	Total distance towed (m)	Dredging efficiency (m^{-1}) *Ai.* Live	*Ai.* Dead	*Gh.* Live	*Gh.* Dead	*Gg.* Live	*Gg.* Dead
SB	5	2463	<0.001	0.002	0	0.008	0	0
SM	4	2121	0	<0.001	0	0.010	0	0
M	2	1329	0	0	0	0	0	0
TP	1	882	0	0	0	0	0.004	0.154
MD	3	2053	0	0.300	0	0.14	0	0

Table 6 – 1: Details of the number of tows, total distance towed and the dredging efficiency (number of clams collected metre^{-1} dredged) for Arctica islandica (Ai), Glossus humanus (Gh) and Glycymeris glycymeris (Gg). Site names as in Figure 2 – 2.

Site	No. of Dives	No. of *Ai* and *Gh* collected live	Diving notes for each site
SUN01	3	*Ai* 16	Ai very common once the divers hit the patch
SUN02	21	*Ai* 16	No distinct accumulations; no more than 2 *Ai* on any one dive with plenty of barren dives
SUN03	13	*Ai* 5	Lots of barren/singles specimens per dive to start off with, then found a patch
SUN04	2	*Ai* 2; *Gh* 1	*Ai* very common

Table 6 – 2: Total number of dives completed at each site in Loch Sunart and diving notes regarding the observations/ successful collection of A. islandica at each site. Site locations as in Table 2 – 2 in Chapter 2.2.

Dredging was extremely effective at collecting large numbers of *G. glycymeris* from the Tiree Passage, However; the true density of *G. glycymeris* in the Tiree Passage is likely to be underestimated and is probably >0.004m^{-2} due to the difficulties the dredge encountered with the seabed in the Tiree Passage. Here the dredge was critically damaged after the first tow, with the forks severely bent by large rocks on the sea bed. To obtain an accurate assessment of the true density of *G. glycymeris* in the Tiree Passage alternative approaches would need to be adopted (video sled or diving survey) which would overcome the problems encountered by mechanised Day grab/ dredge sampling. Of the *G. glycymeris* shells collected, 55% of the dead-collected material had been severely bored. These borings, although minor in appearance on the external shell surface, form large holes within the internal shell layers, and as a result

any shell cross-section which includes such borings cannot easily be used to obtain a growth record series.

6.3 Species distribution

The modern day (live) distributions of *G. humanus*, *G. glycymeris* and *A. islandica* in British waters were identified and assessed by investigating the published literature (Dahlgren *et al.*, 2000; Nicol, 1951; Owen, 1953), online sighting records - including the National Biodiveristy Network (NBN) (http://www.nbn.org.uk/) and the Global Biodiversity Information Facility (GBIF) (http://www.gbif.org/), museum archives – including the Natural History Museum (London), Smithsonian Natural History Museum (Washington) and the Scottish National Museum (Edinburgh), opportunistic collections through local Scottish fisheries and finally the collections made whilst conducting this project through the NFSD team and the dredging by the RV *Prince Madog*.

It is apparent from examining these sources that the distributions of *A. islandica* and *G. glycymeris* are relatively well documented with numerous observations throughout their respective distributions within the North Atlantic region (Figure 6 – 1). The distribution of *G. humanus,* however, is not well understood, records of sightings being scarce, for example within the NBN gateway (Figure 6 – 2). Therefore the current understanding of *G. humanus* distribution is constrained to museum collection data and records published by Nicol, (1951a). In order to further our knowledge of the *G. humanus* distribution within British and European waters, the records and collection details obtained within this thesis along with various physical and environmental parameter timeseries for the corresponding locations were submitted for geographical spatial analysis applications. The analysis, conducted by Dr Mike Tetley, correlates the biological and physical timeseries at the sites with known *G. humanus* populations in order to identify a range of environmental parameters common between each of the localities.

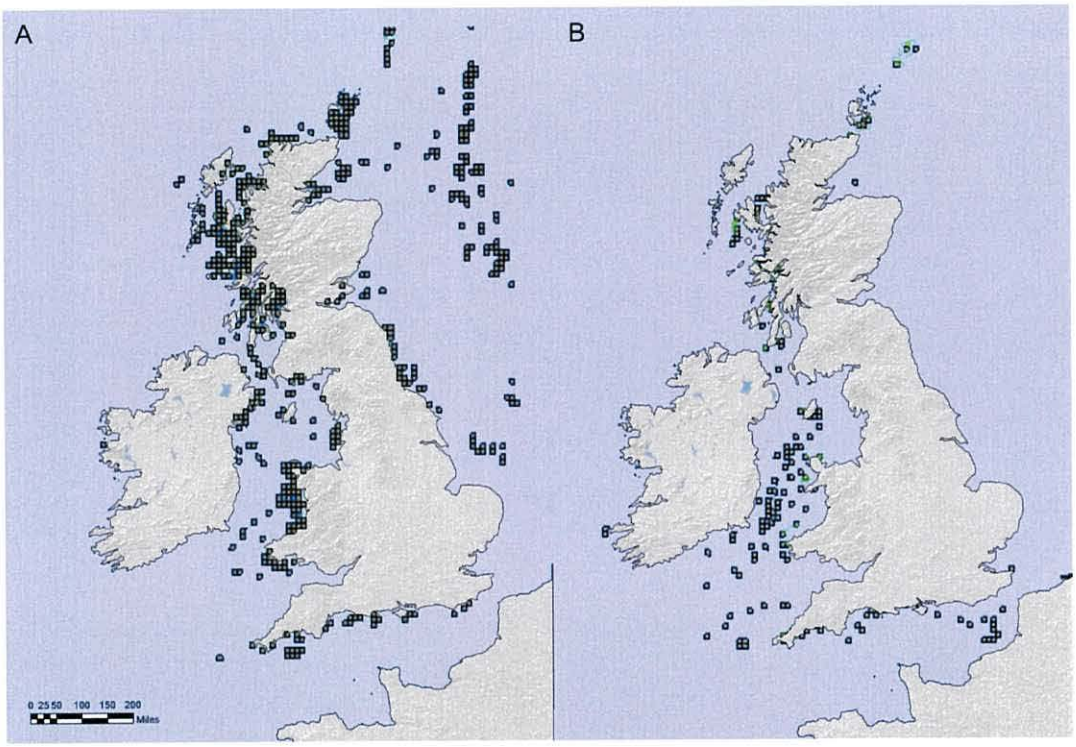

Figure 6 – 1: Maps showing the UK distributions of A) Arctica islandica and B) Glycymeris glycymeris. Data provided by the National Biodiversity Network.

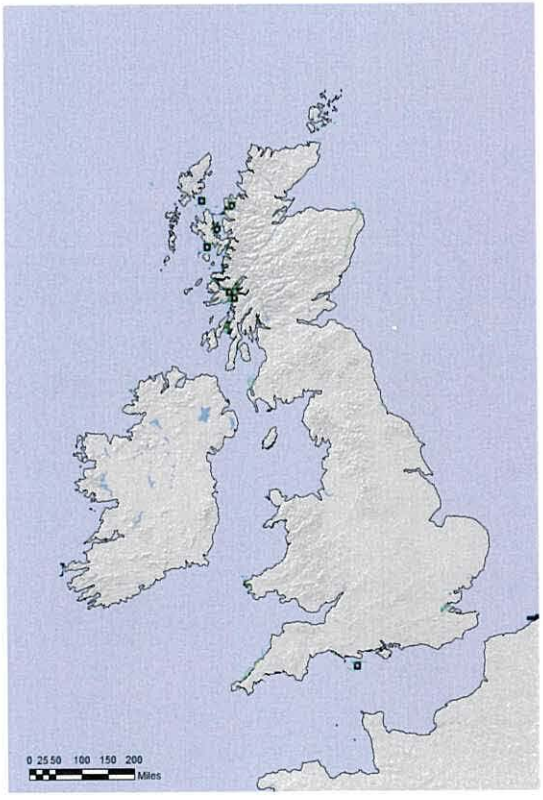

Figure 6 – 2: Distribution of Glossus humanus as depicted by the records on the National Biodiversity Network

The analysis examines the spatial physical and biological timeseries across the entire geographical area, identifying localities with common signature characteristics as found within the sightings loci. The habitat suitability within each longitudinal and latitudinal grid box is then scored by percentage denoted as a colour (Figure 6 – 3). For additional methods of the analysis see appendix A-GD. Figure 6 – 3 presents the results of the habitat distribution mapping. The areas of highest habitat suitability (shown as orange to red shaded areas in Figure 6 – 3) are predominantly near-shore subtidal locations; this is consistent at both the small- and larger-scale plots for the Hebridean shelf and north-western Europe respectively. Areas identified as moderately suitable (shaded green) are generally located further offshore. Detailed analysis of the model outputs is constrained by the spatial resolution of the physical and biological timeseries as well as possible sampling bias in the sightings records; the map published by Nicol (1951a), for example, does not give specific locations and instead large "pin points" are used to denote the collection locations.

Comparison of the species distribution, sightings records and *G. humanus* habitat suitability maps showed that the distribution of the three species, although latitudinaly similar, have complementary modern distributions constrained by contrasting preference for specific sediment grades. Owen (1953) signifies that *G. humanus* was constrained to sediment grades "too soft for *Arctica islandica* to inhabit", due to *A. islandica* on average having a greater mass compared with *G. humanus,* which might lead individuals to "sink" within the sediment should the sediment grade be too fine. However, the RV *Prince Madog* cruise material suggests that it is probable that there is some degree of overlap between the habitats suitable for *A. islandica* and *G. humanus* with recent (past 300 years) dead-collected material being recovered from the same sites within Loch Sunart. The *G. glycymeris* populations, however, appear to be restricted to habitats distinct from both *A. islandica* and *G. humanus* populations with unique habitat preferences constrained to the coarse sand and gravel substrata characteristic of higher energy environments such as those found in the Tiree Passage.

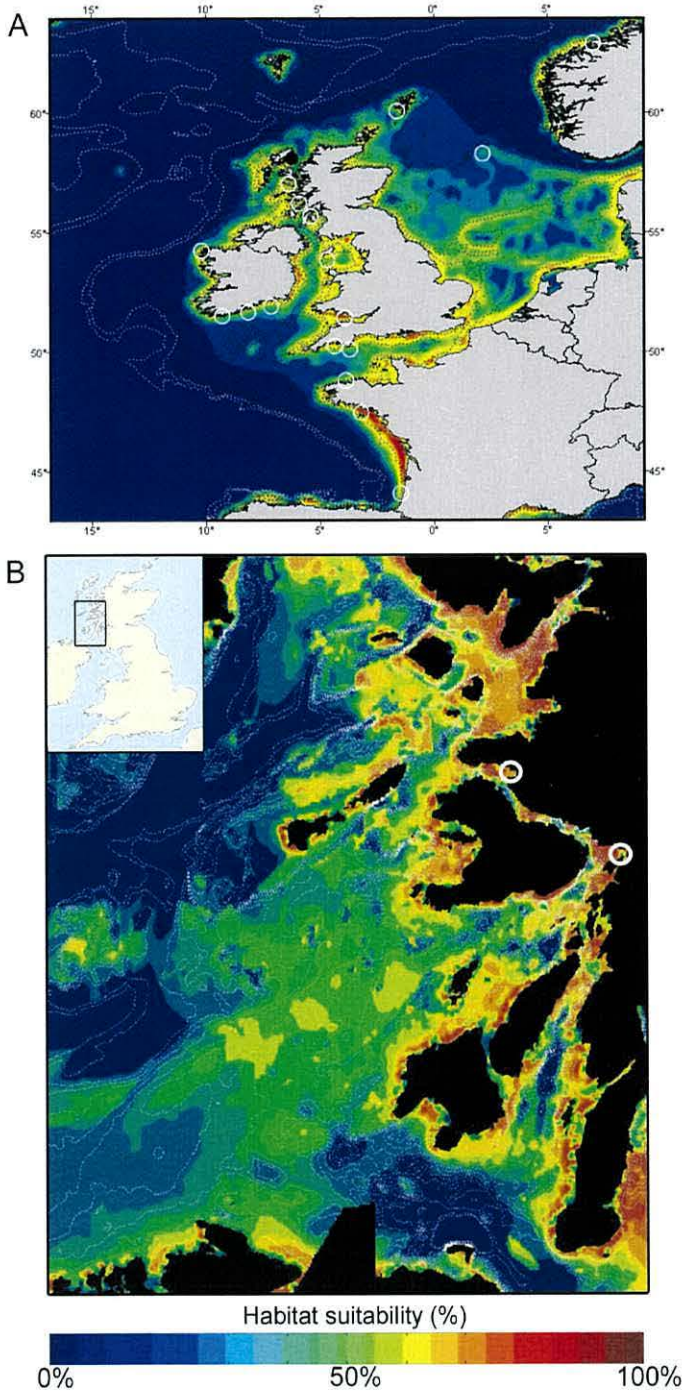

Figure 6 – 3: Habitat suitability maps (given as percentage) for Glossus humanus across A) NW Europe and B) Western Scotland. White circles represent locations from which G. humanus have been collected/ recorded.

The ^{14}C dating of the Sound of Mull *G. humanus* chronology and the presence of live-collected *G. humanus* within the Natural History Museum (London) archive suggest qualitatively that over the latter half of the twentieth century there may have been a substantial reduction in the numbers of *G. humanus* in

the Hebridean shelf seas. However, it is not possible to state definitively, within the context of this thesis, that populations have declined or to propose reasons for any decline. In order to assess the temporal stability of *G. humanus* populations over the last 100 years, a more rigorous quantitative survey approach would need to be undertaken, such as Day grab sampling to sample defined areas of the sea bed. Sampling positions could be determined by the habitat suitability maps (Figure 6 – 3) to select areas likely to yield *G. humanus* samples.

The temporal and spatial extent of the fossil distributions of each of the three species differs significantly. Records within the Natural History Museum in London and presented by Nicol (1951a) suggest that the extent of the fossil *G. humanus* distribution occupied a more southerly region than that of its modern day distribution, occupying the shallow waters within the Mediterranean as well as the shelf seas of NW Europe and the British Isles. However, it is clear from examining all the sources available that at no point within the recent geological record has *G. humanus* been particularly prevalent; this relative scarcity of both live and dead *G. humanus* material could prohibit the use of the species as an important independent sclerochronological archive.

The modern day and fossil *A. islandica* and *G. glycymeris* distribution have been well documented due to their commercial importance, increasing use as environmental archive species (*A. islandica*) and occurrences at key archaeological sites (*G. glycymeris*). *Arctica islandica*, the sole extant species within its genus, is common along the shelf seas of the North Atlantic, including the USA, Iceland and many northwest European countries (Dahlgren *et al.*, 2000). Since the early works of Nicol (1951b) there has been extensive research published describing the fossil distribution of *A. islandica* and how it has changed through time, (Zatsepin and Filatova, 1961; Funder and Weidick, 1967; Raffi, 1986; Salvigsen *et al.*, 1992; Galkin, 1998). The stratigraphical range of *the* Arcticidae *extends* back to the Cretaceous epoch, (Dahlgren *et al.*, 2000). Such a distribution makes the species an extremely useful archive for the temperate to sub-polar North Atlantic.

Glycymeris glycymeris is one of four extant members of the family Glycymeridae that inhabit the European coastal shelf seas. Data provided by the GBIF suggest that fossil records of Glycymeridae species are present to some extent within the coastal shelf seas of all non-polar continents (Figure 6 – 1). The stratigraphical range of fossil Glycymeridae are thought to extend into the Cenomanian (Upper Cretaceous, *ca.*93.5-99.6 Ma; Squires, 2010). This broad temporal and spatial distribution could provide an unrivalled resource of shell material from which to build sclerochronologies across the globe. Such records could provide invaluable archives of both local and global scale changes at annual to sub-annual resolution for areas hitherto devoid of annually-resolved records both within the northern and southern hemispheres.

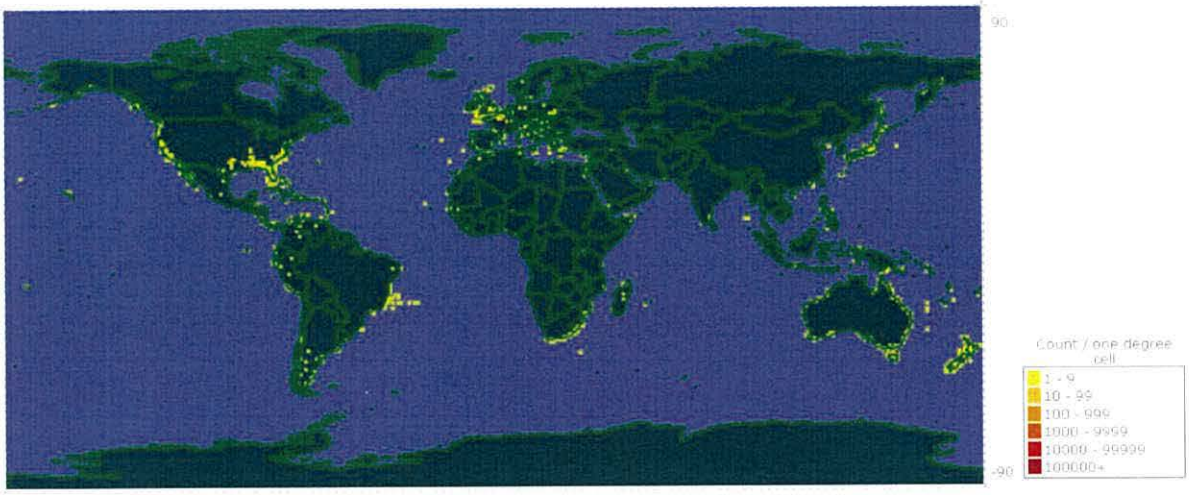

Figure 6 – 4: Distribution of collections or sightings of fossil or extant populations of Glycymeridae. Data provided by the GBIF (http://data.gbif.org/welcome.htm).

6.4 Growth increment analysis

Growth increment series, digitally recorded from acetate peel replicas constructed from the etched polished shell sections, from each of the three species examined, exhibit similar ontogenetic trends (see chapter 4.5). They can be expressed as a negative exponential curve. The amplitude of the ontogenetic growth curve, inter-annual variability and the standard deviation of growth between individuals of *A. islandica* and of *G. humanus* are similar. The growth of *G. glycymeris* (within the umbone), however, although similar in shape to both *G. humanus* and *A. islandica*, is reduced in amplitude, with the mean maximum growth of <400µm yr^{-1} compared with *ca.*1000µm yr^{-1} for both

A. islandica and *G. humanus*. The inter-annual variability of growth in *G. humanus* is also less than *A. islandica*, with the maximum variability during the first 40 years of growth decreasing to a stable variability for the remainder of the lifespan. The reduced variability in growth equates to an increase in the complacency of the growth record. The dendrochronological literature indicates that complacent records, or complacency within the record, hinders the use of the archive as a palaeoenvironmental archive as it is the inter-annual variability in growth that is driven by the environmental forcings. The inference is that reduced inter-annual variability (increased complacency) indicates that environmental factors are not a strong driver of annual growth. However, within the published literature there is no statement regarding a critical defined level of inter-annual variability or complacency. In order to ensure that the measurements of inter-annual growth within *G. glycymeris* accounted for true inter-annual variability, repeat measurements (three) were taken of each growth increment and a mean value calculated. This approach reduced measurement noise caused by human error allowing for the true variability to be assessed.

The maximum longevity of each of the three species significantly differs within the Loch Sunart and Tiree Passage area. *Glossus humanus* reached a maximum longevity of 78 years (gh00013) which is significantly shorter than the maximum longevity of both *A. islandica* (198 years) and *G. glycymeris* (192 years) for the region. The mean longevities of each of the three species are similarly diverse, with the mean *G. humanus* longevity being 45 years compared with 74 years for *A. islandica* and 101 years for *G. glycymeris*. Although *G. humanus* reach a maximum longevity within the Loch Sunart area significantly shorter than that of *A. islandica*, it is still of sufficient length to yield growth increment series that can produce statistically significant cross-matches. The longevities of both *A. islandica* and *G. glycymeris* within the Loch Sunart environment, although significantly shorter lived than those of *A. islandica* collected from the waters north of Iceland (>400 years maximum longevity, Wanamaker *et al.*, 2009) and more recently reclassified as >500 years (Butler *et al.*, submitted; Wanamaker *et al.*, in review), they are still of sufficient length to enable cross-matching.

It is important to note that the estimates of maximum longevity given here are only representative for specimens collected within the Hebridean shelf. Both *G. glycymeris* and *A. islandica* have previously been reported in the literature using specimens collected from a range of locations at various water depths and latitudes. The corresponding estimates of maximum longevity vary widely, with the previous maximum longevity of *G. glycymeris* being reported at *ca.*100 years (Ramsay *et al.*, 2001) and *A. islandica* >500 years (Butler *et al.*, submitted). It is likely that numerous biotic and abiotic factors contribute to the maximum longevity of these organisms. It could therefore be likely that the true maximum longevity of both *G. humanus* and *G. glycymeris*, as with *A. islandica*, is far greater than that found in the specimens collected and examined within this thesis.

6.5 Cross-matching and chronologies

Growth increment widths derived from both dead- and live-collected *G. humanus* and *G. glycymeris*, in addition to the established sclerochronological archive *A. islandica*, were able to be cross-matched using SHELLCORR (see Chapter 4.5). The following subsections discuss the results of the cross-matching and master chronology construction (data from Chapter 4) as well as the validation of the cross-matching using the AMS ^{14}C determination results (from Chapter 5) for each species respectively.

6.5.1 *Glossus humanus*

Significant Pearson correlation coefficients were identified between seven *G. humanus* dead-collected from both the Sound of Mull and Salen Bay sites in the main basin of Loch Sunart. The Pearson correlation coefficients implied that the *G. humanus* growth series could be grouped to construct a single series incorporating the growth increment series of both the shells from Salen Bay and the Sound of Mull. Both sites are situated within the main basin of Loch Sunart. Calibration of the initial four ^{14}C determinations, which were provided by the Aarhus AMS radiocarbon laboratory (Denmark), (see Chapter 5.2.2 and 5.2.3), however, suggest that shell gh00046, which originated from Salen Bay, was significantly older than the two shells (gh00013 and gh00015) sampled from the Sound of Mull. These calibrated ^{14}C determinations indicate that the statistical

cross-match between the shells collected from the Sound of Mull and the Salen Bay are spurious, with the shells collected from Salen Bay originating from the 15th - 17th centuries AD whilst the shells cross-matched within the sound of Mull cross-matches dating to the 19th and 20th centuries AD. This result emphasises the need to validate using AMS ^{14}C dating any cross-matches between *G. humanus* growth series.

The single ^{14}C AMS determination, within the initial submission, derived from the ventral margin of shell gh00013 was determined to be of modern origin (post AD1950). The post-bomb ^{14}C calibration of sample (AAR11601) date the sample at the peak of the ^{14}C bomb pulse curve (AD 1967). This allows a very precise calibration of the ^{14}C determination and provides an "anchor" for the Sound of Mull sclerochronology in the absence of any live-collected *G. humanus*.

The second tranche of ^{14}C AMS determinations, which were analysed in order to further validate the cross-matching within each of the Salen Bay and Sound of Mull *G. humanus* chronologies, returned complementary results to the initial ^{14}C AMS determinations (see Chapter 5.2). The calibrated ^{14}C determinations provide an independent validation of the cross-matches within the Sound of Mull sclerochronology. In this sclerochronology, however, the calibrated ^{14}C determinations highlight that shell gh00024 had been spuriously cross-matched into the Salen Bay chronology (see Chapter 5.2.3) and should therefore be removed from the sclerochronology.

Taking into account the results of the cross-matching and the ^{14}C AMS determinations, two independent sclerochronologies have been constructed from the shells collected from the Sound of Mull and Salen Bay respectively (see Chapter 4.6.1). Both chronologies were constructed using the standard techniques as outlined in Chapter 3. Given the total numbers of shells successfully cross-matched within each *G. humanus* chronology (three) and the total number of shells collected at each site (22 in the Sound of Mull and 20 from Salen Bay, giving a 14% cross-match success rate), it would be necessary

to collect *ca.*86 shells at any site in order to construct a statistically robust master chronology.

6.5.2 *Glycymeris glycymeris*

Significant Pearson correlation coefficients were identified between the growth increment series recorded from the live- and dead-collected *G. glycymeris*. In total ten dead-collected *G. glycymeris* cross-matched with significant Pearson correlation coefficients. In addition to the dead-collected shells, the two long-lived *G. glycymeris* also cross-matched. However the link between the dead- and the live- collected *G. glycymeris* was of insufficient period to form a statistically robust cross-match. The two ^{14}C determinations (SUERC-28453 and SUEERC-28455), which originate from the ventral margin of the two longest-lived *G. glycymeris,* were calibrated to the post-bomb era AD 1965 – AD 1994 and AD 1968 – AD 1984. These ^{14}C determinations provided independent validation for the statistical cross-matching between the dead- and the live-collected *G. glycymeris*. It was therefore possible to construct a single absolutely dated master *G. glycymeris* sclerochronology incorporating both the dead- and live-collected shell material. The resulting series (see Chapter 4.6.2) spans the period from AD 1805 – AD 2006. The chronology EPS is greater than the recommended 0.85 over the period from AD 1880 – AD 2006. Prior to AD 1870 the EPS is reduced due to the lower sample depth within the sclerochronology despite the high Pearson correlation between the series.

6.6 Multi-species cross-matching

In addition to using a single species to build a sclerochronology, there are clear advantages in adopting a multi-species approach sclerochronology construction. The multi-species approach could allow areas to be investigated in which no great numbers of any individual long-lived species are found. By utilising numerous species from within a single hydrographic or oceanographic setting it may be possible to construct a robust and statistically significant sclerochronology.

Only a single previous study has been published that examines the inter-annual variations in growth across multiple species in an attempt to form a single

master multi-species sclerochronology. The approach taken by Witbaard *et al.*, (2006) was to build individual absolutely-dated sclerochronologies for each of three species. Each of these master sclerochronologies incorporated only live-collected specimens. Witbaard *et al.*, (2006) found, using a sign-test (percentage of common variability, given as percentage common variability or PCV) to compare between the master sclerochronologies, a similarity of 69.4 and 78.6% between a master sclerochronology constructed using *A. islandica* with two sclerochronologies constructed using the shorter-lived *Mya truncata* and *Chamelea striatula* respectively, and a similarity of 69% between the chronologies constructed using *M. truncata* and *C. striatula* from AD 1960 to 2004.

The approach adopted by Witbaard *et al.*, (2006) of comparing the master sclerochronologies indicates that there is a potential for a multi-species sclerochronology. However, the method used by Witbaard *et al.* (2006), although presenting a robust assessment of the validity of using multiple species within a single master sclerochronology, required the investigator to have enough specimens of each species to build individual single-species master sclerochronologies. Such an approach is likely to yield significant positive results providing species are used that have similar geographical ranges and that are collected from within the same hydrographic or oceanographic setting. This is because the dendrochronological statistical techniques used for constructing the master sclerochronologies use the growth signal that is common amongst the series included within the sclerochronology. This common signal, or common variability in growth, is attributed to growth that has been driven by external environmental forcing. In constructing three independent master sclerochronologies, any species specific variability in growth should be removed and thus it may be more likely that some degree of commonality is identified between the respective species if it is present at all.

An alternative approach to building a master multi-species sclerochronology is to consider the growth series of each of the separate species as a "single species", cross-matching each of the species with each other, then building the master sclerochronology using the growth series from all the cross-matched

growth series irrespective of species. This method permits a master sclerochronology to be constructed using species which are less well represented within the modern day and fossil records.

The following sub-sections discuss the cross-matches between the three species *G. humanus*, *G. glycymeris* and *A. islandica*.

6.6.1 *Glossus humanus* and *Glycymeris glycymeris*

Only the Sound of Mull *G. humanus* sclerochronology was cross-matched with the *G. glycymeris* Tiree Passage sclerochronology as the ^{14}C determinations of the shells within the Salen Bay *G. humanus* sclerochronology, which only incorporates fossil shell material, indicated that it pre-dates the *G. glycymeris* sclerochronology. The Sound of Mull *G. humanus* sclerochronology, which incorporates fossil *G. humanus* shells that were collected from outside the outer sill of Loch Sunart at the intersection with the Tiree Passage and the Sound of Mull, is in close proximity to the site of collection of the *G. glycymeris* in the Tiree Passage that constitutes the *G. glycymeris* sclerochronology. In addition the ^{14}C determinations from the Sound of Mull *G. humanus* sclerochronology show that the most modern portion of the sclerochronology is post-bomb, with sample AAR11601 from the ventral margin of shell 00013.

Given the relative difficulty in cross-matching between specimens of *G. humanus*, initial attempts at cross-matching were made between individual *G. humanus* shells and the *G. glycymeris* master sclerochronology. Figure 6 – 6 indicates significant positive correlations between the detrended growth series in the *G. humanus* sclerochronology and the absolutely dated *G. glycymeris* sclerochronology. It is noticeable, however, that the temporal stability in the Pearson correlation coefficients (calculated over a 21 year window) differs between each of the shells cross-matched, with the correlation coefficients between shell 00015 and the master sclerochronology maintained at $R>0.4$ between AD 1890-1904 before being reduced to ca. 0.25. The correlations between the longest lived *G. humanus* (00013) and the master *G. glycymeris* sclerochronology, however, were lower than of those between shell 00015 and

the master sclerochronology, but similarly showed relative temporal variability, generally varying between 0.1 -0.5 over the period AD 1890-1970.

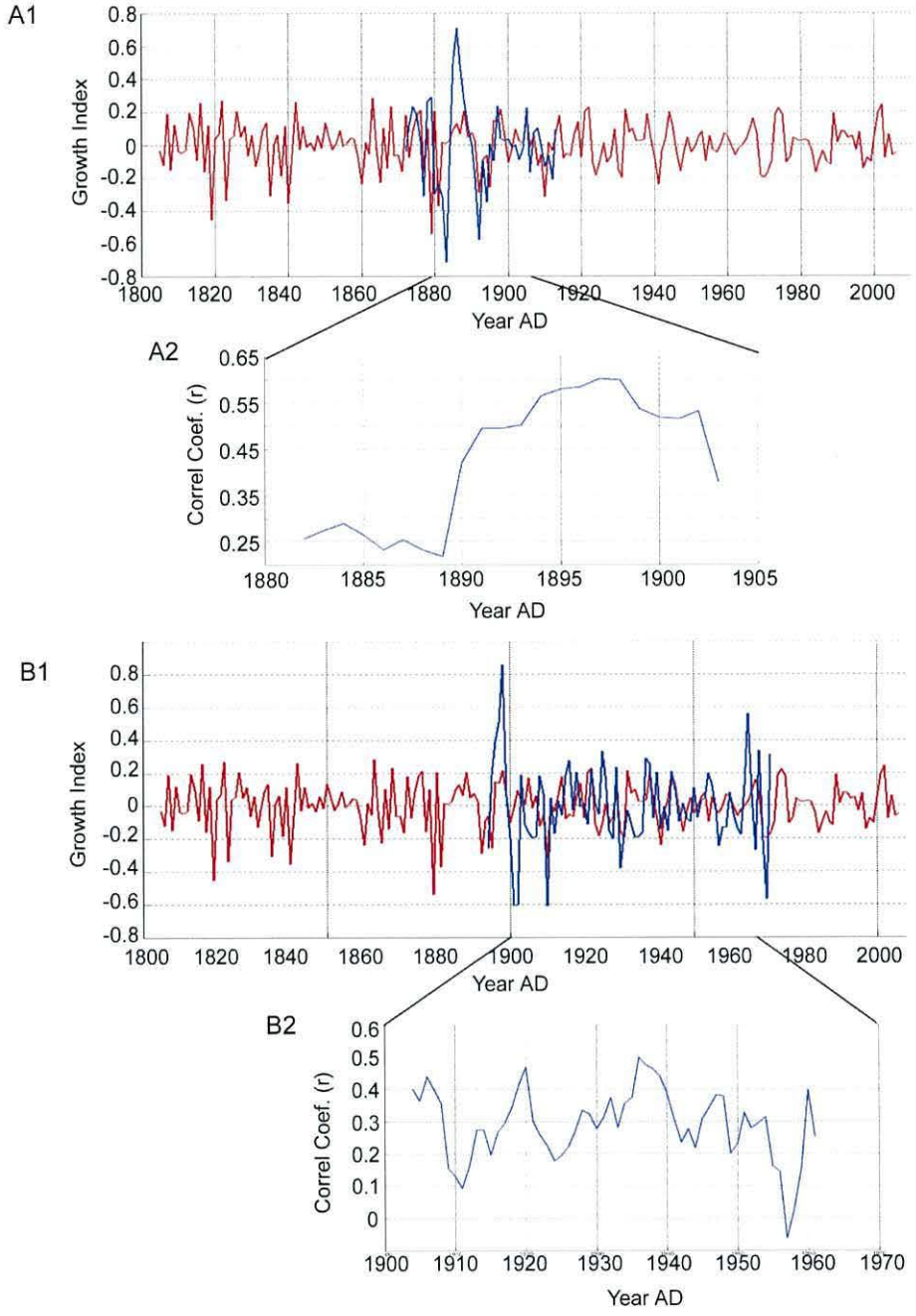

Figure 6 – 6: Graphs illustrate the cross-match identified between the Glycymeris glycymeris and Glossyus humanus. A1) Standardised growth index values for Glossus humanus 00015 (blue) and the master Glycymeris glycymeris chronology (red)); B1 Standardised growth index values from the longest lived Glossus humanus 00013 (blue) with the master Glycymeris glycymeris chronology (red): with corresponding Pearson correlation coefficients (A2 and B2 respectively). Correlations calculated over a 21-year running window.

The significant Pearson correlation coefficients between the absolutely dated *G. glycymeris* sclerochronology and the floating Sound of Mull *G. humanus* sclerochronology, in conjunction with the ^{14}C determinations within the Sound of Mull *G. humanus* sclerochronology provided a dated anchor for the Sound of Mull *G. humanus* sclerochronology.

6.6.2 *Glycymeris glycymeris* and *Arctica islandica*

Cross-matching between *G. glycymeris* and *A. islandica* shells was undertaken using the raw growth series derived from the live-collected specimens. The raw *A. islandica* and *G. glycymeris* growth series, (see Chapter 2), were cross-matched as if they had originated from a single species (see Chapter 3). Figure 6 – 7 highlights significant Pearson correlation coefficients identified between one of the live-collected *G. glycymeris* shells and two of the live- collected *A. islandica* shells. The Pearson correlation coefficients, which have been calculated using a 21-year window, are relatively stable over the *ca.*30 year period ranging from 0.6-0.85 and 0.3-0.6. This result shows for the first time, that the growth series derived from multiple bivalve species, providing they are derived from species with similar geographical range, and have been collected from within the same hydrographic or oceanographic setting, can be treated as if they were a single species within a sclerochronology. This indicates that it is possible to construct an absolutely dated multispecies master sclerochronology.

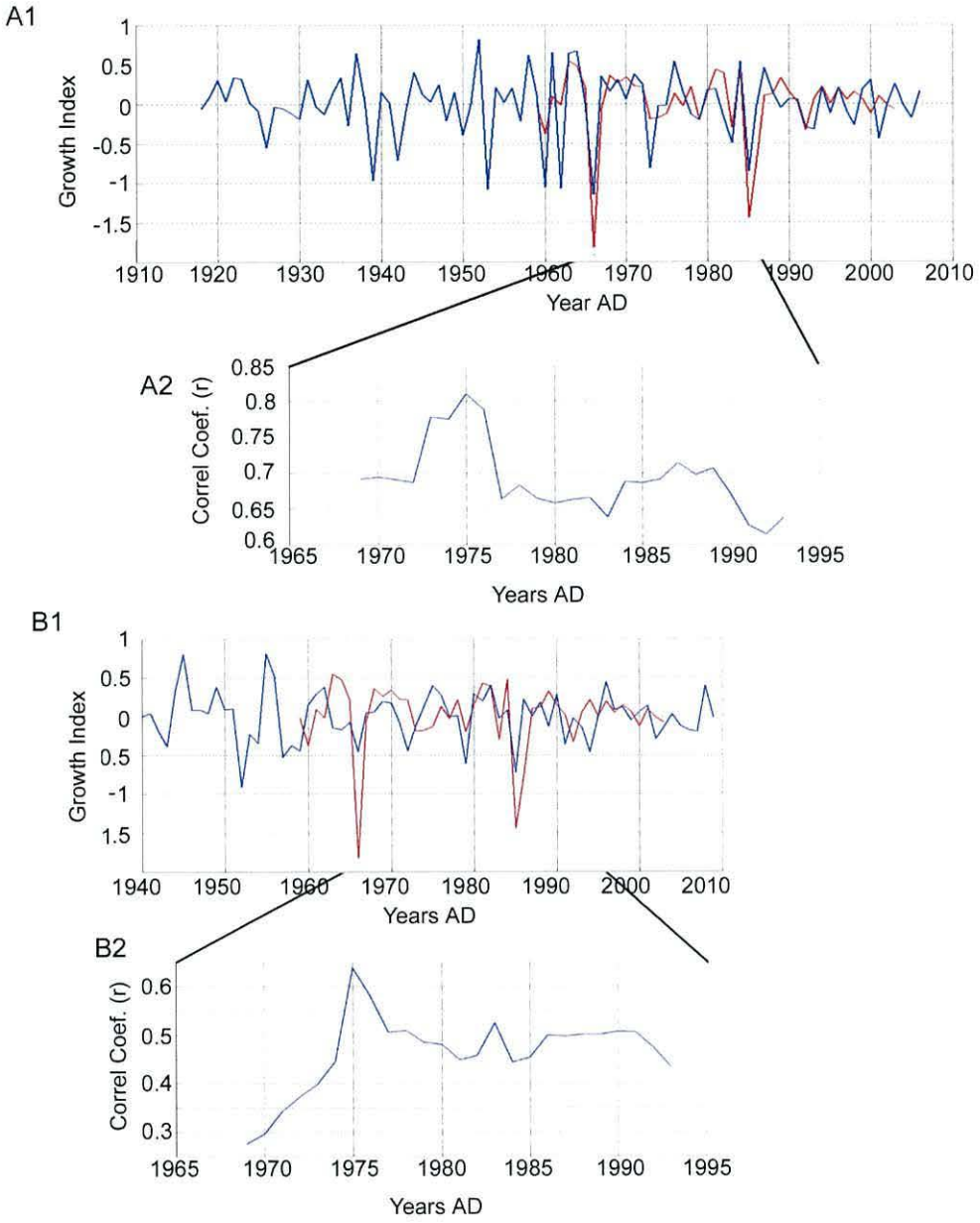

Figure 6 – 7: Graphs illustrate the cross-matchs found between Glycymeris glycymeris and Arctica islandica, A1) Standardised Growth index of Arctica islandica 100025 (blue line) with Glycymeris glycymeris 00025 (red line): and B1) Arctica islandica 108002 (blue line) with Glycymeris glycymeris 00025 (red line); with corresponding Pearson correlation coefficients (A2 and B2 respectively). Correlations calculated over a 21-year running window.

6.7 Master multi-species sclerochronology

Using all the shells that had been successfully cross-matched between the species (see Chapter 6.5) a single absolutely dated multi-species master sclerochronology was constructed using ARSTAN (for methods see Chapter 3.4).

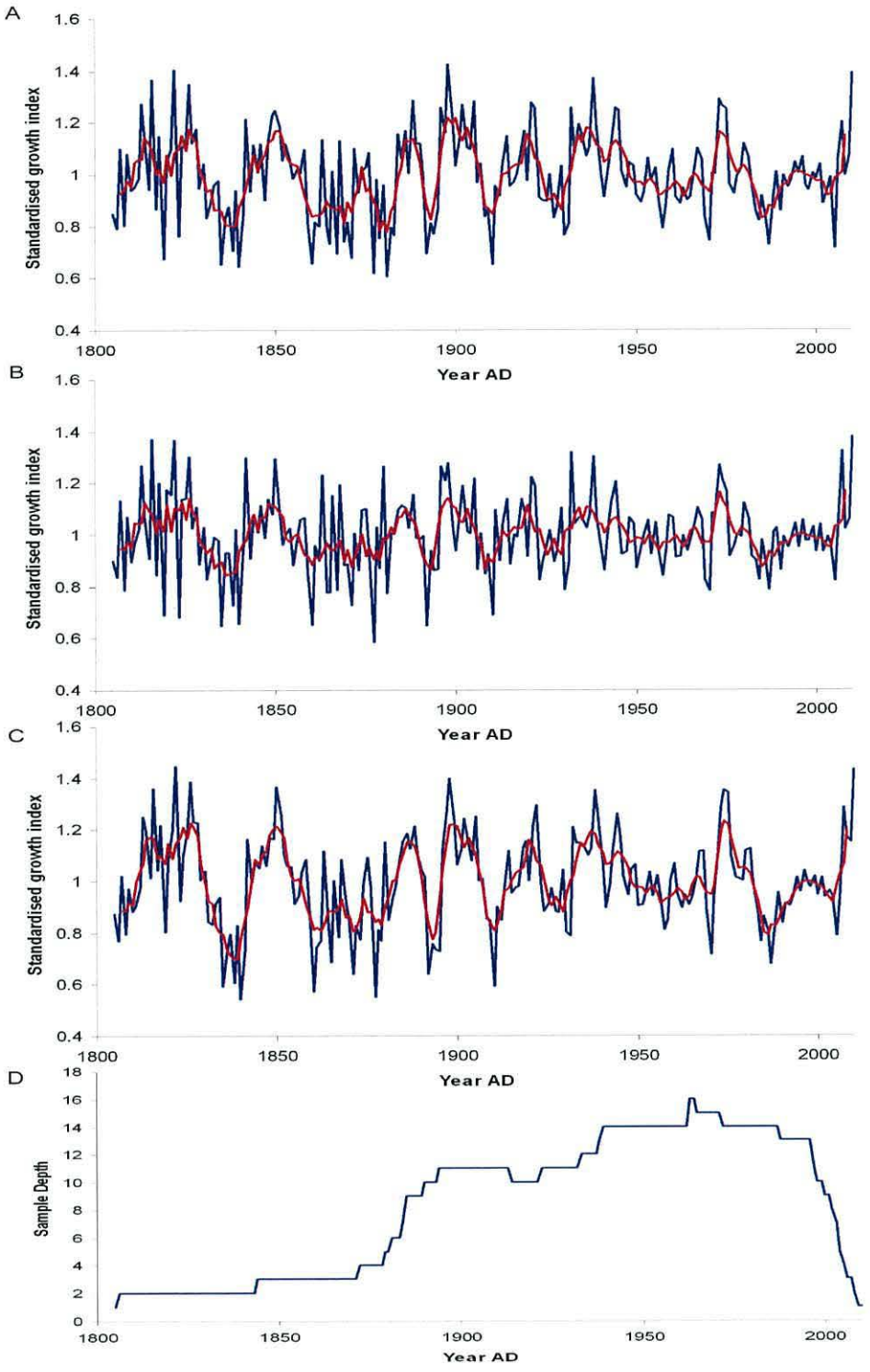

Figure 6 – 8: Arstan chronology outputs for the first multi-centennial multi-species master sclerochronology constructed from live- and dead-collected Glossus humanus, Arctica islandica and Glycymeris glycymeris from sites within the Sound of Mull/ mouth of Loch Sunart and the Tiree Passage. A) Standardised chronology; B) Residual chronology: C) Arstan chronology; and D) Running sample depth values throughout the master sclerochronology.

In total 18 shells were incorporated into the master sclerochronology including, two dead-collected *G. humanus*, four live-collected *A. islandica*, two live- and ten dead-collected *G. glycymeris*. The mean EPS for the master multi-species sclerochronologies over the entire 201 year period is 0.865, higher than the benchmark level of 0.85 suggested in the dendrochronological literature. The master sclerochronologies presented in figure 6 – 8 therefore represent the first robust multi-centennial absolutely dated multi-species master sclerochronologies.

The ability to find significant correlations between the growth patterns of different long-lived molluscs implies that a common environmental variable is forcing shell growth across all three species. This facilitates the construction of robust multi-species sclerochronologies enabling the investigation of regions where hitherto no significant numbers of any individual mollusc species have been found. It is likely, however, that the successful cross-matching between multiple species presented in this thesis and in the construction of the master multi-species sclerochronology has been aided by the fact that the geographical distribution of the species investigated are similar, being constrained to mid-latitude European coastal waters. It is likely therefore that each of the species will have a common response to fluctuations to biotic or abiotic environmental forcings.

6.8 Chronology comparisons

Each of the master sclerochronologies produced in this chapter were compared to each other as well as to an independently-produced dendrochronological record in order to assess any further temporal coherences. The dendrochronological record was obtained from Dr E. Woodley and Dr N. Loader (BGS and Swansea University respectively). It is constructed from the growth increment widths of 15 live-sampled Scots Pine (*Pinus sylvestris* L.) trees growing near Loch Hourne in the Southern Glens of western Scotland (57° 5'N 5° 9'W, 350m altitude) (Woodley, 2010). The ontogenetic growth curves were removed using standard dendrochronological techniques and master dendrochronologies constructed using Arstan (as in Chapter 3.5). The three chronologies are shown in figure 6 – 9.

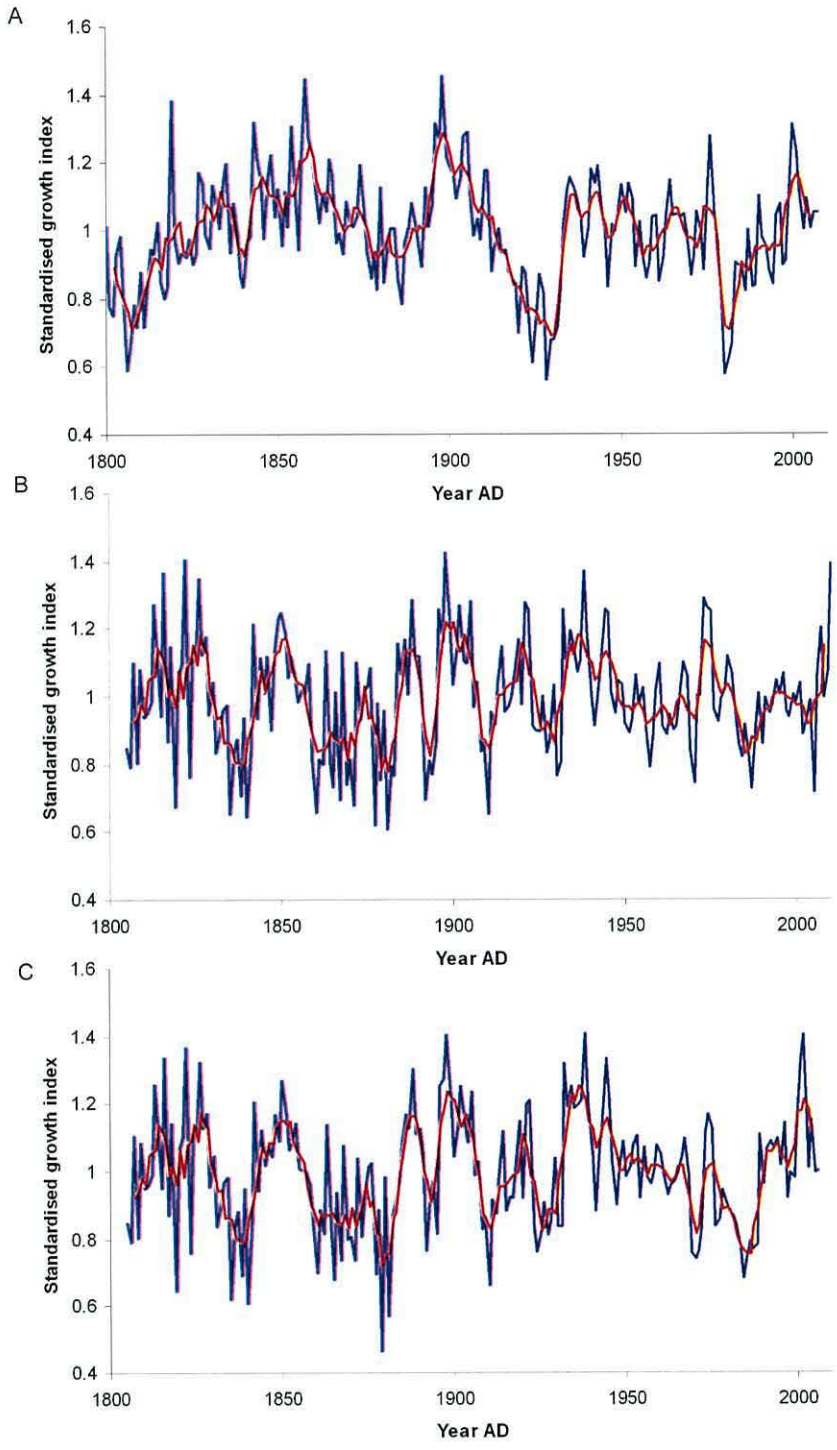

Figure 6 – 9: Graphs comparing the master chronologies constructed from A) Pinus sylvestris B) molluscan multi-species and C) Glycymeris glycymeris. The blue line represents annual standardised growth indices, the red line represents a five year moving average.

As expected significant Pearson correlation coefficients were identified between the *G. glycymeris* sclerochronology and the multi-species sclerochronology over

the entire common period (r=0.862 n=201 and P<0.005 at annual resolution and r=0.846, n=197 and P<0.005 between the five year smoothed data). Significant Pearson correlation coefficients were found between the *G. glycymeris* master sclerochronology and the *P. sylvestris* dendrochronology over the common period using both the annually resolved data and the smoothed (five year running mean) data sets, (r=0.238, P<0.005, n=201 and r=0.340, P<0.05, degrees of freedom (DF) = 40 respectively). The multi-species sclerochronology and the *P. sylvestris* dendrochronology exhibit reduced positive Pearson correlations compared with those between the *G. glycymeris* chronology and the *P. sylvestris* dendrochronology (r=0.131, n=202, p=0.032 at annual resolution and r=0.188, DF=40 and P<0.005 for the five year smoothed).

Periods of the chronology that contains fewer than three growth increment series should be treated with caution when they are compared with other archives or instrumental series as the common signal is weighted by individual growth series and thus may not be a true common signal. This generally reflected in a reduction of the (running) EPS statistic. The analysis of the *G. glycymeris* and the multi-species sclerochronologies should therefore be constrained to periods that incorporate growth series of more than three shells (AD1870-2006). Constraining the period examined to AD 1870-2006 results in an increase in the Pearson correlation coefficients between the *G. glycymeris*/multi-species sclerochronology and the *P. sylvestris* dendrochronology (annual resolution data r=0.418 and 0.266 respectively, P<0.005, n=136 and 137 respectively; five year smoothed data r=0.544 and 0.348 respectively, P<0.005 n=132 and 133 respectively). However, Pearson correlation coefficients between the *G. glycymeris* and multi-species sclerochronologies are reduced over this period with r=0.780 and 0.783 (p<0.005) at annual resolution and five-year smoothed respectively. The reduction in Pearson correlation coefficients over this period is likely due to a difference in the common signal across the multiple species that is incorporated within the sclerochronology when constructed using the Arstan program. The difference in the common signal could be a result of differing biological constraints on growth, for example, the length different growing seasons.

Chapter 7

Discussion: Palaeoenvironmental Reconstructions From Growth Increment Series

7.1 Introduction

This chapter discusses the temporal and spatial correlations between the master *G. glycymeris* chronology and the other species chronologies and compares these chronologies with localised and gridded oceanographic and meteorological instrumental datasets

7.2 SST timeseries

In order to allow the full investigation of correlations between temperature and the growth increment chronologies, timeseries other than the Tiree Passage instrumental record have also been used. Although the Tiree oceanographic mooring represents the longest current meter and specific temperature record for the NW European shelf (Inall *et al.*, 2009), the temperature record contains large periods with incomplete data or no data at all. Only using the Tiree Passage data would thus seriously constrain the growth increment temperature reconstructions and result in the construction of statistically unreliable reconstructions. Basic statistical analyses were therefore carried out to examine the temporal coherence between the Keppel Pier and North Atlantic Current sea surface temperature index (NAC SSTI) data (constructed in section 7.4.1) and the Tiree Passage data (Figure 7 – 1). Both the Keppel Pier and the NAC SSTI timeseries are of sufficient length (57 and 140 years respectively) and allow the full statistical assessment of the temporal coherence between SSTs and the growth increment chronologies.

Linear regression analysis of the three respective SST timeseries over the common period (AD 1985-2005) showed statistically significant positive correlations, r^2= 0.593 N=21 P<0.005 between Keppel and the NAC SSTI; r^2=0.81 N=13 P<0.005 Keppel Pier and Tiree Passage; and r^2=0.729 N=13 P<0.005 for the Tiree Passage and NAC SSTI. The most noticeable difference between the three timeseries is the amplitude of the overall series means, with the NAC SSTI being significantly warmer than the Tiree Passage series which is in turn warmer than the Keppel Pier series. The NAC SSTI series is warmer due to the geographical range which is incorporated within the timeseries (see section 7.4.1). However the differences between the Tiree Passage and Keppel Pier timeseries, which is the inverse of the latitudinal temperature gradient generally observed, suggests a strong component of NAC-sourced waters within the Tiree Passage which has the effect of increasing series mean. Although the direction of inter-annual variability is statistically significant and visually apparent in Figure 7 – 1, the amplitude of such changes differs substantially between series with the standard deviations for the SSTs within the Tiree Passage and Keppel Pier being 0.66 and 0.54 respectively compared to 0.25 for the NAC SSTI.

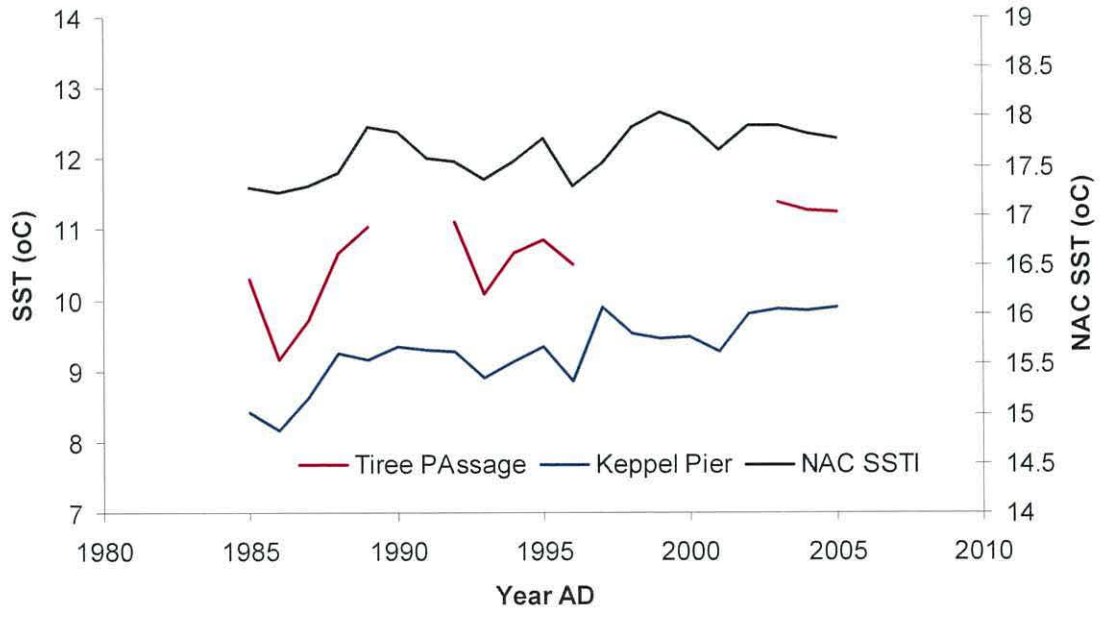

Figure 7 - 1: Mean annual Tiree Passage, Keppel Pier and North Atlantic Current SSTs for the common period of AD 1985 - 2005.

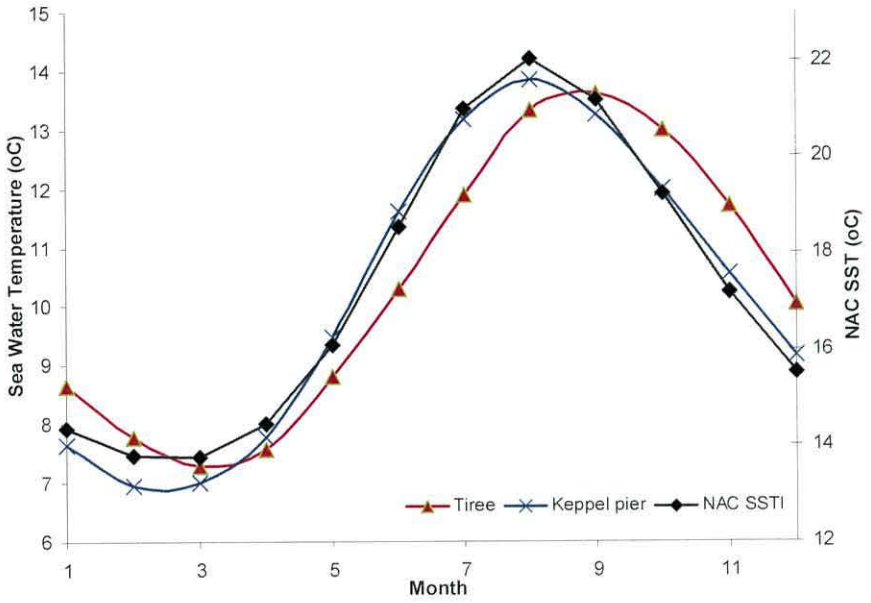

Figure 7 – 2: Mean monthly SSTs values for Keppel Pier (Blue line) and the Tiree Passage (red line) and NAC SSTI (Black line).

Figure 7 – 2 highlights notable differences in the observed seasonality within the NAC, Tiree Passage and Keppel Pier timeseries. Most notable is the temporal offset of the seasonal cycle in the Tiree Passage timeseries compared with the NAC SSTI and Keppel Pier timeseries (ca. 21 days), with the warmest month in the Keppel Pier SST record being on average August, whilst in the Tiree Passage it is September. The amplitude differences between the two timeseries are subtle, (ignoring the temporal offset). The mean summer temperatures are very similar, however the winter temperatures differ, with the more southerly Keppel Pier showing the greatest reduction in temperatures over the winter and spring months. It is likely that the warmer waters found within the Tiree Passage during winter are strongly modulated by the influx of warmer North Atlantic waters.

In conclusion, the three timeseries show significant coherence across the common period and accordingly either the Keppel Pier or the NAC SSTI can be used instead of the patchy Tiree Passage timeseries to allow a more statistically robust examination of the relationships found between the master growth increment sclerochronologies and SSTs.

7.3 Spatial correlation analysis

Spatial correlations, calculated using the Royal Netherlands Meteorological Institute KNMI Climate Explorer facility (http://climexp.knmi), were used to qualitatively assess the spatial extent of correlations between the two sclerochronologies (*G. glycymeris* and multi-species) and gridded monthly-resolved HadISST1 and CRU TS3 datasets. The KNMI facility calculates Pearson correlation values (r) between the proxy series and the target parameter within each individual grid box. The spatial resolution of the analyses is constrained by the resolution of the target parameter. The calculated Pearson correlation values are then displayed on maps. Areas that have been calculated to have statistically significant Pearson correlation values are colour coded allowing quick visual analysis of the spatial extent of Pearson correlation coefficients. The following subsections detail the spatial analysis between the two respective chronologies and sea surface temperatures, air temperatures and precipitation records.

7.3.1 Sea surface temperatures (HadISST1)

The spatial correlation analysis shows that both the *G. glycymeris* and multi-species sclerochronologies significantly correlate with the SSTs from the North Atlantic and coastal shelf seas of NW Europe over the common period of AD 1870-2006 (Figure 7 – 3 and 7 – 4). The *G. glycymeris* sclerochronology shows significant positive correlations across the N. Atlantic following the trajectory of the Gulf Stream/ North Atlantic Current (GS/NAC) (Figure 7 – 3). Peak correlations were found between the *G. glycymeris* sclerochronology and mean March to August GS/NAC SSTs. The multi-species sclerochronology appears to have reduced correlations with the GS/NAC SSTs (Figure 7 – 4) compared to those identified between the *G. glycymeris* sclerochronology and the GS/NAC SSTs. There are subtle differences in the degree of the correlations within the Baltic Sea area, with the multi-species sclerochronology appearing to correlate more strongly. Peak correlations between the multi-species sclerochronology and HadISST1 SSTs are, as with the *G. glycymeris* sclerochronology, with mean March to August SSTs.

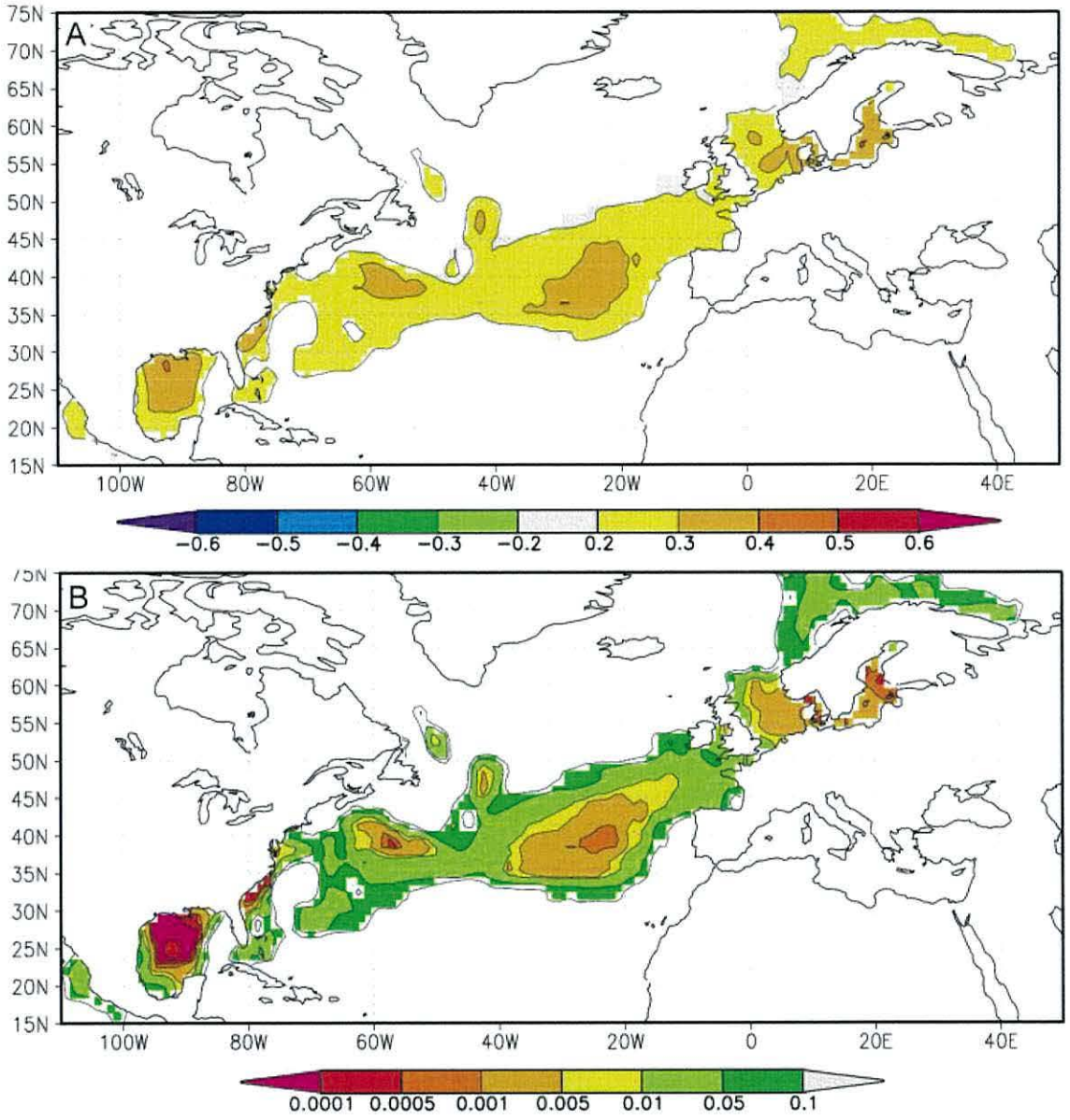

Figure 7 - 3: A) Average correlation values calculated using the KNMI spatial correlation model between mean March to August HadISST1 SSTs and G. glycymeris mean standardized growth index between AD 1870 and 2006; and B) corresponding probability values. Regions with correlation of ~zero are white.

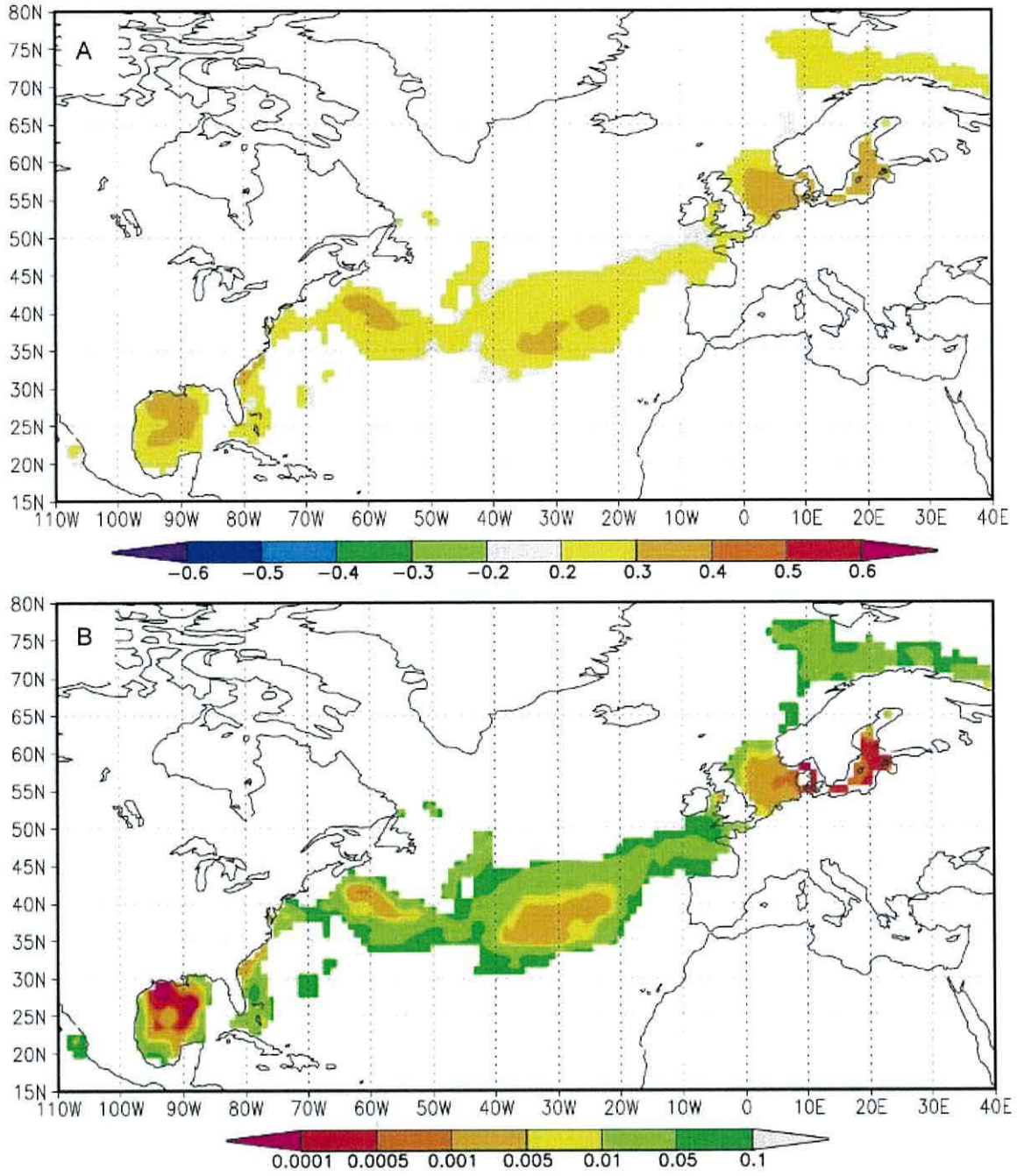

Figure 7 - 4: A) Average correlation values calculated using the KNMI spatial correlation model between mean March to August HadISST1 SSts and multi-species mean standardized growth index between AD 1870 and 2006; and B) corresponding probability values. Regions with correlation of ~zero are white.

7.3.2 Air temperature (CRU TS3)

Spatial correlation analysis between the *G. glycymeris* and multi-species sclerochronologies with the CRU TS3 monthly air temperature dataset shows

significant positive correlation coefficients over the common period (AD 1901 – 2006), (Figure 7 – 5). Peak correlations were identified between the *G. glycymeris* sclerochronology with mean November to March air temperatures in northwest Scotland, Scandinavia and to a lesser extent from northern France extending across to NW Russia.

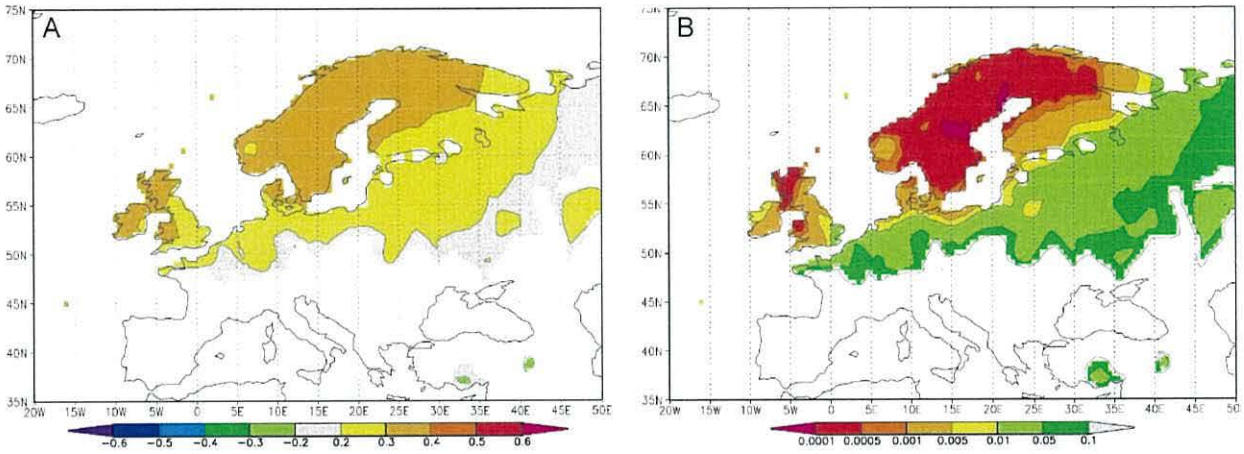

Figure 7 – 5: A) Spatial correlation coefficients and B) associated probabilities calculated between CRU TS3 gridded air temperature series (0.5° spatial resolution) for mean November to April air temperatures AD 1901-2006 and the G. glycymeris master sclerochronology. Regions with correlation of ca.0 are white.

Significant Pearson correlations were also identified between the multi-species sclerochronology and mean November to April air temperatures (CRU TS3) over NW Europe (Figure 7 – 6). The correlations identified in Figure 7 – 6 appear to be spatially inconsistent (most notably in Figure 7 – 6B). The *G. glycymeris* sclerochronology exhibits consistent strong correlations across Northern Scandinavia which is reflected in the probabilities which are similarly consistent across the Scandinavian region ((Figure 7 – 5B). Despite the overall reduction in spatial stability, the multi-species sclerochronology more strongly correlates with mean November to April air temperatures across NW Scotland. This trend is likely due to the incorporation of the *A. islandica* and *G. humanus* shells from the outer sill of Loch Sunart. One theory for this would be that the common growth signal within the *A. islandica* and *G. humanus* shells is more strongly related to localised climatic variability within Loch Sunart, whilst the *G.*

glycymeris growth signal reflects the larger scale climate variability due to the open nature of the Tiree Passage site and its connection with the NAC linked to N. Atlantic weather systems. Alternatively *G. humanus* and *A. islandica* growth may be less sensitive to climatic variability across larger spatial extents due to being more infaunal species compared to *G. glycymeris*.

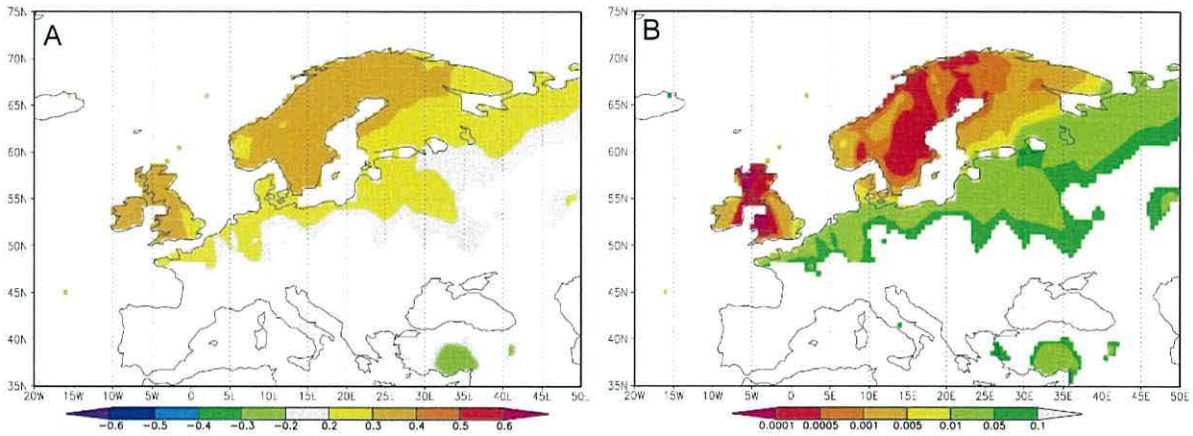

Figure 7 – 6: A) Spatial correlation coefficients and B) associated probabilities calculated between CRU TS3 gridded air temperature series (0.5° spatial resolution) for mean November to April air temperatures AD 1901-2006 and the multi-species master sclerochronology. Regions with correlation of ca.0 are white.

7.3.3 CRU TS3 Precipitation

The spatial correlation analysis shows significant Pearson correlations between both the *G. glycymeris* and multi-species sclerochronologies with CRU TS3 precipitation across Europe (Figure 7 – 7 and 7 – 8). The *G. glycymeris* sclerochronology shows significant positive correlations with mean February to June precipitation along the Norwegian coastline, whilst over the same period significant positive correlations are identified for precipitation over coastal Portugal and Spain and NW France. This precipitation trend is consistent with North Atlantic Oscillation (NAO) variability (Hurrell an Van Loon 1997).

Figure 7 – 8 identifies that, similarly to the *G. glycymeris* sclerochronology, the multi-species sclerochronology shows significant positive Pearson correlations with precipitation in coastal Norway as well as significant negative correlation over central France. Interestingly, however, the timing of the peak positive and

negative correlations differ with peak positive correlations being with mean February to June and the peak negative correlation being with mean March to July precipitation.

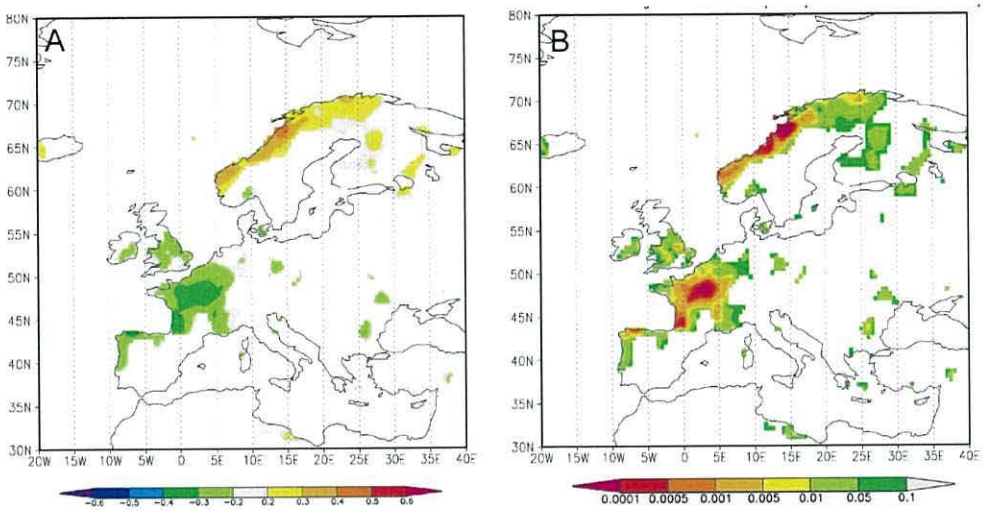

Figure 7 - 7: A) Spatial correlation coefficients and B) associated probabilities calculated between CRU TS3 gridded precipitation series (0.5° spatial resolution) for mean February to June precipitation AD 1901-2006 and the G. glycymeris master sclerochronology. Regions with correlation of ~zero are white.

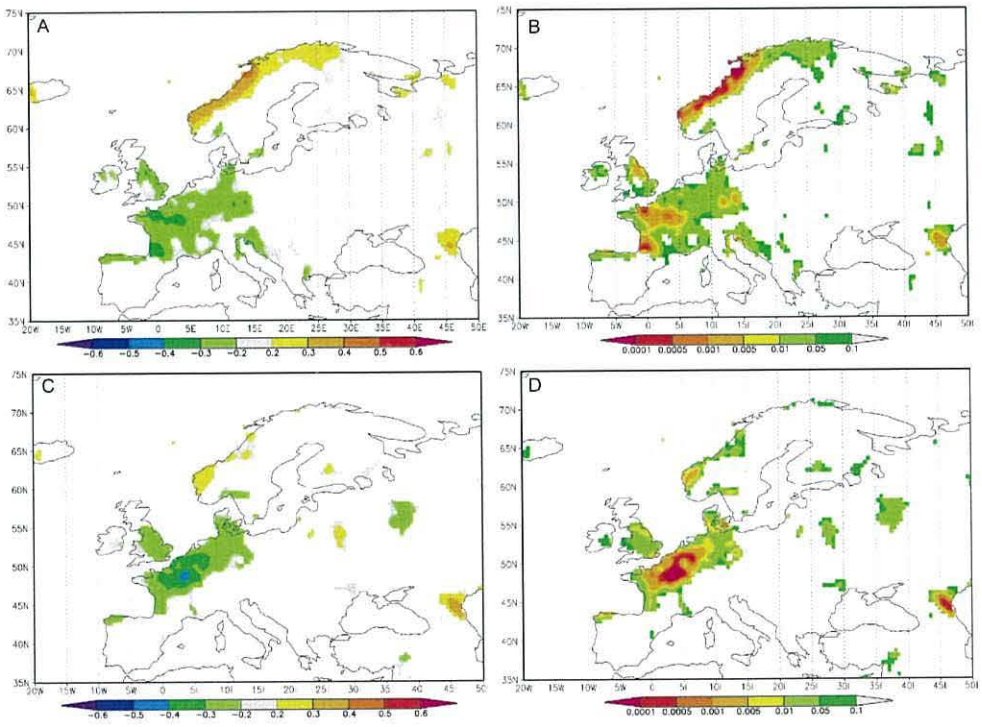

Figure 7 - 8: Spatial correlation analysis between the multispecies sclerochronology and A) mean February to June and C) mean March to July CRU TS3 precipitation timeseries AD 1901-2006. B and D) display the corresponding probability values. Regions with correlation of ~zero are white.

Despite both chronologies significantly correlating with CRU TS3 precipitation, it was considered inappropriate to attempt to reconstruct precipitation using either of the sclerochronologies. The principal reason for this is that the correlations identified between the SSTs and air temperature are stronger than those with the CRU TS3 precipitation data, as might be expected for a marine proxy.

7.4 Temporal stability of correlations

In order to precisely quantify and assess the temporal stability of the correlations identified by the spatial correlation analysis, composite temperature series were constructed using the methods described in Chapter 3.6. The North Atlantic Current sea surface temperature index (NACSSTI) was constructed from the mean of eleven 10° x 10° composite grid boxes from the HadISST1 monthly sea surface temperature data (1° raw spatial resolution). A NW European winter air temperature (NWEWAT) index was constructed from four 10° x 10° sub grid boxes of CRU TS3 monthly air temperature data (0.5° raw resolution). The following two sections (7.4.1 and 7.4.2 for SST and air temperatures respectively) discuss the results of the temporal analysis of the resulting composites.

7.4.1 North Atlantic Current sea surface temperatures

Examination of the Pearson correlation coefficients (r) calculated between the *G. glycymeris* sclerochronology and the NACSSTI over the common period (AD 1870-2006) identified the strongest positive correlations between the individual months of March through to September excluding June (Figure 7 – 8). The strongest seasonal correlations were identified between the *G. glycymeris* chronology and mean annual, spring (mean March to May) and summer (mean June to August) SSTs. The highest correlation identified was with the "growing season" of March to August ($r=0.391$ $n=137$ and $P<0.005$) as well as spring ($r=0.387$ $n=137$ and $P<0.005$).

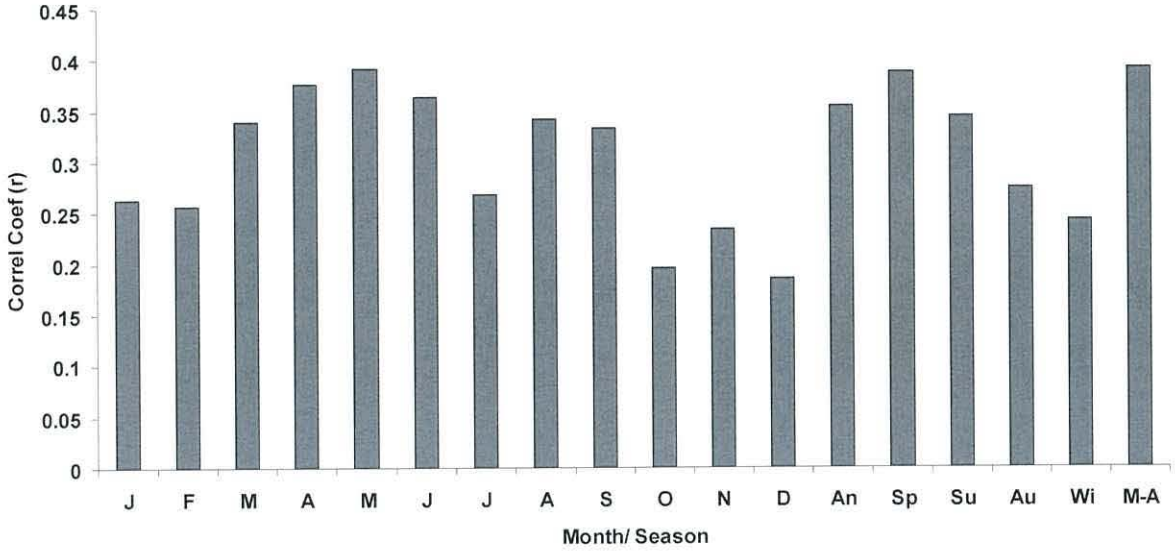

Figure 7 – 9: Pearson correlation coefficients calculated between the G. glycymeris chronology and the NACSSTI over the entire common period (AD 1870-2006, n = 137). For a 99% significance level the critical R = 0.2 (n=136).

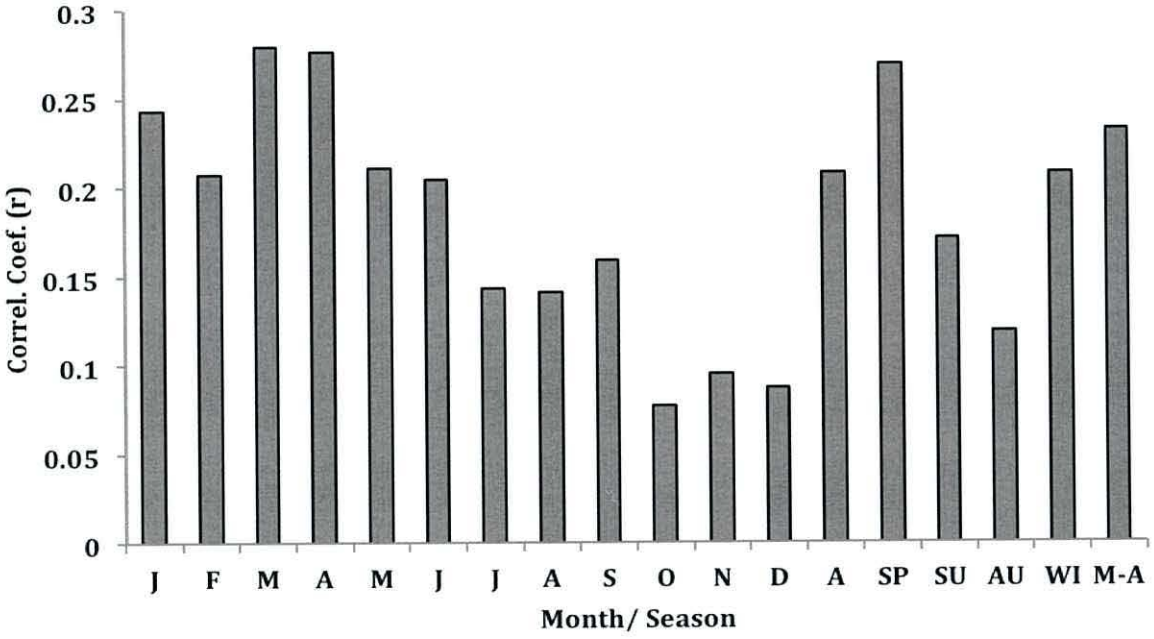

Figure 7 – 10: Pearson correlation coefficients calculated between the multi-species sclerochronology and the NACSSTI over the common period AD 1870-2006. For a 99% significance level the critical R = 0.2 (n=136).

Although the spatial analysis techniques identified significant correlations between the NACSSTI and the multi-species sclerochronology (see section 7.3.1), quantitative assessment of the correlations per month, season and presumed growing season (March to August) shows that for the majority of the

months and seasons the correlations are no higher than would be expected from a randomly generated series. The months of March and April, as well as the spring season, do however show significant correlations (r=0.279, 0.276 and 0.269 respectively, n= 136 and P<0.005). The relative reduction in correlation between NAC SSTs and the multispecies sclerochronology compared to the *G. glycymeris* sclerochronology is likely due to the reduced influence of the NAC within Loch Sunart on the *A. islandica* and *G. humanus* shell growth. As such it is probable that the common growth signal identified within the multi-species sclerochronology may represent a climatic signal with a more acute spatial range. The weaker correlation precludes the use of the multi-species sclerochronology for reconstructing NAC SSTs.

Despite the highly significant nature of the correlations between the *G. glycymeris* sclerochronology and mean March to August NAC SSTS over the entire common period, analysis of the 15-year and 21-year running Pearson correlation coefficients identified temporal instabilities (Figure 7 – 11). Despite these minor temporal instabilities, examination of the correlation statistics using calibration verification techniques (see Chapter 3.7 and 3.9) identified significant positive correlations over both the calibration and verification periods (r=0.49 and 0.47, σ=0.16 and 0.21 respectively) (calibration period AD 1940-2006 and verification period AD 1870-1939).

Linear regression analysis between the 21-year running Pearson correlation coefficients, calculated between the NACSSTI and the *G. glycymeris* sclerochronology, and low pass filtered (21-year moving average) Atlantic Multi-decadal Oscillation (AMO, see Chapter 2.10) index indicates a highly significant positive correlation (r=0.822, n=115, P<0.005). Such a significant relationship might imply that AMO cyclicity has a major influence on the water masses within the Tiree Passage and the Hebridean shelf. Periods of positive AMO denote periods of increased strength of the NAC system, which correspond to periods with the strongest correlation between the *G. glycymeris* series and the NACSSTI. These define periods with enhanced incursions of NAC waters onto the Hebridean shelf. These conditions could provide more optimal conditions for planktonic growth providing increased food availability for the *G. glycymeris*

population. Conversely however, and more significantly, during periods when the AMO is reduced or negative, the *G. glycymeris* sclerochronology has little coherence with the NACSSTI series. The degree of correlation between the *G. glycymeris* sclerochronology and NAC SSTI during the periods of reduced AMO is often no greater than can be attributed to chance, and as such a reconstruction based on those periods would be statistically non-robust.

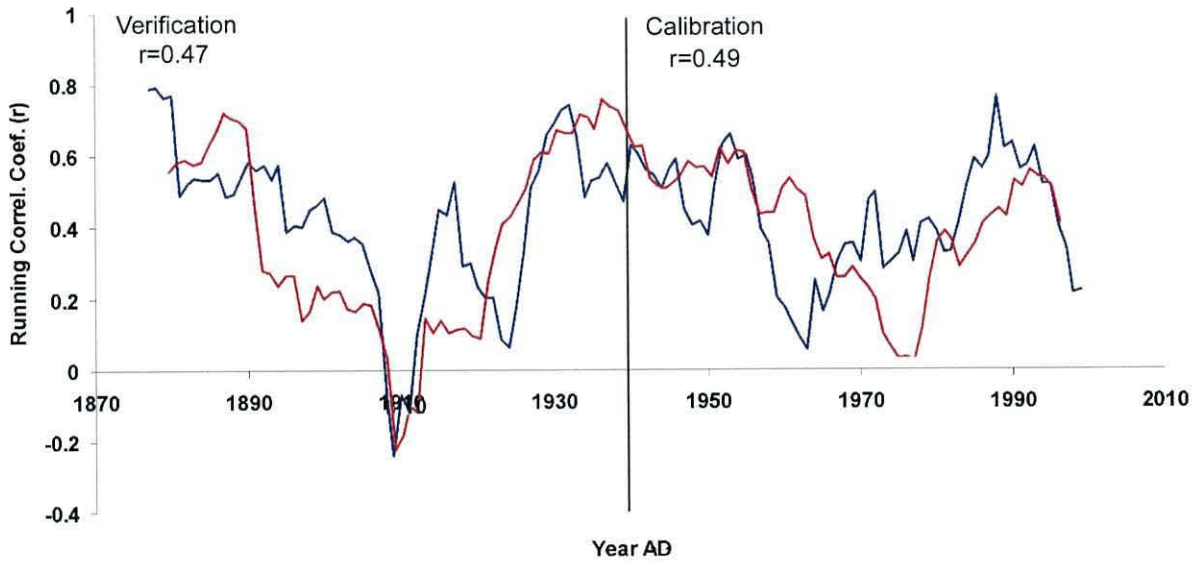

Figure 7 – 11: Fifteen year (blue line) and 21-year (red line) running Pearson correlation coefficients (r) calculated between the G. glycymeris series and mean March to August NAC SSTs. Mean correlation coefficients over the calibration and verification periods are 0.49 and 0.47 respectively (calibration period AD 1940-2006 and verification period AD 1870-1939).

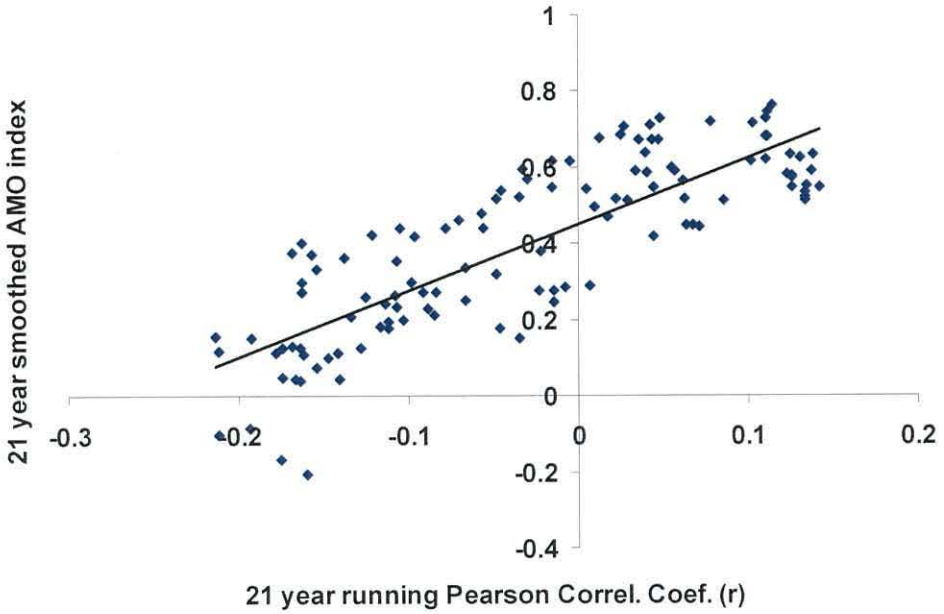

Figure 7 – 12: Linear regression analysis between the 21 year running Pearson correlation coefficients, calculated between the NACSSTI and the G. glycymeris series, with low pass filtered (21-year running mean) AMO index . The regression line can be described by the equation y = 1.741x + 0.4521 (r=0.822, DF=6, P<0.05).

Figure 7 – 13 presents the linear regression and data-scaled *G. glycymeris* derived NACSSTI reconstructions, both at annual resolution (blue lines) and with 5-year smoothing (red lines). Although the inter-annual variability within each reconstruction is identical, the standard deviation for the data scaling reconstruction (σ=0.344) is more than double that of the linear regression reconstruction (σ=0.161). this difference is implicit to the methods of reconstruction, with the data scaling method depicting the full amplitude of the variability within the target parameter, whilst the linear regression reconstruction is regarded as generally containing more precision and skill (Esper *et al.*, 2005). The robustness of each chronology is discussed in section 7.5.

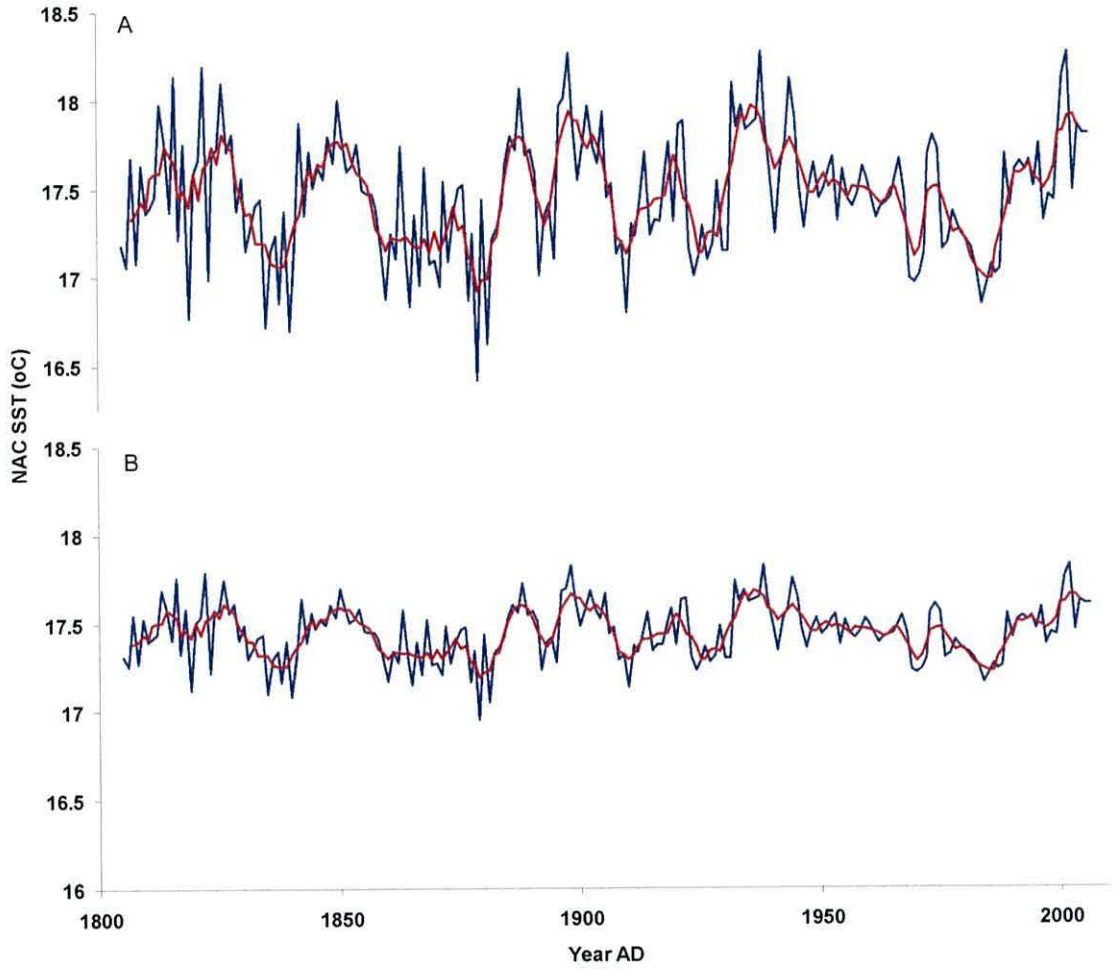

Figure 7 – 13: annually reconstructed NAC SSTs (blue line) with five-year running average (red) line constructed from the G. glycymeris sclerochronology using A) data scaling and B) linear regression methods.

7.4.2 Air temperature

Quantitative analysis of the Pearson correlation coefficients between the *G. glycymeris* sclerochronology and mean monthly and seasonal CRU TS3NW European air temperatures identified statistically significant positive correlations over the common period (AD 1901-2006). Figure 7 – 14 indicates that the *G. glycymeris* series most strongly correlates with mean November to April, annual and winter air temperatures ($r=0.362$ and 0.357 respectively, $n=105$ and $P<0.005$).

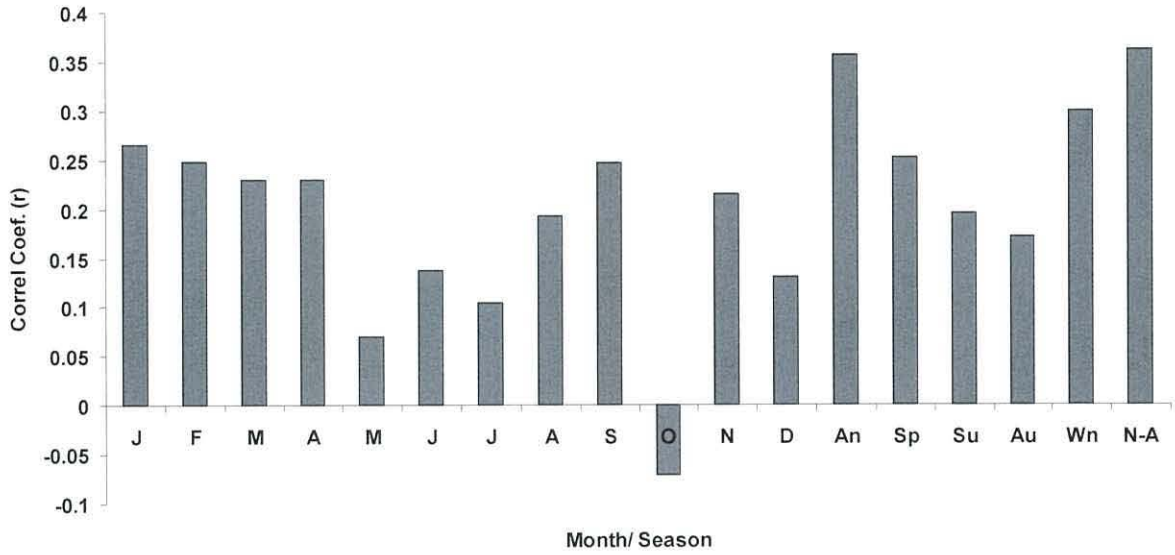

Figure 7 - 14: Pearson correlation coefficients calculated between the G. glycymeris and mean monthly and seasonal composite air temperatures for Britain/ Scandinavia constructed from the CRU TS3 dataset calculated over the entire period (AD 1901-2006, n=106). Critical R = 0.23 (n=106 and P<0.01).

The Pearson correlation coefficients calculated between the multi-species sclerochronology and NW European monthly and seasonal air temperatures (Figure 7 – 15) indicates a reduction in correlations compared within the *G. glycymeris* series. It is likely that, as with the SSTs, this reduction is due to the influence of environmental factors within Loch Sunart on the shell growth of *A. islandica* and *G. humanus*. It is therefore likely that the climate forcing which is driving the growth in these species reflects a more localised microclimate and thus it is probable that the reconstructions based on the multi-species sclerochronology relate to local conditions for the same reasons as mentioned in section 7.3.2.

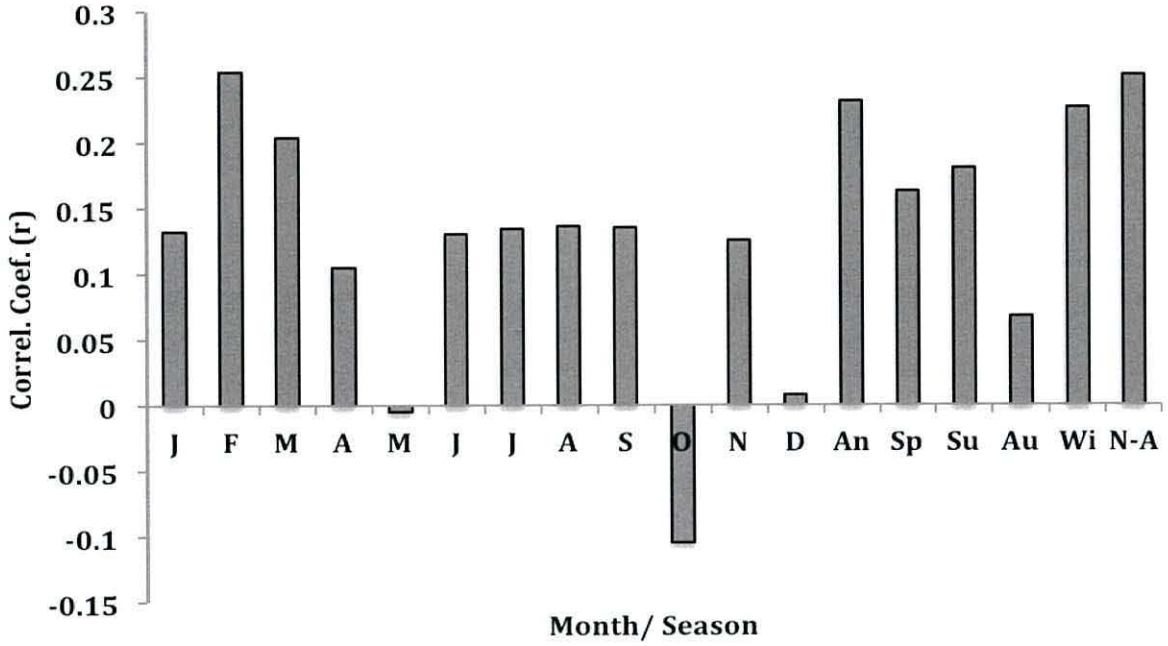

Figure 7 – 15: Pearson correlation coefficients (r), calculated between monthly and seasonal NW European air temperatures (CRU TS3) and the multi-species master sclerochronology over the common period of AD 1901-2006. Critical R = 0.23 (n=106 and P<0.01).

The running correlations between the *G. glycymeris* sclerochronology and the mean November to April air temperature in NW Europe (Figure 7 – 13), show significant temporal instabilities. Examination of the mean Pearson correlation coefficients over the calibration and verification period indicates a significant drop in the correlations from the calibration to the verification period (r=0.47 and 0.29 respectively). The standard deviation of the 15-year running Pearson correlation coefficients over their calibration and verification periods are σ=0.21 and σ=027 respectively. An attempt was made to ascertain the nature of the reduction in Pearson correlations across this period calculated by means of linear regression analysis with other climatological parameters. Figure 7 – 17 indicates that there is an insignificant positive correlation between the 21-year running Pearson correlation coefficients calculated between the *G. glycymeris* sclerochronology and the mean November to April air temperatures within NW Europe, and the AMO index (r=0.324 DF=4 and P>0.05).

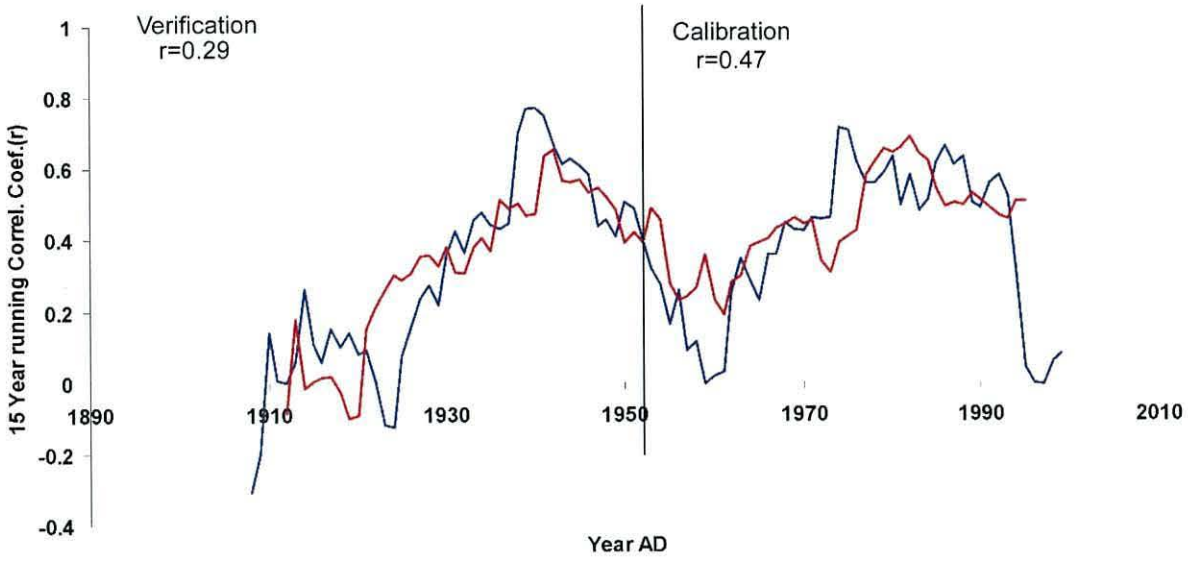

Figure 7 – 16: Fifteen-year (blue line) and 21-year (red line) running Pearson correlation coefficients (r) calculated between the G. glycymeris sclerochronology and mean November to April NW European air temperatures. Mean Pearson correlation coefficient over the calibration and verification periods are r=0.47 and 0.29 respectively (calibration period is AD 1953-2006 and verification period AD 1902-1952).

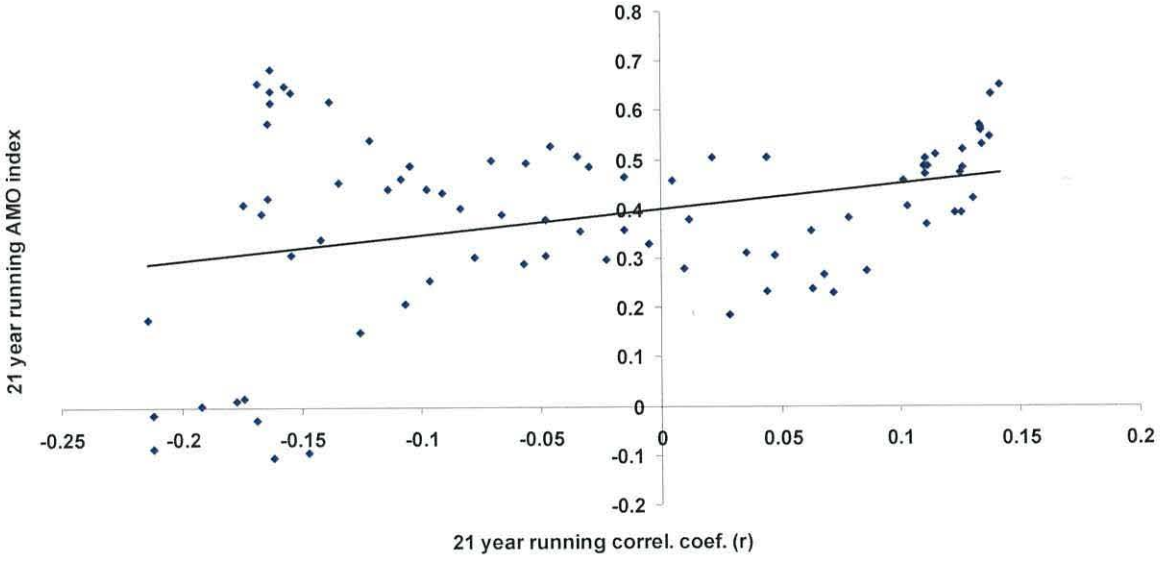

Figure 7 – 17: Linear regression analysis between 21-year running Pearson correlation coefficients, calculated between the G. glycymeris sclerochronology and mean November to April NW European air temperatures, and the AMO index which has been low pass filtered (21-year running average). The regression line can be described by the following equation y = 0.5209x + 0.4 (r=0.324 DF=4 and P>0.05).

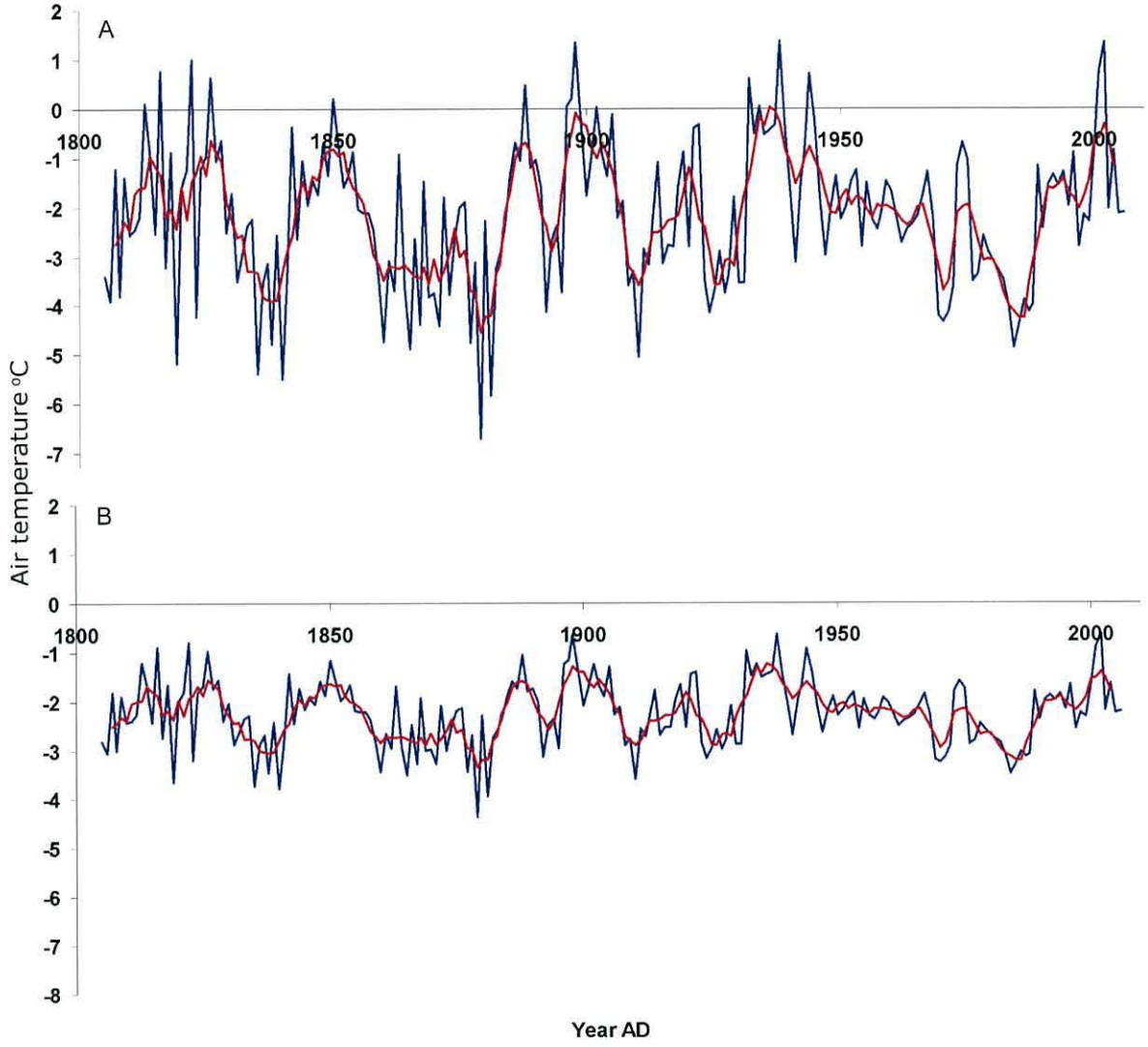

Figure 7 – 18: Reconstructed mean November to April NW European November to April air temperatures (blue line) with five-year running average (red) line constructed from the G. glycymeris sclerochronology using A) data scaling and B) linear regression methods.

7.5 Assessment of reconstruction precision and skill

Standard dendrochronological methods for the analysis of reconstruction precision and skill (reduction of error and coefficient of efficiency statistics) were used to assess the reliability of each of the reconstructions described in sections 7.4.1 and 7.4.2. For detailed methods see Chapter 3.9 or NRC (2006).

In order to get a true assessment of the precision and skill of any proxy reconstruction the RE, CE and Pearson correlations need to be taken into account to provide the assessment of proxy-target coherence across the widest spectrum of frequency domains. Table 7 – 1 provides the details of each of the

tests which need to be considered. The correlation coefficients assess the ability of the proxy to accurately represent the direction of the inter-annual variability within the target parameter; this encompasses the highest frequency domain. The coefficient of efficiency statistics assess the ability of the proxy to accurately detect long term shifts within the mean values over the calibration and verification periods. A CE or RE of ≤0 implies that the proxy is the same (if zero) or worse than (if <0) using a linear reconstruction based on the target parameters mean value over that period. If the RE statistic is >0 but the CE statistic is <0 it would imply that the proxy has predictive skill over the calibration period, but does not have the sensitivity to detect the shift in the mean between the calibration and verification period. The RE and CE statistics therefore examine the mid to low frequency precision and skill of the proxy reconstruction. Values for mean squared error are also given which provide a quantitative assessment for the mean error (in °C) incorporated within the proxy reconstructions.

Reconstruction	**Correlations**	**MSE**				
	r (r^2)	**Linear reg.**	**Scaled**		**Linear reg.**	**Scaled**
NWEAT.						
1902-1953	0.29 (0.0841)	1.15	2.28	**CE**	-0.04	-1.05
1954-2006	0.47 (0.2209)	1.27	1.747	**RE**	0.21	-0.08
NACSSTI						
1870-1939	0.47 (0.2209)	0.132	0.21623	**CE**	-1.49	-3.08
1940-2006	0.49 (0.2401)	0.058	0.0809	**RE**	0.31	0.04

Table 7 – 1: Correlation coefficients (r and r^2), reduction of error (RE) and coefficient of efficiency (CE) statistics and the mean squared error (MSE) calculated for the reconstructions derived from the G. glycymeris chronology using both the data scaling and linear regression techniques over the defined calibration and verification periods.

Examination of the RE statistics (Table 7 – 1) demonstrates that all of the proxy reconstructions derived from the *G. glycymeris* sclerochronology, bar the scaled NWEAT, contain greater precision than a linear reconstruction based on the target parameter mean value over the calibration period. All the proxy reconstructions contain CE statistics <0, however, implying that over the verification period the proxy reconstructions (which are based on the proxies

relationship to the calibration period only) are worse than a linear reconstruction based on the mean value calculated over the calibration period. This suggests that none of the reconstructions are sensitive to subtle changes in the long-term mean. Examination of the Pearson correlation coefficients, which are consistently significant over both the calibration and verification periods for both the NWEAT and the NACSSTI, suggests that the *G. glycymeris* record does contain predictive skill for reconstructing the inter-annual fluctuations within the target series. Figure 7 – 15 illustrates the clear differences between the coherence of the reconstructions and the target parameters across frequency domains (raw data, high pass filtered and low pass filtered).

In terms of actual error within the proxy reconstructions, both the linear regression and the scaled reconstructions of NACSSTI contain very low (MSE <0.1°C during the calibration period and 0.13 and 0.21°C over the verification period). The decrease in the precision over the verification period is due to the inability of the reconstruction to fully follow the low frequency variability within the target parameter. The reconstructions of the NWEAT contain more error, with values being >1°C using both the scaled and linear regression methods over both the calibration and verification period.

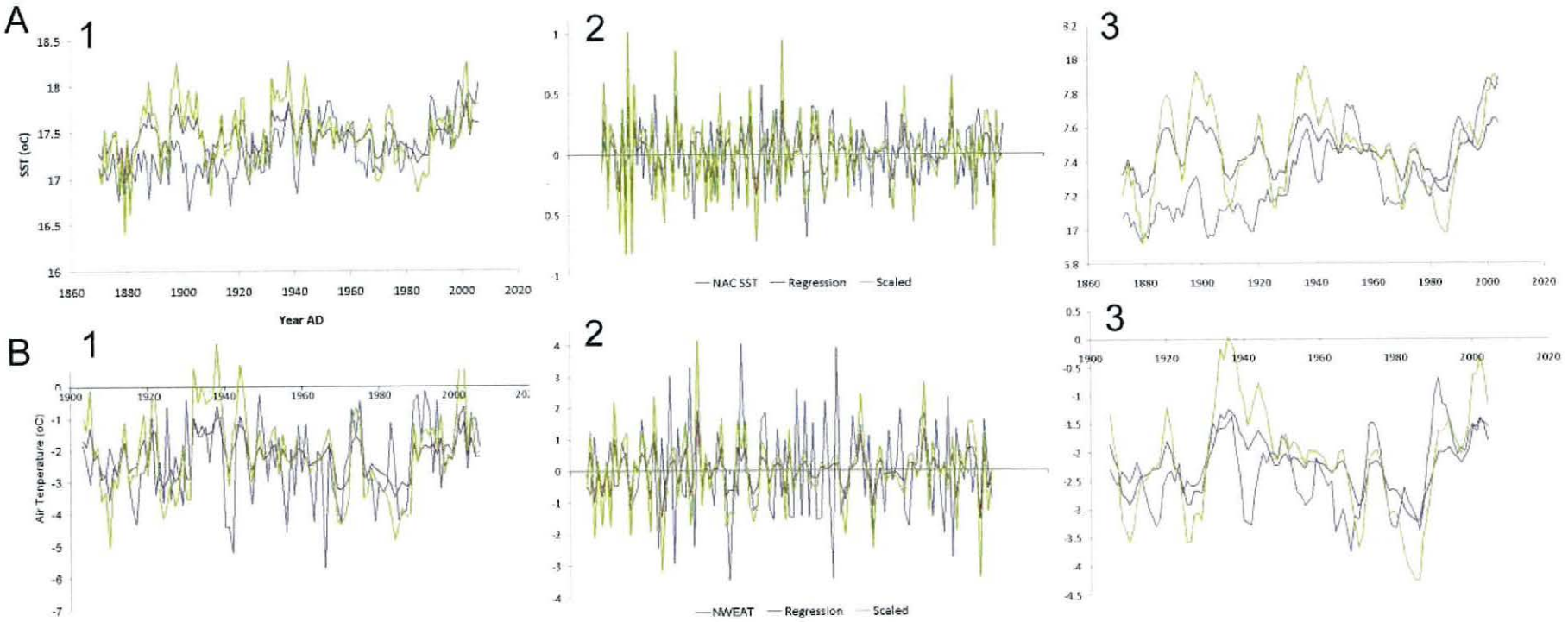

Figure 7 – 19: Differences in the coherence between 1) the raw climatic indices (blue line), linear regression reconstruction (red line) and scaled reconstruction (green line); 2) high pass filtered (first differenced, inter annual variability): and 3) low pass filtered (five year running mean) for A) NACSSTI and B) NWEAT.

Chapter 8

Discussion: Geochemistry

8.1 Introduction

The radiocarbon determinations used to verify independently the nature of the cross-matching, presented in chapter four, are used to determine the localised offset from the global marine reservoir (ΔR). These values are compared with previously published values for Scottish coastal waters. Analyses of stable isotopic concentrations presented in Chapter Four are compared with other geochemical archives from Scotland and the Irish Sea.

8.2 Radiocarbon ΔR

Determinations of the regional offset from the global marine reservoir (ΔR) are invaluable for facilitating more accurate ^{14}C dating calibrations as well as for indicating long term shifts in water masses (Wanamaker *et al.*, submitted). Radiocarbon determinations derived from dendrochronological sources have been fundamental in providing ^{14}C determinations from absolutely-dated material for the construction of robust ^{14}C calibration curves. The homogeneous distribution of atmospheric ^{14}C is not, however, reflected within aquatic or marine systems, with temporal offsets in the distribution of modern ^{14}C within the hydrosphere throught about by varying rates of mixing brought about by the various transport mechanisms such as rivers, ice caps and oceanic currents. Although marine derived ^{14}C determinations can be calibrated using various marine ^{14}C calibration curves, such as Marine04 (Hughen *et al.*, 2004)) and Marine09 (Reimer *et al.*, 2009), these curves are based on a mean global marine reservoir for the surface mixed layer based on box modelling. Such a

calibration can over simplify the marine reservoir as it assumes a homogeneity of modern ^{14}C throughout the hydrosphere which within shallow coastal waters (or indeed any other location) may be incorrect. Sclerochronological archives can provide a powerful tool for investigating regional ΔR values as they can provide absolutely dated calcium carbonate samples from which ^{14}C dates can be derived to provide calibration based on empirical observations rather than modelling. Comparison of the observed ^{14}C determination with that predicted by the marine calibration curve for the given sample year allows the localised offset from the marine ΔR to be calculated (see Equ. 8.1).

Equ 8.1 $$\Delta R = A_{sample} - A_{marine}$$

where A_{sample} represents the uncalibrated ^{14}C determination of the sample and A_{marine} represents the corresponding ^{14}C age from the associated calibration curve.

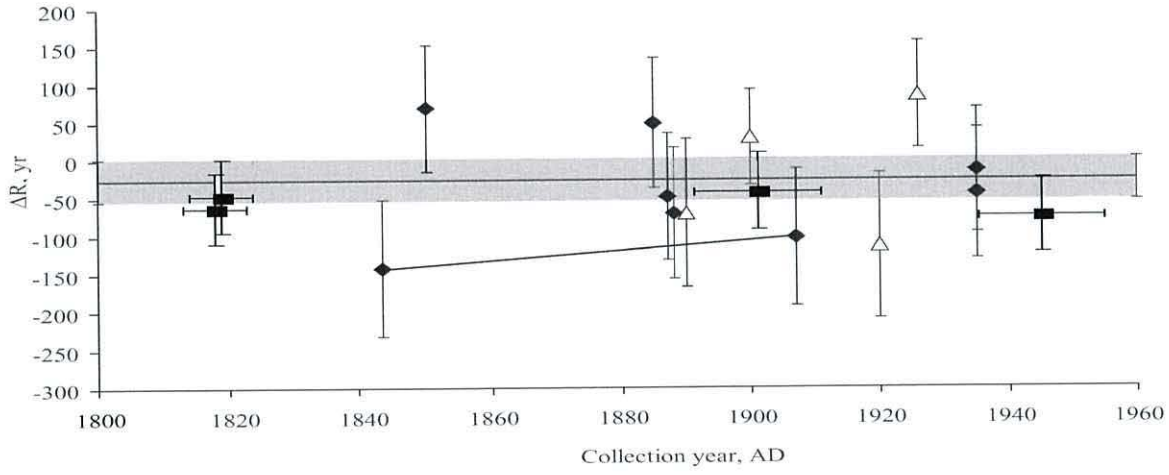

Figure 8 – 1: Hebridean shelf sea ΔR values; modification of Figure 4 of Cage et al. (2006) to incorporate the absolutely-dated G. glycymeris and G. humanus ΔR values derived from the ^{14}C determinations (black squares). The black diamonds and white triangles represent samples of gastropods and bivalves collected from sediment cores and analysed by Cage et al. (2006). The solid black line represents the mean value for the series with shaded grey the error (-26 ±14 years).

Cage *et al.*, (2006) present ΔR values for the Hebridean shelf seas utilising ^{14}C determinations derived from several gastropod and bivalve mollusc species

collected from dated cores collected from six sea lochs (Loch Creran, Loch Fyne, Upper Loch Fyne, Tarbert, Wemyss Bay, and Oban) located on the NW Scottish Coast.

The mean ΔR determined from the ^{14}C samples analysed from both *G. glycymeris* and *G. humanus* shell samples is -57years ± 29 (2σ of the four samples). Each of the individual sample ΔR values, as well as the mean value, are in agreement (within error) with the mean ΔR value calculated over the 19th and 20th centuries by Cage *et al.* (2006). The negative ΔR indicates a regional marine reservoir age which is less than the modelled mean global marine reservoir age. Ascough *et al.* (2004) compared ^{14}C determinations derived from paired marine and terrestrial materials from archaeological sites in the Shetlands and Hebridean islands. Although the dated material was significantly older, originating from *ca.*2000BP, than the samples analysed in this thesis and those examined by Cage *et al.* (2006), and different methodologies were used, the ΔR derived by Ascough *et al.* (2004) is within the error range of both Cage *et al.*, (2006) and the results given in table 8 – 1, (-79 years ± 17). These ΔR determinations provide no evidence that suggest the regional offset from the marine reservoir within the Scottish coastal waters has been temporally unstable over the past two centuries and thus the region has been hydrographically stable. Such stability has also been found within the ΔR record obtained from ^{14}C data derived from absolutely dated *A. islandica* from the Irish Sea over the past 500 years (Butler *et al.*, 2009b).

Shell ID	Sample date	Shell pMc	Shell error	Model pMc	Model error	ΔR	ΔR error
0020	1815	471	37	519	23	-48	47.88528
6004	1814	455	35	519	23	-64	46.14109
0013	1900	411	35	454	23	-43	50.53712
0015	1945	389	33	464	23	-75	48.76474

Table 8 – 1: Details of the four ^{14}C determinations used to calculate ΔR within Loch Sunart and the Tiree Passage.

8.3 $\delta^{13}C$ analysis

The annually resolved $\delta^{13}C$ values derived from the live-collected *G. glycymeris* (gg00024) show a significant linear decline (r^2=0.886, P<0.001) encompassing four repeating cycles with a period of 7 – 8 years, over the 28 years between AD 1976 – AD 2004. Such a decline is indicative of the depletion in ^{13}C values reported from *A. islandica* records from the Isle of Man (Butler *et al.*, 2009) and within foraminifera from Western Scotland (Cage and Austin, 2010; both shown in Figure 8 – 2). The trend towards depleted ^{13}C values is interpreted in both studies as an effect of the increased burning of fossil fuels that has taken place since the late 18th century AD (Butler *et al.*, 2009) i.e. the Suess Effect.

The *G. glycymeris* $\delta^{13}C$ record differs significantly from the Butler *et al.*, (2009) and Cage and Austin (2010) records (referred to here after as the Butler and Cage records respectively), both in temporal resolution and length, with both earlier records being, on average, decadally resolved compared with the annual resolution of the *G. glycymeris* record. However, over the common period all three records show a significant trend towards depleted $\delta^{13}C$ values. Within the Butler and Cage $\delta^{13}C$ records the gradient of the decline in $\delta^{13}C$ over the same 28 year period represented by the *G. glycymeris* record is *ca.*0.002‰yr^{-1}. The *G. glycymeris* record, however, exhibits a decline of 0.004‰yr^{-1}, double that of the Butler and Cage records. Ontogenetic trends have been identified within the $\delta^{13}C$ records obtained from *A. islandica* over the first forty years of growth (Schöne *et al.*, 2005; Butler *et al.*, 2009). It is hypothesised that the increased rate of calcium carbonate precipitation may lead to incorporation of metabolic ^{13}C which leads to an "exaggerated" Suess Effect signal. Figure 8 – 3 indicates that, as in *A. islandica*, there is a significant ontogenetic trend in the $\delta^{13}C$ record derived from a single *G. glycymeris* (R^2 = 0.5622, n=28 and P<0.005).

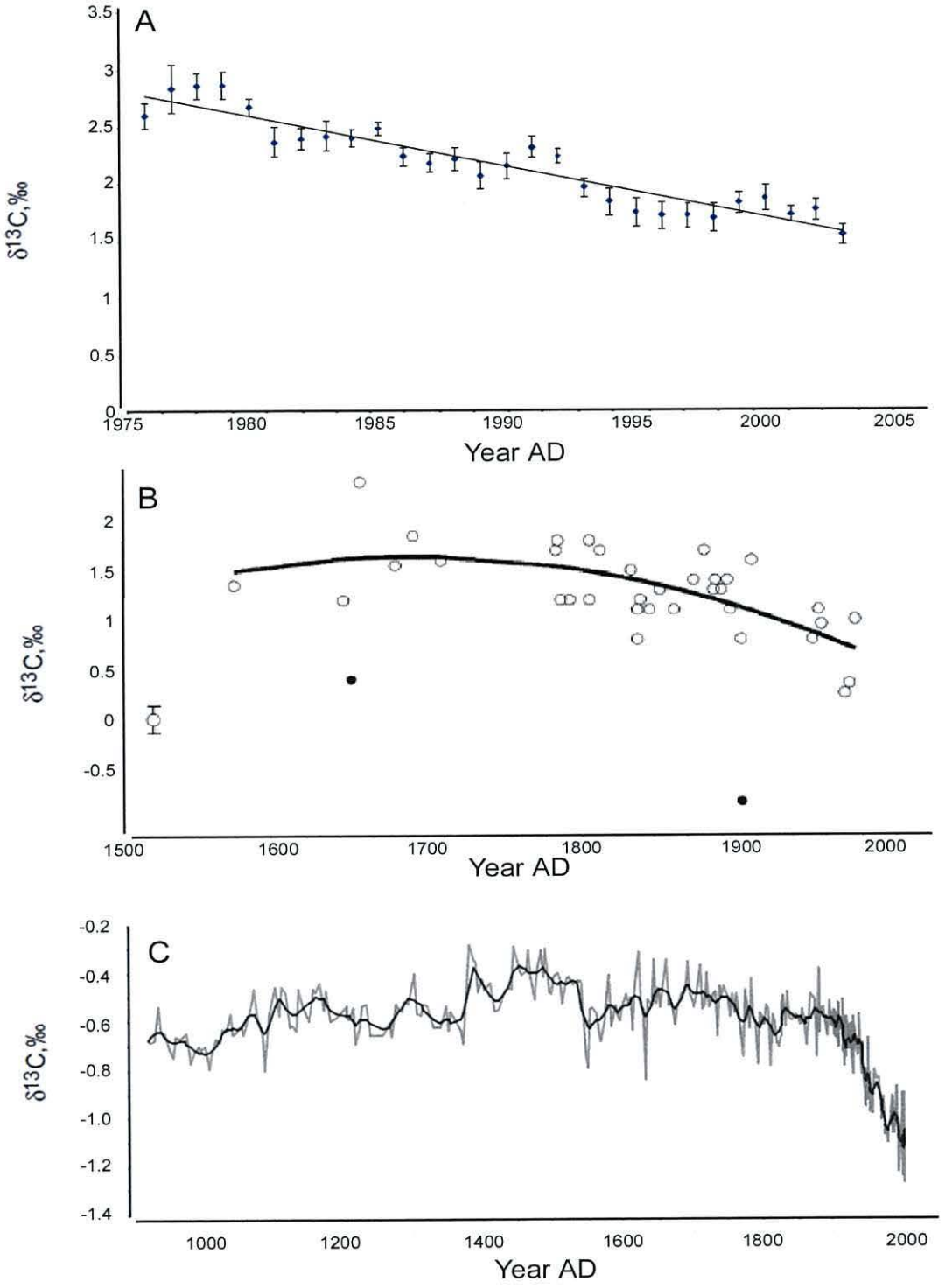

Figure 8 – 2: A) Annually resolved $\delta^{13}C$ values derived from a single live collected G. glycymeris shell valve collected from the Tiree Passage. B) Annually resolved $\delta^{13}C$ derived from multiple A. islandica valves collected from the coastal waters near the Isle of Man, UK (Butler et al., 2009b). C) $\delta^{13}C$ values derived from the benthic foraminifera Ammonia beccarii within a dated sediment core from Loch Sunart (Cage and Austin, 2010).

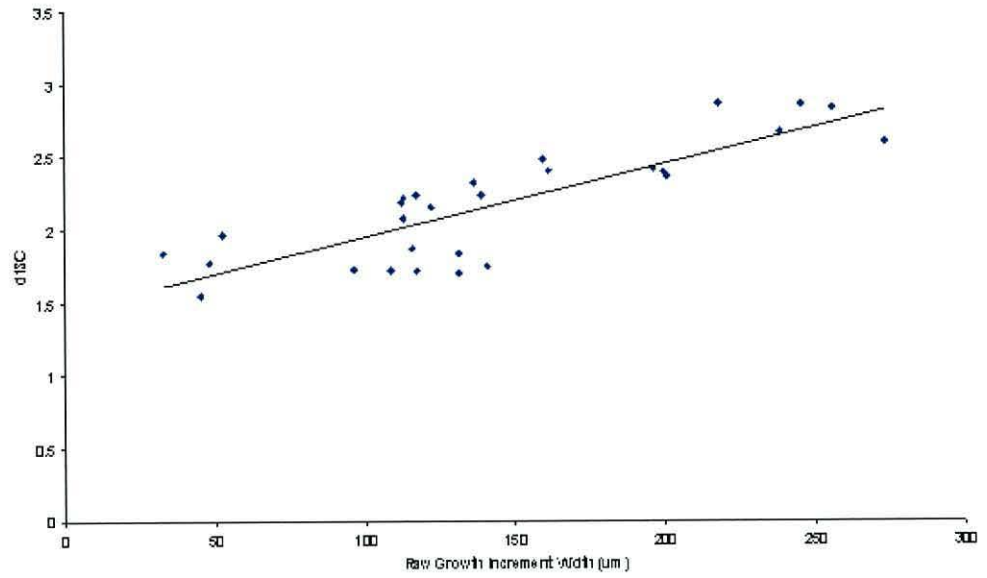

Figure 8 – 3: Linear regression analysis between the raw growth increment widths and associated $\delta^{13}C$ (‰) values. The linear regression line is described by the equation y = 0.0049x + 1.5018 (r^2 = 0.5622, n=28 and P<0.005)

A secondary dual linear regression was completed on the same $\delta^{13}C$ data to assess if there was a critical growth increment width i.e. if increments are narrower than a defined critical width it could be hypothesised that no metabolic $\delta^{13}C$ is incorporated and thus data within this portion could be ascribed to the Suess Effect signal. Figure 8 – 4 identifies that growth increments less than 150µm in width do not contain a significant correlation with $\delta^{13}C$ values (r=0.141), but that growth increments that are wider than 150µm do still significantly correlate with $\delta^{13}C$.

Although these results are only derived from a single shell over a limited time scale, they represent the highest resolution $\delta^{13}C$ record produced for the Western Scottish coastal shelf seas. The *G. glycymeris* $\delta^{13}C$ series highlights the need for further analysis of multiple shells of differing ontogenetic ages to ascertain the full impact of ontogenetic growth on $\delta^{13}C$ values.

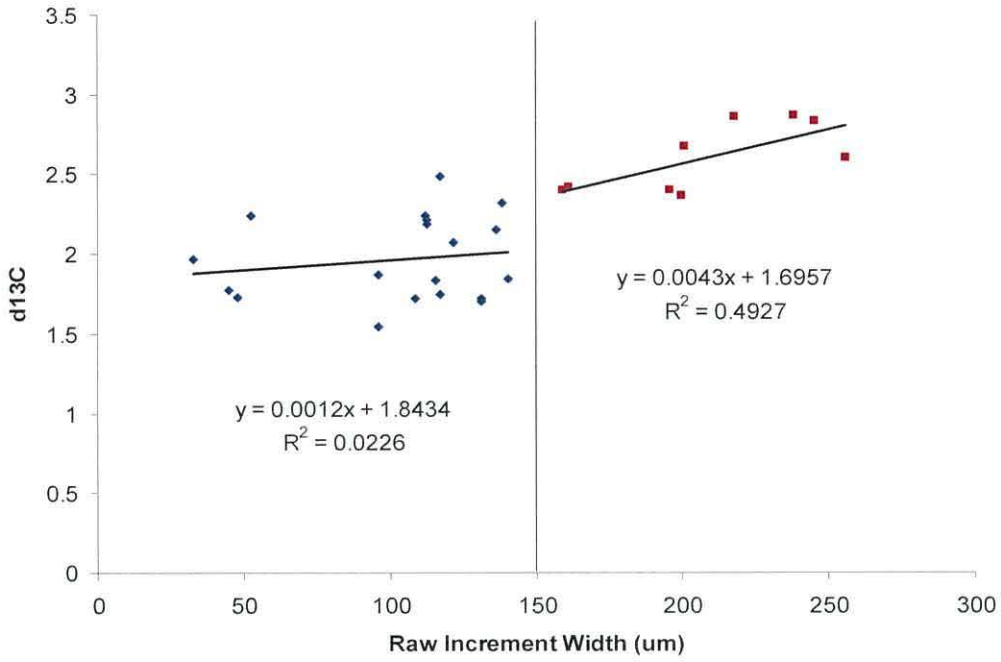

Figure 8 – 4: Dual linear regression analyses between the raw growth increment widths and associated $\delta^{13}C$ (‰) values. The solid black line denotes the separation between growth increments that may incorporate metabolic CO_2 (growth increment widths >150um) and those growth increments that show no statistically significant correlation with $\delta^{13}C$ (growth increment widths <150um).

8.4 – $\delta^{18}O$ Palaeotemperature

The 28 $\delta^{18}O$ values derived from the annual growth increments within the live-collected *G. glycymeris* 00024 significantly correlate with localised SSTs from Keppel Pier, Millport ($r=0.53$, $n=28$ $P<0.005$; Figure 8 - 5). Since the earliest classical studies (Urey *et al.*, 1947; Epstein *et al.*, 1953) it has been well documented that $\delta^{18}O$ values negatively correlate with sea water temperatures. More recent studies have identified that the same negative correlation is found between $\delta^{18}O$ values and calcium carbonate material derived from molluscs (Grossman and Ku, 1986; Schöne *et al.*, 2005; Wanamaker *et al.*, 2006). The positive Pearson correlation found between the *G. glycymeris* $\delta^{18}O$ and SSTs must therefore be an indirect correlation. Such an inversion in the relationship between $\delta^{18}O$ and temperature could be explained by stratification events within the Tiree Passage during the peak *G. glycymeris* growing season. As the surface waters warm a thermocline develops and the waters below the

thermocline remain relatively cool. Such events can result in an inverted (i.e. positive) correlations between shell $\delta^{18}O$ and SSTs.

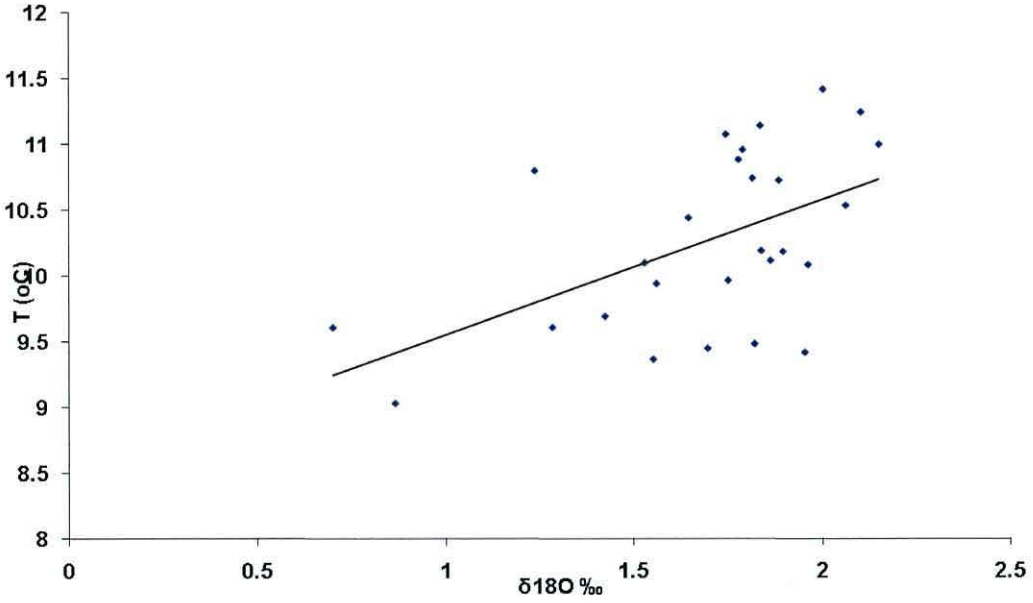

Figure 8 – 5: Linear regression analysis between the 28 year annually resolved G. glycymeris $\delta^{18}O$ series and annual Keppel Pier SSTs. The regression line can be described by the equation y = 1.0269x + 8.5256 (r=0.53, n=28 and P<0.005).

Studies examining stable isotopes of foraminifera in sediment cores taken from the Celtic Sea identified a negative correlation between $\delta^{18}O$ and $\delta^{13}C$ values in benthic foraminifera during shelf sea stratification onset (Austin and Scourse, 1997; Scourse *et al.*, 2002). This is due to an increase in remineralisation of the surface formed isotopically light organic matter during the transition from a mixed to a stratified water column. Linear regression analysis between $\delta^{18}O$ and $\delta^{13}C$ (Figure 8 – 6) also shows a negative correlation, thus supporting the idea that the Tiree Passage becomes stratified during the peak *G. humanus* growing season.

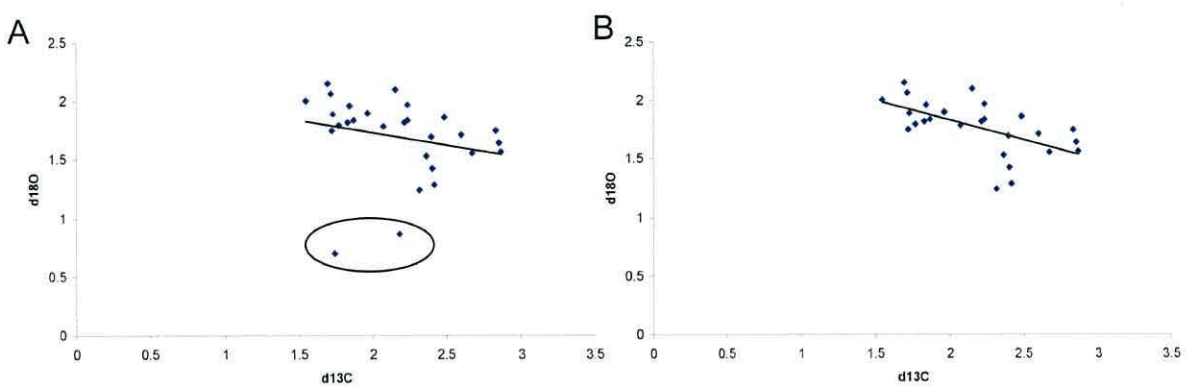

Figure 8 – 6: Linear regression analysis between $\delta^{18}O$ values and $\delta^{13}C$. A) analysis of all the raw stable isotope values. The regression line is expressed by the equation y = -0.2118x + 2.1556 (r^2= 0.0585, n=28 and 12). B) excludes two samples with depleted $\delta^{18}O$ values circled in A. The regression line is expressed by the equation y = -0.3346x + 2.4974 (r^2=0.3289, n=26 and P<0.005).

The raw $\delta^{18}O$ values were converted to palaeotemperatures using the Grossman and Ku (1986) palaeotemperature equation. However, a small modification of their equation was required because they report oxygen isotope values of seawater ($\delta^{18}O_{water}$) in SMOW – 0.27 ‰ (see footnote in Dettman *et al.*, 1999). The corrected function is as follows (Equ. 8.2):

Equ. 8.2 $$T(°C) = 20.60 - 4.34 \times (\delta^{18}O_{aragonite} - (\delta^{18}O_{water} - 0.27))$$

where $\delta^{18}O_{aragonite}$ denotes the $\delta^{18}O$ values derived from biogenic aragonite, $\delta^{18}O_{water}$ denotes the $\delta^{18}O$ value of the ambient water. The Cage and Austin (2010), mixing line equation (Equ. 8.3) for Loch Sunart was used to calculate a representative value for $\delta^{18}O_{water}$ based on mean salinity within the Tiree Passage:

Equ. 8.3 $$\delta^{18}O_{water} = 0.18 \times salinity - 6$$

where *salinity* is the ambient water salinity in PSU.

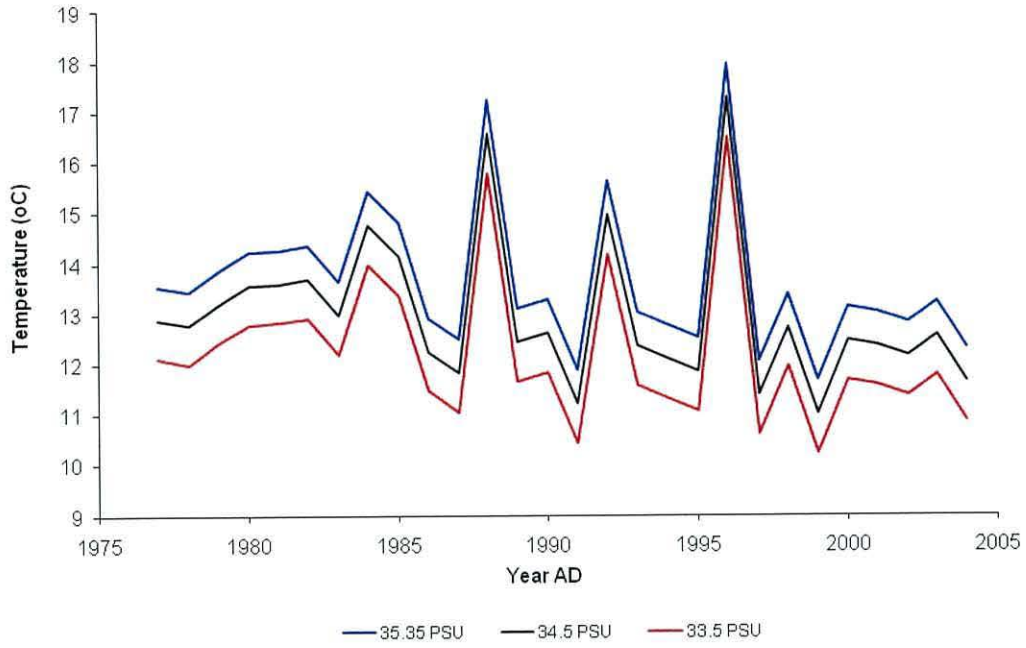

Figure 8 – 7 Sea water temperature values reconstructed using the G. glycymeris $\delta^{18}O$ timeseries using three different $\delta^{18}O_{water}$ values calculated for three salinities, 35.35PSU (European Slope Current Salinity; Inall et al., 2009) 34.5PSU (Loch Sunart main basin salinity; Cage 2005) and 33.5PSU (minimum Tiree passage surface salinity; Inall et al., 2009).

Cage *et al.*, (2005) reported mean salinity values within the main basin of Loch Sunart as 34.2 PSU. However, Inall *et al.*, (2009) report that the Tiree Passage is marginally more saline at 35.35 PSU; they also report that there is a weak seasonal effect in the salinity. They further report that accurate measurement of salinity only started in the Tiree Passage in 2002, so a mean value is adopted here in order to convert the $\delta^{18}O$ into palaeotemperatures.

Edwards and Edelsten, (1977) and Inall *et al.*, (2009) highlight that within narrow sided fjord systems, halo circulation plays a larger part in stratification of the water column than in thermal regimes. Additionally, within the Tiree Passage, Inall *et al.*, (2006) report a high degree of spatial and temporal variability in surface salinity, with measurements ranging from *ca.*33.5 to 35.5. Such salinity variability in the Tiree Passage would cause a range in the mean reconstructed temperatures (using Equ. 9.2 and 8.3) over the 28 year period from AD 1977 to AD 2004 of 12.2°C to 13.64°C . It is likely that the two pronounced peaks in reconstructed temperature in 1988 and 1996 are likely

due to inflated salinity values within the Tiree Passage. As salinity is an indicator of the fresh water influx, inflated volumes of fresh water through riverine or resulting directly as precipitation lead to a reduction in salinity, furthermore the fresh water input, which has been isotopically fractionated during the evaporation processes within the hydrological cycle, forces a shift in the marine system towards more depleted $\delta^{18}O_{water}$ values. Conversely the influx of more saline waters from the North Atlantic would contain isotopically enriched water.

Analysis of the raw $\delta^{18}O$ *G. glycymeris* values, using linear regression analysis, identifies an increase of 0.325‰ between the AD 1977 and AD 2004. Such an increase would normally correspond to a decrease in water temperatures of 1.34°C. However, examination of the Keppel Pier SSTs at both annual and seasonal level indicates that mean annual SSTs have increased by 1.27°C, spring SSTs by 1.06°C summer SSTs by 1.46°C, autumn SSTs by 0.953°C and winter SSTs by 1.05°C over the same 28 year period. However, the temperatures that result from converting the *G. glycymeris* $\delta^{18}O$ values using Equ. 8.2 and 8.3 indicate a decrease in temperature i.e. as the surface waters become warmer so the bottom waters in the Tiree Passage become cooler. This difference in trend between isotopically derived water temperatures and observed surface water temperatures could indicate a transition towards more strongly stratified water during the peak *G. glycymeris* growing season.

8.5 Spatial analysis

Analogous to the spatial analysis techniques applied to the growth increment chronologies (see chapter 7.3), the $\delta^{18}O$ timeseries was analysed using the KNMI Climate Explorer facility (http://climexp.knmi.nl) spatial correlation tool against the HadISST1 0.5° resolution SST dataset. Significant positive correlations were identified between the 28-year $\delta^{18}O$ *G. glycymeris* series and HadISST1 SSTs. Mean August to September SSTs showed the highest Pearson correlation coefficients as well as the widest spatial distribution (Figure 8 – 9).

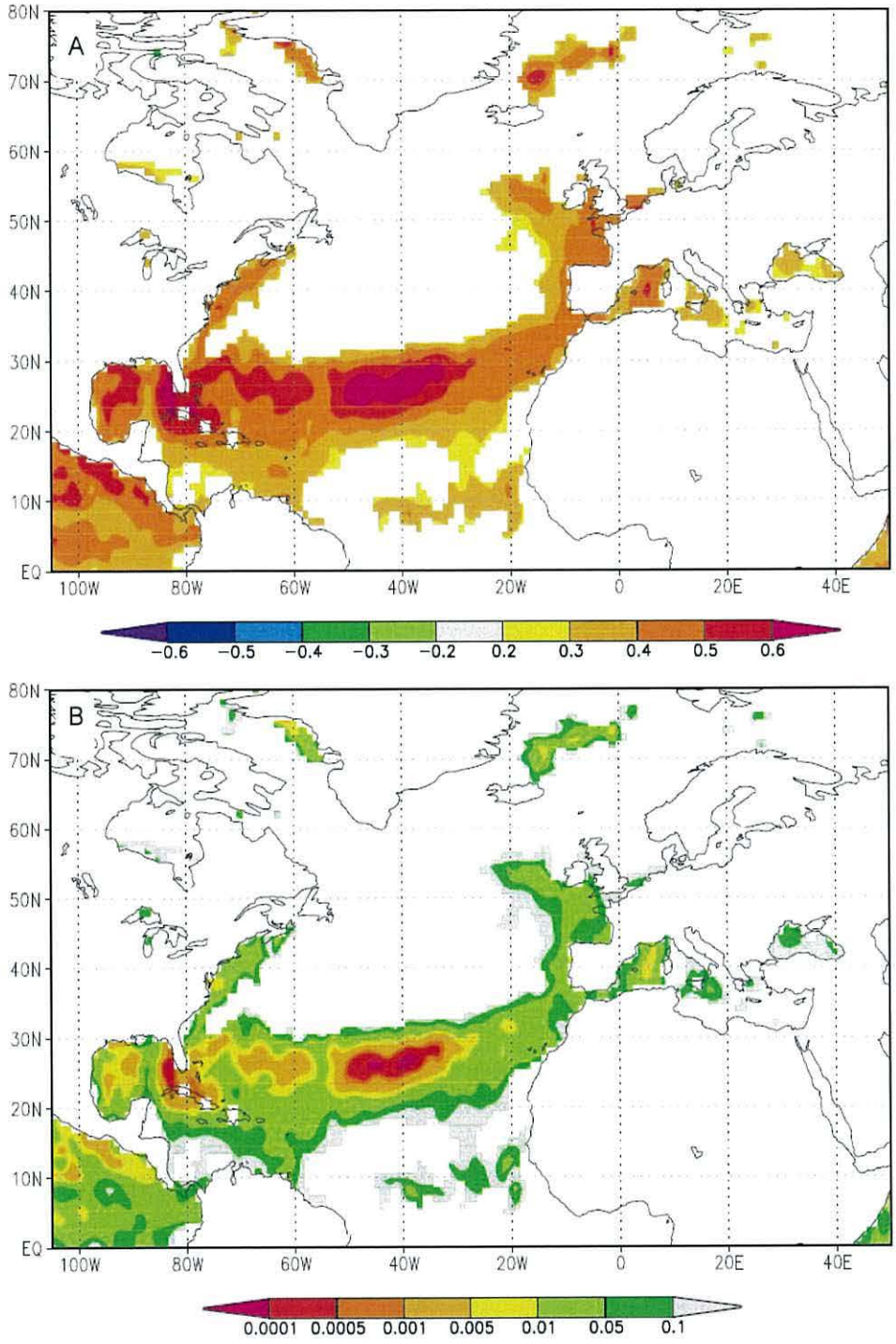

Figure 8 – 8 A) Correlation coefficients between mean August to September HadISST1 0.5° resolution SSTs and the 28 year $\delta^{18}O$ series obtained from the single G. glycymeris shell valve over the period AD1976 - 2004 and B) the corresponding probability values. Regions with correlations ~zero are coloured white.

Unlike the spatial analysis between the *G. glycymeris* growth increment series and the HadISST1 SSTs (Chapter 7), the area of the North Atlantic identified by this spatial correlation analysis, although similarly stretching from the Gulf of Mexico across to Western Europe and the British Isles, is significantly further south when compared with the trajectory of the NAC. It would, therefore, be unlikely that the $\delta^{18}O$ record represents actual NAC SSTs. However, similarities can be identified between the spatial correlation plot in Figure 8 – 8 and the $\delta^{18}O$ composition of global surface waters (Figure 8 – 9) as well as the isotopic composition of precipitation (Figure 8 – 10).

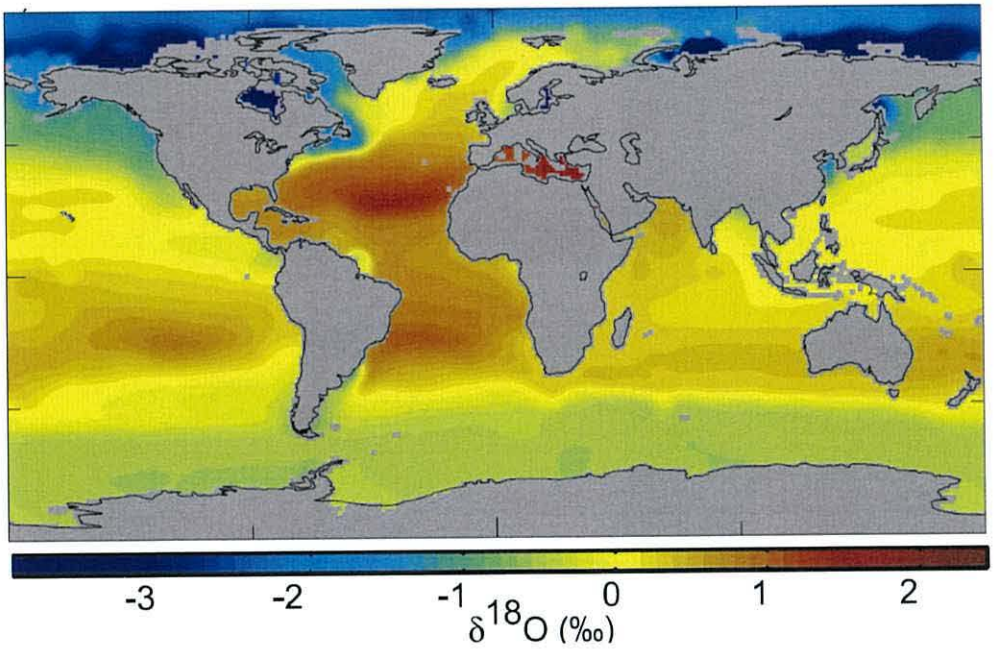

Figure 8 – 9: Gridded surface water $\delta^{18}O$ values (1° resolution) as presented by LeGrande and Schmidt (2006, Figure 1).

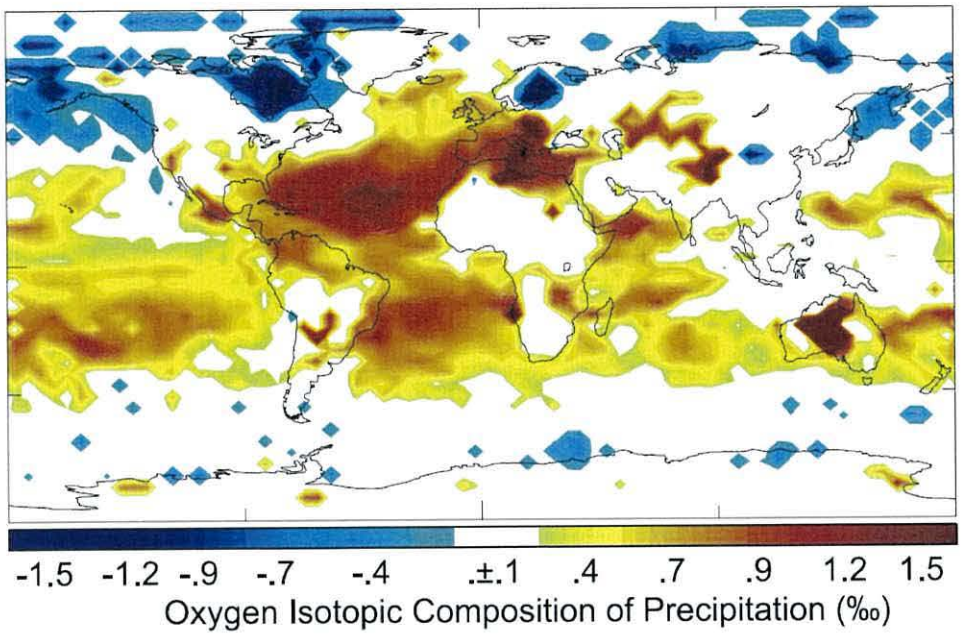

Figure 8 – 10: The simulated difference in the oxygen isotopic composition of precipitation using the GISS Model between setting the surface boundary condition of $\delta^{18}O$ as in Figure 8 - 9 and defining it as 0%. The difference between the last 5 years of 11 year runs is plotted and values less than the t-test 95% confidence intervals have been masked out.

This spatial relationship is intriguing and suggests that the $\delta^{18}O$ values in the Tiree Passage are at least partially controlled by the isotopic composition of precipitation over Scotland since it is highly likely that this region of the sub-tropical to warm temperate North Atlantic is the moisture source for air masses with westerly trajectories over NW Europe. Future isotopic analysis, from multiple *G. glycymeris*, is needed to extend the $\delta^{18}O$ record. Doing so would enable the full temporal stability and spatial extent of the correlations to be examined. It is of particular interest to examine the temporal stability of correlations calculated between both the $\delta^{18}O$ with SSTs and $\delta^{18}O$ with growth increment widths. It is hypothesised that interpretation of these records could facilitate the reconstruction of the AMO at annual resolution. Undertaking this would facilitate the interpretation of the *G. glycymeris* growth increment temperature reconstruction allowing greater precision across AMO cycles.

Chapter 9

General Conclusions

9.1 Introduction

This chapter summarises the results and discussions encompassing the biology, geochemistry, chronological analysis and palaeoenvironmental reconstructions. It also sets out some ideas and recommendations for possible future work.

9.2 Collections and general biology

The sampling methods employed, mechanical dredge and NFSD collections, yielded adequate numbers of *G. glycymeris* and *A. islandica* to construct absolutely dated robust master sclerochronologies. The low numbers of *G. humanus* that were collected from Loch Sunart have precluded the construction of an absolutely dated sclerochronology. It is likely that the relative rarity of *G. humanus* will severely constrain its use as a sclerochronological archive.

Sclerochronological examination of the internal growth increments in both *G. humanus* and *G. glycymeris* allowed the third and fourth key criteria of bichronological archives to be assessed (Thompson and Jones, 1977). Examination of the mean and range of longevities exhibited by *G. humanus* and especially *G. glycymeris* confirmed that they both reach longevities sufficient for cross-matching and as a result pass the third criterion set out by Thompson and Jones (1977). The shell valves of both *G. humanus* and *G. glycymeris* exhibit growth lines throughout the internal shell matrix in much the same way as *A. islandica*. Comparison of the ^{14}C determinations derived from both the umbone and ventral margin material from each of two *G. glycymeris* and *G. humanus*

with the sclerochronoloigcally derived ages confirmed that the growth lines were deposited throughout the lifespan of these organisms. It is concluded therefore that both *G. humanus* and *G. glycymeris* form growth increments over their entire longevities and thus fulfil criterion four (Thompson and Jones, 1977).

9.3 Construction of sclerochronologies

The internal growth increments of the three species were examined from digital photomosaics taken from the etched polished shell sections cut from the umbone to the ventral margins. The resulting growth increment series of all three species were then cross-matched using standard dendrochronological and sclerochronological techniques. In addition to the pre-existing sclerochronological archive (*A. islandica*) it was found that the growth increment series in both live- and dead-collected *G. humanus* and *G. glycymeris* could be successfully cross-matched. Due to the relatively short longevity and difficulties in identifying the growth increments it was essential to independently validate the cross-matching of the *G. humanus* growth series by means of ^{14}C dating; ^{14}C measurements were also undertaken from two dead-collected *G. glycymeris* that had been successfully cross-matched. The ^{14}C determinations successfully validated the cross-matching in the *G. glycymeris* sclerochronology and also confirmed the link between the live- and dead-collected *G. glycymeris* allowing a single absolutely dated sclerochronology to be constructed. In the *G. humanus* series, however, the ^{14}C data indicated that the shells collected from the Salen Bay site significantly pre-dated those shells from the Sound of Mull and had therefore been spuriously cross-matched. The ^{14}C dating did nevertheless confirm that the cross-matching of the shells from each site was relatively successful, although one shell from the Salen Bay site had still been spuriously cross-matched.

The confirmation that the growth increments within both *G. glycymeris* and *G. humanus* cross-match provide evidence that the growth increments are formed in synchrony between individuals living within populations driven by a common environmental forcing; this is the first of the four key criteria set out by Thompson and Jones (1977). The ability to cross-match dead- and live-collected individuals is fundamental for the construction chronologies that

extend beyond the lifetime of any single individual and for the conversion floating chronologies into absolute chronologies. It will therefore be possible to extend the sclerochronologies back through time constrained only by the availability of material within the fossil record; currently the extent of the fossil record for each of the species within Loch Sunart is unknown.

From the numbers of live and dead shells collected, by both dredging and NFSD collection it is unlikely that *G. humanus* will become a key sclerochronological archive. *G. glycymeris* and *A. islandica,* however, were present in good numbers at each of the sites examined. Therefore it is likely that further collections and research within the Tiree Passage and outer Loch Sunart will extend the sclerochronologies constructed as part of this thesis. Given the relative success in building and applying the *G. glycymeris* sclerochronology it is, therefore, likely that *G. glycymeris* will become a key sclerochronological archive.

9.4 Construction of the first multi-species master sclerochronology

The growth increment series of live- and dead-collected *G. glycymeris*, dead-collected *G. humanus* and live-collected *A. islandica* were successfully cross-matched, and verified by means of ^{14}C dating. The growth series which were successfully cross-matched were then used to construct the first statistically robust (EPS>0.85) multi-centennial annually resolved multi-species master sclerochronology. The ability to construct a sclerochronology utilising multiple species is a significant breakthrough in that it provides the foundation for the construction of further sclerochronologies in areas with insufficient series based on individual species. These data also indicate that the different species are growing in synchrony across a range of habitats and environments in the Tiree Passage and Loch Sunart. Therefore it is likely that the environmental factor(s) forcing the growth of these three species are operating across the entire region.

9.5 Comparison of the sclerochronologies to other late Holocene archives

Significant positive correlations were identified between the *G. glycymeris* sclerochronology and the independently constructed *P. sylvestris* dendrochronology from the Southern Glens. Such a coherent relationship is

likely due to large-scale climatic forcings linked to the North Atlantic climate system. The temporal stability within the correlations between the dendrochronology and the sclerochronologies provides independent validation of the dating within each of the series. However, the multi-species sclerochronology exhibits reduced correlations with the *P. sylvestrus* dendrochronology. This is attributed to the common signal within the series reflecting a more localised climatic signal due to the incorporation of *A. islandica* and *G. humanus* from Loch Sunart.

9.6 Geochemistry

Radiocarbon determinations derived from the biogenic aragonite of both *G. glycymeris* and *G. humanus* shell valves provided an invaluable independent assessment of the nature of cross-matching prior to the construction of the master sclerochronologies. Two ^{14}C determinations derived for each of two *G. glycymeris* as well as two *G. humanus* shells, derived from ventral margin and umbone calcium carbonate, were used to provide a comparison for the sclerochronologically determined ages, in order to provide a test of the annual periodicity of growth line formation. In all instances, the calibrated ^{14}C determinations agreed (within error), with the sclerochronologically determined ages assuming the growth increments were formed on an annual basis. Therefore these data provide confirmation that the growth lines in *G. glycymeris* are annual and the first evidence that annual lines are deposited in *G. humanus*. As such both species fulfil the second criteria set out by Thompson and Jones (1977) that a biochronical must possess consistent growth increments of known periodicity.

Four of the ^{14}C determinations, which were derived from the shell material that was then able to be absolutely dated as a result of their inclusion within the master sclerochronologies, were able to be converted into assessments of the localised offset from the marine reservoir. The assessments obtained from these determinations (-57±17) fall within the error of previous published assessments of ΔR for this region.

Stable isotope analysis ($\delta^{18}O$ and $\delta^{13}C$) of the biogenic aragonite derived from a single *G. glycymeris* from the Tiree Passage showed significant trends over the 28-year period from AD 1976-2004. The $\delta^{13}C$ data exhibited a significant decline, which can be attributed to an enhanced Suess effect amplified by the possible incorporation of metabolic carbon due to ontogenetic processes. The $\delta^{18}O$ data showed a negative correlation with SSTs from Keppel Pier. Such a trend is typical of a stratified water column in which the bottom water cools relative to the surface waters as the stratification develops. Linear regression analysis between the $\delta^{18}O$ and $\delta^{13}C$ data showed an inverse relationship. Such a trend has been shown to occur when a mixed watermass stratifies and isotopically light ($\delta^{13}C$) organic matter, which originates within the surface waters, remineralises as it descends through the thermocline into the cooler bottom waters generating lighter $\delta^{13}C_{seawater}$ values, (Austin and Scourse, 1997)

Spatial analysis of the $\delta^{18}O$ data identified significant correlation with the waters in the tropical Atlantic from the Gulf of Mexico to the NW coast of Africa. This region has been identified within the literature as a key source of the precipitation across NW Europe. These results warrant further analysis.

9.7 Palaeoclimate reconstructions

The data presented show that the master sclerochronologies constructed from the internal growth lines of bivalve molluscs collected from climatically sensitive areas, such as the Tiree Passage, can be used to reconstruct SSTs within the NAC and air temperatures across NW Europe. Inclusion of growth series from *A. islandica* and *G . humanus* from the mouth of Loch Sunart in the first multi-species sclerochronology showed lower correlations between the master sclerochronology and SSTs ; this may indicate that *G. humanus* and *A. islandica* are responding to climatic forcing originating from within Loch Sunart, albeit they still show some degree of response, although insignificant, to fluctuations within the NAC SSTs.

The temporal instabilities found within the running Pearson correlation coefficients between the *G. glycymeris* sclerochronology and NAC SSTI and NWEAT series showed significant correlations with the AMO cyclicity. Such a

trend, given our current understanding of the AMO, highlights the significance of the application of the *G. glycymeris* sclerochronology in reconstructing NAC SSTs. Further study is required to investigate the full effects of the AMO upon the Tiree Passage *G. glycymeris* populations as well as on stratification within the water column.

Both the stable isotopic data and the correlations between the *G. glycymeris* sclerochronology suggest that *G. glycymeris* can grow even when the water column becomes stratified. The $\delta^{18}O$ data, which positively correlate with SSTs, suggests that the bottom water temperatures are inversely proportional to the SSTs. As the growth increment widths positively correlate with the SSTs, this suggests that the growth increments are responding indirectly to changing SSTs. It is highly likely, therefore, that the *G. glycymeris* are responding to changes within food availability (plankton) controlled by changes in SST and stratification.

9.8 Areas of future research

Whilst conducting this study it has become apparent that there are key areas of future research which could follow the completion of this thesis. The following sub-sections detail by species the areas identified as key future objectives.

9.7.1 *Glossus humanus*

There has been very little work done regarding the biology or ecology of *G. humanus* since the seminal works of Nicol (1951) and Owen (1953) . The field collections undertaken during this project and the examination of the museum collections, - Natural History Museum (London), Smithsonian Natural History Museum (Washington) and the Scottish National Museum (Edinurgh) - as well as examination of the online databases - the National Biodiversity Network and the Global Biodiversity Information Facility - suggest that the abundance of extant *G. humanus* populations have declined over the past decades. Currently, however, there are no quantitative data regarding the extent of the modern day distribution or distributions within the fossil record for this large bivalve. It may be possible, by utilising the multi-species sclerochronology as a dating tool, to date more dead-collected material from the main basin within Loch Sunart to

generate a temporal perspective on the *G. humanus* populations. It would be recommended, however, that any such study should validate any successful cross-matching with independent ^{14}C determinations.

9.7.2 *Glycymeris glycymeris*

The dog cockle *G. glycymeris* has shown great potential for becoming a key palaeoceanographic archive, both by means of statistical sclerochronological analysis and by using geochemical proxies. Further examination of the biology and ecology of the organism is required to understand what drives the growth of the organism and the forcing behind the periodic growth lines and to fully understand the mechanisms underlying the linkages between the proxy and climatic variability. Further development of the multi-proxy reconstructions, (utilising the statistical analysis of the growth increment widths and the stable isotope geochemistry), is likely to enable more extensive palaeoceanographic reconstructions leading to a greater understanding of ocean-atmosphere coupled climatic variability over past millennia at annual to sub-annual resolution.

Prior to the application of *G. glycymeris* as a geochemical proxy it is first recommended that an in-depth investigation into the full effects of the thermo-halocline within the Tiree Passage, as well as the varying effects of each environmental parameters and ontogenetic age on the isotopic content of the biogenic aragonite with *G. glycymeris* shell valves, is undertaken.

9.7.3 *Arctica islandica*

It is likely now that with the more comprehensive shell collections obtained by the NFSD dive team that a statistically robust master sclerochronology could be constructed utilising both the live- and dead-collected shells from several of the sites within the main basin of Loch Sunart. Doing so may allow for the assessment of the hydrography of the main basin on shell growth as well as potentially allowing further investigation of the late Holocene palaeoclimate. It would be very interesting to compare a master *A. islandica* sclerochronology with the Tiree Passage *G. glycymeris* sclerochronology; doing so may deconvolve the NAC- and Loch Sunart-derived climate signals.

References

Ambrose, W.G., Carroll, M.L. Greenacre,M., Thorrold, S.R., and McMahon, K.W., 2006. Variation in *Serripes groenlandicus* (Bivalvia) growth in a Norwegian high-Arctic fjord: evidence for local- and large-scale climatic forcing, *Global Change Biology*, ***12***, 1595-1607.

Ascough, P.L., Cook, G.T., Dugmore, A.J., Barber, J., Higney, E. and Scott, E.M., 2004. Holocene variations in the Scottish marine radiocarbon reservoir effect. *Radiocarbon*, **46**(2), 611-620.

Austin, W.E.N. and scourse, J.D., 1997. Evolution of seasonal stratification in the Celtic Sea during the Holocene. *Journal of the Geological Society*, **154,** 249-256.

Berthou, P., Blanchard, M., Noel, P. and Vergnaud-Grazzini, C., 1986. The analysis of stable isotopes of the shell applied to the determination of the age of four bivalves of the "Normano-Breton" Gulf, Western Channel. *ICES,* **K:16**, 1-13.

Black, B.K., 2009. Climate-driven synchrony across tree, bivalve and rockfish growth-increment chronologies of the northeast Pacific. *Marine Ecology Progress Series*, **378**, 37-46.

Briffa, K.R., Jones, P.D., Bartholin, T.S., Eckstein, D., Schweingruber, F.H., Karlén, W., Zetterberg, P. and Eronen, M., 1992. Fennoscandian summers from AD 500: temperature changes on short and long timescales*. *Climate Dynamics*, **7**, 111-119.

Bronk Ramsey, C., 1994. Analysis of Chronological Information and Radiocarbon Calibration : The Program OxCal. *Archaeological Computing Newsletter,* **41**, 11-16.

Bronk Ramsey, C., 2001. Development of the radiocarbon calibration program OxCal. *Radiocarbon,* **43**(2A), 355-363.

Butler, P.G., 2009. *Establishing the Arctica islandica archive*. PhD thesis, Bangor University.

Butler, P.G., Richardson, C.A., Scourse, J.D., Wanamaker Jr. A.D., Shammon, T.M. and Bennell, J.D., 2009a. Marine climate in the Irish Sea: analysis of a 489-year marine master chronology derived from growth increments in the shell of the clam *Arctica islandica*. *Quaternary Science Reviews,* doi:10.1016/j.quascirev.2009.07.010.

Butler, P.G., Scourse, J.D., Richardson, C.A., Wanamaker Jr., A.D., Bryant, C.L. and Bennell, J.D., 2009b. Continuous marine radiocarbon reservoir calibration and the 13C Suess effect in the Irish Sea: Results from the first multi-centennial shell-based marine master chronology. *Earth and Planetary Science Letters*, **279**, 230-241.

Butler, P.G. Wanamaker Jr, A.D., Scourse, J.D., Richardson, C.A. and Reynolds, D.J., 2011. Long-term stability of δ13C with respect to biological age in the aragonite shell of mature specimens of the bivalve mollusk *Arctica islandica. Palaeogeography, Palaeoclimatology Palaeoecology,* **302**, 21-30.

Butler, P.G., Wanamaker Jr., A.D., Scourse, J.D., Richardson, C.A. and Reynolds, D.J., Submitted. Variability of marine climate on the North Icelandic Shelf in a 1,357-year cross-dated *Arctica islandica* chronology. *Palaeogeography, Palaeoclimatology Palaeoecology.*

Cage, A.G., 2005. *The modern and late Holocene marine environments of Loch Sunart, N.W. Scotland.* Ph.D. thesis. School of Geography & Geosciences, University of St Andrews, St Andrews. pp. 399.

Cage, A.G., Heinemeier, J. and Austin, W.E.N., 2006. Marine radiocarbon reservoir ages in scottish coastal and fjordic waters. *Radiocarbon*, **48**(1), 31–43.

Cage, A.G. and Austin, W.E.N., 2010. Marine climate variability during the last millennium: The Loch Sunart record, Scotland, UK. *Quaternary Scince Reviews*, doi:10.1016/j.quascirev.2010.01.014.

Cook, E.R. and Peters, K., 1981. The smoothing spline: a new approach to standardizing forest interior tree-ring width series for dendrochronological studies. *Tree-ring Bulletin*, **41**, 45-58.

Cook, E.R. and Holmes, R.L., 1986. Guide for computer program ARSTAN. In: Holmes, R.L., Adams, R.K., and Fritts, H.C. (Eds.). Tree-ring chronologies of Western North America. California eatern Origon and northern Great Basin. Laboratory of Tree-ring Research, University of Arizona, Tucson, USA, 50-65/.

Cook, E.R. and Kairiukstis, L.A., 1990. *Methods of Dendrochronology: applications in the environmental sciences*. Boston, MA: Kluwer Academic Publishers.

Cook, E.R. and Peters, K., 1997. Calculating unbiased tree-ring indices for the study of climate and environmental change. *Holocene*, **7**(3), 359-368.

Cook, E.R. and Krusic, P.J. 2007. *ARSTAN – A tree-ring standardization program based on detrending and auto-regressive timeseries modelling with interactive graphics.* Tree Ring Laboratory, Lamont Doherty Observatory of Columbia University Palisades, NY.

Cullen, H.M., D'Arrigo, R.D. and Cook, E.R., 2001. Multiproxy reconstruction of the North Atlantic Oscillation. *Paleoceanography*, **14**, 27-39.

Dahlgren, T.G., Weidberg, J.R. and Halanych, K.M., 2000. Phylogeography of the ocean quahog (*Arctica islandica*): influences of palaeoclimate on genetic diversity and species range. *Marine Biology*, **37**, 487-495.

Dettman, D.L., Reische, A.K. and Lohmann, K.C., 1999. Controls on the stable isotope composition of seasonal growth bands in aragonitic fresh-water bivalves (Unionidae). *Geochimica et Cosmochimica Acta*, **63**(7-8), 1049-1057.

Edwards, A. and Edelsten, D.J., 1977. Deep-water renewal of Loch Etive: a three basin Scottish fjord. *Estuarine and Coastal Marine Science,* **5**, 575–593.

Epstein S., Buchsbaum R., Lowenstam H.A. and Urey H.C. 1953. Revised carbonate-water isotopic temperature scale. *Geological Society of America Bulletin.* **64**, 1315–1326.

Esper, J., Frank., D.C., Wilson, R.J.S. and Briffa, K.R., 2005. Effect of scaling and regression on reconstructed temperature amplitude for the past millennium. *Geophysical Research Letters*, **32**, L07711.

Fritts, H.C., 1976.*Tree Rings and Climate*. Academic Press, London.

Funder, S. and Weidick, A., 1991. Holocene boreal molluscs in Greenland – palaeoceanographic implications. *Palaeogepgraphy, Palaeoclimatology and Palaeoecology,* **85**, 123-135.

Galkin, Y., 1998. Long-term changes in the distribution of molluscs in the Barents Sea related to the climate. *Reportings of Polar Research*, **287**, 100-143.

Gillibrand, P.A., Cage, A.G. and Austin, W.E.N., 2005. A preliminary investigation of basin water response to climate forcing in a Scottish fjord: evaluating the influence of the NAO. *Continental Shelf Research*, **25**, 571–587.

Grossman, E.L. and Ku, T.L., 1986. Oxygen and carbon isotope fractionation in biogenic aragonite: Temperature effects. *Chemical Geology*, **59**, 59-74.

Hayward, P.J. and Ryland, J.S., (eds.) 1995. *Handbook of the marine fauna of north-west Europe*. Oxford University Press.

Helama, S., Schöne, B.R., Kirchhefer, A.J., Nielsen, J.K., Rodland, D.L. and Janssen, R., 2007. Compound response of marine and terrestrial ecosystems to varying climate: Pre-anthropogenic perspective from bivalve shell growth increments and tree-rings. *Marine Environmental Research,* **63**(3), 185-199.

Helama, S., Läänelaid, A., Tietäväinen, H., Fauria, M.M., Kukkonen, I.T., Holopainen, J. Nielsen, J.K. and Valovirta, I., 2009. Late Holocene climatic variability reconstructed from incremental data from pines and pearl mussels – a multi-proxy comparison of air and subsurface temperatures. *Boreas*, **39**, 734-748.

Hudson, H.J., Shinn, E.U., Halley, R.B. and Lidz, B., 1976. Sclerochronology: A tool for interpreting past environments. *Geology*, **4**, 361-364.

Hughen, K.A., Baillie, M.G.L., Bard, E., Beck, J.W., Bertrand, C.J.H., Blackwell, P.G., Buck, C.E., Burr, G.S., Cutler, K.B., Damon, P.E., Edwards, R.L., Fairbanks, R.G., Friedrich, M., Guilderson, T.P., Kromer, B., McCormac, G., Manning, S., Bronk Ramsey, C., Reimer, P.J., Reimer, R.W., Remmele, S., Southon, J.R., Stuiver, M., Talamo, S., Taylor, F.W., van der Plicht, J. and Weyhenmeyer, C.E., 2004. Marine04 marine radiocarbon age calibration, 0-26 cal kyr BP. *Radiocarbon,* **46**(3), 1059-1086.

Hurrell, J.W., 1995. Decadal trends in the North Atlantic Oscillation regional temperatures and precipitation. *Science*, **269**, 676-679.

Hurrel, J.W. and Van Loom, H., 1997. Decadal variations in climate associated with the north atlantic oscillation. *Climate Change*, **36**, 301-326.

Inall, M., Gillibrand, P., Griffiths, C., MacDougal, N. and Blackwell, K., 2009. On the oceanographic variability of the North-West European Shelf to the West of Scotland. *Journal of Marine Systems*, **77**, 210–226.

Knutson, D.W., Buddemeier, R.W. and Smith, S.V., 1972. Coral chronometers: Seasonal growth bands in reef corals. *Science*, **177**, 270-272.

Jones, P.D., Jónsson, T. and Wheeler, D., 1997: Extension to the North Atlantic Oscillation using early instrumental pressure observations from Gibraltar and South-West Iceland. *International Journal of Climatology,* **17**, 1433-1450.

Jones, D., 1980. Annual cycle of shell growth increment formation in two continental shelf bivalves and its palaeoecologic significance. *Paleobiology,* **6**(3), 331-340.

Jones, D.S., Williams, D.F., Arthur, M.A. and Krantz, D.E., 1984. Interpreting the palaeoenvironmental, palaeoclimatic and life history records in mollusc shells. *Geobios, Memoir Special*, **8**, 333-339.

Owen, G., 1953. On the biology of *Glossus humanus*. *Journal of the Marine Biological Association of the United Kingdom*, **32**, 85-106.

Manley, G., 1953. Mean temperature of central England. *Quarterly Journal of the Royal Meteorological Society*, **79**, 242-261.

Manley, G., 1974. Central England temperatures monthly means 1959 to 1973. *Quarterly Journal of the Royal Meteorological Society*, **100**, 389-326.

Mantua, N.J., Hare, S.R., Zhang, Y., Wallace, J.M. and Francis, R.C., 1997. A Pacific interdecadal climate oscillation with impacts on salmon production. *Bulletin of the American Meteorological Society*, **78,** 1069-1079.

Marchitto, T.M., Jones, G.A., Goodfriend, G.A. and Weidman, C.R., 2000. Precise temporal correlation of Holocene mollusc shells using sclerochronology. *Quaternary Research*, **53(3)**, 236-246.

Nicol, D., 1951a. Recent species of the cyrenoid pelecypod *Glossus*. *Journal of the Washington Academy of Science*, **41**, 142-146.

Nicol, D., 1951b. Recent species of the veneroid pelecypod *Arctica*. *Journal of the Washington Academy of Science*, **41**, 102-106.

NRC, 2006. Surface temperature reconstructions for the last 2000 years. Commitee on Surface Temperature Reconstructions for the last 2000 years, National Research council. ISBN 0-309-66144-7.

Pachauri, R.K. and Reisinger, A. (eds.). IPCC, 2007: Climate Change 2007: Synthesis Report. Contribution of Working Groups I, II and III to the Fourth Assessment Report of the Intergovernmental Panel on Climate Change Geneva, Switzerland.

Parker, D.E., Legg. T.P. and Folland, C.K. 1992. A new daily central England temperature series, 1772-1991. *International Journal of Climatology*, **12**(4), 317-342.

Raffi, S., 1986. The significance of marine boreal molluscs in the early Pleistocene faunas of the Mediterranean area. *Palaeogeography, palaeoclimatology and Palaeoecology*, **52**, 267-289.

Ramsay, K., Kaiser, M.J., Richardson, C.A., Veale, L.O. and Brand, A.R., 2000. Can shell scars on the dog cockle, (*Glycymeris glycymeris* L.) be used as an indicator of fishing disturbance? *Journal of Sea Research*, **43**, 167-176.

Ramsay, K., Richardson, C.A. and Kaiser, M.J., 2001. Causes of shell scaring in dog cockles *Glycymeris glycymeris*. *Journal of Sea Research* **45**, 131-139.

Rayner, N.A.; Parker, D.E., Horton, E.B.; Folland, C.K. Alexander, L.V. Rowell, D.P. Kent, E.C., Kaplan, A., 2003. Global analyses of sea surface temperature, sea ice, and night marine air temperature since the late nineteenth century. *Journal of Geophysical Research,* **108**(D14), 4407 10.1029.

Rayner, N.A., Brohan, P. Parker, D.E., Folland, C.F., Kennedy, J.J. Vanicek, M., Ansell, T. and Tett, S.F.B., 2006. Improved analyses of changes and uncertainties in sea surface temperature measured in situ since the mid-nineteenth century: the HadSST2 data set. *Journal of Climate,***19**(3), 446-469.

Reimer, P.J., Baillie, M.G.L., Bard, E., Bayliss, A., Beck, J.W., Blackwell, P.G., Bronk Ramsey, C., Buck, C.E., Burr, G.S., Edwards, R.L., Friedrich, M., Grootes, P.M., Guilderson, T.P., Hajdas, I., Heaton, T.J., Hogg, A.G., Hughen, K.A., Kaiser, K.F., Kromer, B., McCormac, F.G., Manning, S.W., Reimer, R.W., Richards, D.A., Southon, J.R., Talamo, S., Turney, C.S.M., van der Plicht, J. and Weyhenmeyer, C. E., 2009. IntCal09 and Marine09 radiocarbon age calibration curves, 0-50,000 years cal BP. *Radiocarbon,* **51**(4), 1111-1150.

Rhodes, D.C. and Lutz, R.A., (eds) 1980. *Skeletal growth of aquatic organisms.* New York: Plenium Press.

Richardson, C.A., 2001. Molluscs as archives of environmental change. *Oceanography and Marine Biology*, **39**, 103-164.

Rosenberg, G.D. and Runcorn, S.K., (eds) 1975. *Growth rhythms and the history of the Earth's rotation.* London, Wiley.

Salvigsen, O., Forman, S.L. and Miller, G.H., 1992.Thermophilous molluscs on Svalbard during the Holocene and their palaeoclimatic implications. *Polar Research*, **11**, 1-10.

Schöne, B.R., Freyre Castro, A.D., Freng, J., Houk, S.D., Oschmann, W. and Krönck, I., 2004. Sea surface water temperatures over the period 1884-1983 reconstructed from oxygen isotope ratios on a bivalve mollusc shell (*Arctica islandica*, southern North Sea). *Palaeogeography, Palaeoclimatology Palaeoecology,* **212**, 215-232.

Schöne, B.R., Tanabe, K., Dettman, D.L., and Sato. S., 2003. Environmental controls on shell growth rates and δ^{18}Oof the shallow-marine bivalve mollusc *Phacosoma japonicum* in Japan. *Marine Biology,* **142**, 473-485.

Schöne, B.R., Fiebig, J., Pfeiffer, M., Gleh, R., Hickson, J., Johnson, A.L.A., Dreyer, W. and Oschmann, W., 2005. Climate records from a bivalved Methuselah (*Arctica islandica*, Mollusca; Iceland). *Palaeogeography, Palaeoclimatology Palaeoecology*, **228**, 130-148.

Scourse, J.D, Richardson C., Forsythe, G., Harris, I., Heinemeier, J., Fraiser, N., Briffa, K. and Jones, P., 2006. First cross-matched floating chronology from the marine fossil record: data from growth lines of the long-lived bivalve mollusc *Arctica islandica*. *Holocene*, **16**(7), 967-974.

Scourse, J.D., Austin, W.E.N., Long, B.T., Assinder, D.J. and Huws, D., 2002. Holocene evolution of seasonal stratification in the Celtic Sea refined age model. Mixing depths and foraminifera stratigraphy. *Marine Geology*, **191**, 119-145.

Scourse, J.D. Wanamaker Jr, A.D., Weidman, C., Heinemeier, J. Reimer, P.J. Butler, P.G. Witbaard, R. and Richardson, C.A., in prep. The marine radiocarbon bomb-pulse across the temperate North Atlantic: a compilation of $\delta^{14}C$ time histories from *Arctica islandica* growth increments.

Squires, R.L., 2010. Northeast Pacific upper Cretaceous and Paleocene Glycymeridid bivalves. *Journal of Paleontology*, **84** (5) 895-917.

Stepkowsa, E.T., Pérez-Rodríguez, J.L., Sayagués, M.J. and Martínez-Blanes, J. M., 2003. Calcite, vaterite and aragonite forming On cement hydration from liquid and gaseous phase. *Journal of Thermal Analysis and Calorimetry,* **73** 247.269.

Strom, A., Francis, R.C., Mantua, N.J., Miles, E.L. and Peterson, D.L., 2004. North Pacific climate recorded in growth rings of geoduck clams: a new tool for paleo- environmental reconstruction. *Geophysical Research Letters,* **31**, LO6206. doi:10.1029/2004GL019440.

Steuber, T., 1999. Isotopic and chemical intra-shell variations in low-Mg calcite of rudist bivalves (Mollusca-Hippuritacea): disequilibrium fractionations and late Cretaceous seasonality. *International Journal of Earth Sciences*, **88**(3), 551-570.

Suess, H.E., 1953. *Natural radiocarbon and the rate of exchange of carbon dioxide between the atmosphere and the sea. In: Aldrich, W. (Ed.), Nuclear Processes in Geologic Settings*. University of Chicago Press, Chicago, 52–56.

Surge, D.M., Lohmann, K.C. and Goodfriend, G.A., 2003. Reconstructing estuarine conditions: oyster shells as recorders of environmental change, Southwest Florida. *Esturine Coastal and Shelf Science,* **57**(5-6), 737-756.

Thompson, I. and Jones, D.S., 1977. The ocean quahog, *Arctica islandica*, "tree" of the north Atlantic shelf. *Annual Meeting of the Geological Society of America Abstracts*, 9, 1199.

Thompson, I., Jones, D.S. and Dreibelbis,D.,1980. Annual internal growth banding and life history of the ocean quahog *Arctica islandica* (Mollusca: Bivlavia). *Marine Biology,* **57**, 25–37.

Tourre, Y.M., Paz, S., Kushnir, Y. and White, B., 2010. Low frequency climate variability in the Atlantic basin during the 20th century. *Atmospheric Science Letters*, **11**, 180-185.

Urey, H.C., 1947. The thermodynamic properties of isotopic substances. *Journal of the Chemistry Society*, 562-581. DOI: 10.1039/JR9470000562

Visser, H., Büntgen, U., D'Arrigo, R. and Petersen, A.C., 2010. A. C. 2010. Detecting instabilities in tree-ring proxy calibration. *Climate of the Past Discussions,* **6**, 225-255.

Walker, G.T. and Bliss, E.W., 1932. World Weather V. *Memoir of the Royal Meteorological Society*, **4**, 53-84.

Wanamaker Jr, A.D., Kreutz, K.J., Borns Jr, H.W., Introne, D.S., Feindel, S. and Barber, B.J., 2006a. An aquaculture-based method for calibrated bivalve isotope paleothermometry. *Geochemistry, Geophysics, Geosystems*, **7**, doi:10.1029/2005GC001189.

Wanamaker Jr, A.D., Kreutz, K.J., Schöne, B.R., Pettigrew, N., Borns, H.W., Introne, D.S., Belknap, D., Maasch, K.A. and Feindel, S., 2006b. Coupled North Atlantic slope water forcing on Gulf of Maine temperatures over the past millennium. *Climate Dynamics*, **35**, 183-194.

Wanamaker Jr, A.D., Kreutz, K.J., Scho¨ne, B.R., Maasch, K.A. Pershing, A.J., Borns, H.W., Introne, D.S. and Feindel, S., 2008. A late Holocene paleo-productivity record in the western Gulf of Maine, USA, inferred from growth histories of the long-lived ocean quahog (*Arctica islandica*). *International Journal of Earth Sciences*, **98**, 19-29.

Wanamaker Jr, A.D., Heinemeier, J., Scourse, J.D., Richardson, C.A., Butler, P.G., Eiríksson, J. and Knudsen, K.L., 2009. Very long-lived mollusks confirm 17th century ad tephra-based radiocarbon reservoir ages for north Icelandic shelf waters. *Radiocarbon*, **50**(3), 399-412.

Wanamaker Jr, AD., Kreutz, K.J., Schöne, B.R. and Introne, D.S., 2011. Gulf of Maine shells reveal changes in seawater temperature seasonality during the Medieval Climate Anomaly and the Little Ice Age. *Palaeogeography, Palaeoclimatology Palaeoecology*, **302**, 43-51.

Wanamaker Jr, A.D., Butler, P.G., Scourse, J.D., Heinemeier, J., Eriksson, J., Knudsen K.L. and Richardson, C.A., Submitted. Coherent hydrographic changes in the North Atlantic during the last millennium. *Nature*.

Weidman, C.R., Jones, G.A. and Kyger, C.L., 1994. The long-lived mollusc *Arctica islandica*: a new palaeoceanographic tool for the reconstruction of bottom water temperatures for the continental shelves of the northern North Atlantic Oscillation. *Journal of Geophysical Research*, **99**(9), 18305–18314.

Wigley, T.M.L., Briffa, K. and Jones, P., 1984. On the Average Value of Correlated Time Series, with Applications in Dendrochronology and Hydrometeorology. *American Meteorological Society,* **23**(2), 201-213.

Wilson, R.J.S. and Elling, W., 2004. Temporal instability in tree-growth/climate response in the lower Bavarian Forest region: implications for dendroclimatic reconstruction. *Trees*, **18**(1), 19–28.

Witbaard, R., Jenness, M.I., Van Der Borg, K. and Ganssen, G., 1994. Verification of annual growth increments in *Arctica islandica* L. from the North Sea by means of oxygen and carbon isotopes. *Journal of Sea Research*, **33**, 91-101.

Witbaard, R., Duineveld, G.C.A. and DeWilde, P.A.W.J., 1997a. A long-term growth record derived from *Arctica islandica* (Mollusca, Bivalvia) from the Fladen Ground (northern North Sea). *Journal of the Marine Biological Association of the United Kingdom*, **77**(3), 801–816.

Witbaard, R., Franken, R. and Visser, B., 1997b. Growth of juvenile *Arctica islandica* under experimental conditions. *Helgolander Meeresuntersuchungen*, **51**(4), 417–431.

Witbaard, R. and Bergman, M.J.N., 2003a. The distribution and population structure of the bivalve *Arctica islandica* L. in the North Sea: what possible factors are involved? *Journal of Sea Research*, **50**, 31-25.

Witbaard, R., Jansmab, E. and Sass Klaassenc, U., 2003b. Copepods link quahog growth to climate. *Journal of Sea Research*, **50**, 77-83.

Witbaard, R., Duineveld, G.C.A., Amaro, T. and Bergman, M.J.N., 2006. Growth trends in three bivalve species indicate climate forcing on the benthic ecosystem in the southeastern North Sea. *Climate Research*, **30**, 29-38.

Woodley, E.J., 2010. *Reconstructing the climate of Scotland using stable carbon and oxygen isotopes in tree-rings.* Ph.D. thesis Swansea University.

Zhang, R. and Delworth, T.L., 2006. Impact of Atlantic multidecadal oscillation on India/ Sahel rainfall and Atlantic hurricanes. *Geophysical Research Letters*, **33,** L17712.

Zhang, R., 2007. Anticorrelated multidecadal variations between surface and sub surface tropical North Atlantic. *Geophysical Research Letters,* **34**, L12713.

Zatsepin, V.I. and Filatova, Z.A., 1961. The bivalve mollusc *Cyprina islandica* (L.), its geographic distribution and role in the communities of benthic fauna. *Transactions of the Institute of Ocean studies, Russian Academy of Science,* **46**, 201-216.